

**Copyright**

**by**

**He Liu**

**2006**

**The Dissertation Committee for He Liu Certifies  
that this is the approved version of the following dissertation:**

**Individual variation and hormonal modulation of sodium channel  
alpha and beta1 subunits in the electric organ correlate with  
variation in a social signal**

**Committee:**

---

**Harold Zakon, Supervisor**

---

**Nigel Atkinson**

---

**John Mihic**

---

**George Pollak**

---

**Bing Zhang**

**Individual variation and hormonal modulation of sodium channel alpha  
and beta1 subunits in the electric organ correlate with variation in a  
social signal**

by

**He Liu, B.S.**

**Dissertation**

Presented to the Faculty of the Graduate School of

the University of Texas at Austin

in Partial Fulfillment

of the Requirements

for the Degree of

**Doctor of Philosophy**

The University of Texas at Austin

August 2006

## **Dedication**

This dissertation is dedicated to my parents, Wen-Sheng Liu and Yu-Wen Wang, my sister, Rui Liu and my wife Peixin Chen.

## **Acknowledgements**

I would like to thank my advisor, Harold Zakon, for his guidance and support in the past five years. His knowledge, consideration and friendship have been crucial for me to complete my degree. It indeed took him extra efforts and patience to be the mentor of a foreign student with very different language and cultural background. Mingming Wu spent a lot of time to help me with most of the oocytes recordings and data analysis in this dissertation. Lynne McAnelly helped me with tissue collection. I would also like to thank Nigel Atkinson, who provided facilities for most of the laboratory work in this dissertation and gave me many instrumental advices. Many others also have helped me along the way, including: Nikolai Dembrow, Andrew George, Ying Lu, Yan Wang, Seung K. Rhee and Moon Draper.

**Individual variation and hormonal modulation of sodium channel  
alpha and beta1 subunits in the electric organ correlate with  
variation in a social signal**

Publication No. \_\_\_\_\_

He Liu, Ph.D.  
The University of Texas at Austin, 2006

Supervisor: Harold Zakon

**Abstract**

The electric fish *Sternopygus macrurus* emits an electric organ discharge (EOD) composed of a series of pulses. EOD frequency and duration are individually unique, sexually dimorphic and regulated by steroid hormones. Previous studies have shown the EOD pulse is partially shaped by a sodium current, whose rate and voltage dependence of inactivation correlate with EOD frequency and pulse duration, and are modulated by androgens.

In this study I tested whether the gradient in sodium current inactivation across EOD frequency might be due to regulation on sodium channel  $\alpha$  and  $\beta$ 1 subunits. Full-length sequences of the two sodium channel  $\alpha$  subunits in the electric organ of *Sternopygus macrurus*, smNav1.4a and smNav1.4b were cloned. Furthermore, two smNav1.4b mRNA transcripts (smNav1.4bL and

smNav1.4bS), with alternative first exons and translated into proteins with and without an extended N terminus respectively, were identified. Electric organ expresses smNav1.4a and smNav1.4b at comparable levels and preferentially expresses smNav1.4bL. The mRNA level of smNav1.4bL but not smNav1.4a, correlates with EOD frequency.

I also cloned the sodium channel  $\beta$ 1 subunit in *Sternopygus* and found two splice forms of this gene ( $\beta$ 1L and  $\beta$ 1S). They exhibit a distinct pattern of differential expression in different tissues. In the electric organ, the mRNA levels of  $\beta$ 1 and the splicing preference for  $\beta$ 1S correlate with EOD frequency.

An androgen implant lowered EOD frequency. It also lowered the mRNA levels of smNav1.4bL, smNav1.4bS and  $\beta$ 1, but did not affect smNav1.4a or the splicing preference of  $\beta$ 1.

Expression of smNav1.4bL or smNav1.4bS alone, or together with  $\beta$ 1L or  $\beta$ 1S in *Xenopus* oocytes revealed the kinetic properties of these subunits. Importantly, smNav1.4bL and  $\beta$ 1S, whose expressions correlate with EOD frequency, show faster inactivation rates and negative shifts of voltage dependence, consistent with the natural phenotype of high EOD frequency fish. Furthermore, two mutagenesis studies addressed the functions of the novel regions in smNav1.4bL and  $\beta$ 1S.

These results suggest multiple levels of mRNA control on sodium channel  $\alpha$  and  $\beta$ 1 subunits underlie the cellular excitability in the electric organ and correlate with the variation in an important social signal, EOD, in *Sternopygus*.

# Table of Contents

<b>List of Tables</b>	xi
<b>List of Figures</b>	xii
<b>Chapter 1</b>	
<b>General Introduction</b>	<b>1</b>
Voltage-gated sodium channel	1
Regulation of voltage-gated sodium channels contributes to cellular excitability	3
$\beta$ 1 subunit of voltage-gated sodium channels	5
Alternative mRNA splicing of ion channels	8
Hormonal control of ion channels	10
Electric fish and electric organ	11
Electric organ discharge	13
Androgen modulates EOD and sodium current inactivation kinetics	14
Summary of this dissertation	15
<b>Chapter 2</b>	
<b>Regulation of sodium channel <math>\alpha</math> subunit expression underlies cellular excitability of electrocytes</b>	<b>20</b>
Abstract	20
Introduction	22
Materials and Methods	24
<i>Experimental animals</i>	24
<i>RNA and DNA Isolation</i>	25
<i>RT-PCR, PCR and Cloning PCR products</i>	25
<i>3' and 5' Rapid Amplification of cDNA Ends (RACE)</i>	26
<i>Cloning intron and promoter sequences of smNav1.4b</i>	28
<i>Semi-Quantitative RT-PCR</i>	29
<i>Immunoprecipitation and Western Blot</i>	30
<i>Differential Display RT-PCR</i>	31
<i>Real-time Quantitative RT-PCR</i>	31
<i>DHT treatment</i>	33
<i>Plasmid Construction of Nav1.4bL, Nav1.4bS full-length sequences</i>	33
<i>Site-directed Mutagenesis</i>	34
<i>Expression of Nav1.4 genes in Xenopus oocytes</i>	35
<i>Statistics</i>	37

Results		37
	<i>Cloning of Nav1.4 cDNA sequences in Sternopygus</i>	37
	<i>Both sodium channels are expressed in electric organ at comparable levels</i>	38
	<i>5' RACE revealed complex mRNA variation of smNav1.4b</i>	39
	<i>5' RACE of Nav1.4b in zebrafish and rat</i>	40
	<i>Tissue distribution pattern of smNav1.4 transcripts</i>	42
	<i>Immunoprecipitation and western blot confirmed the existence of smNav1.4b protein</i>	43
	<i>Correlation between gene expression and EOD frequency</i>	43
	<i>DHT affects expression of sodium channels in electric organ</i>	45
	<i>Expression of smNav1.4bL, smNav1.4bS and hNav1.4 in Xenopus oocytes</i>	47
	<i>Deletion of a proline strongly affects the inactivation kinetics</i>	49
Discussion		51
	<i>Variations in the ends of ion channels may allow functional diversity</i>	51
	<i>N terminus of sodium channel affects inactivation</i>	52
	<i>Expression of sodium channels in the electric organ</i>	54
	<i>Hormonal regulation of sodium channel expression</i>	58
	<i>Evolution of sodium channels in electric fish</i>	59
<b>Chapter 3</b>		
<b>Expression and alternative splicing of sodium channel <math>\beta</math>1 subunit contribute to the individual variation of cellular excitability of electrocytes</b>		85
Abstract		85
Introduction		86
Materials and Methods		87
	<i>Cloning <math>\beta</math>1 subunit in Sternopygus</i>	87
	<i>Cloning introns of <math>\beta</math>1 subunit</i>	88
	<i>Tissue distribution of the <math>\beta</math>1 subunit splicing forms</i>	88
	<i>Real-time Quantitative RT-PCR</i>	89
	<i>DHT treatment</i>	89
	<i>Plasmid construction</i>	90
	<i>Site-directed mutagenesis</i>	90
	<i>Co-expression of <math>\beta</math>1 subunits with Nav1.4 in oocytes</i>	90

Results	91
<i>Cloning of sodium channel <math>\beta 1</math> subunits in <i>Sternopygus</i></i>	91
<i>Tissue distribution, gene structure, and alternative splicing of sodium channel <math>\beta 1</math> subunit</i>	92
<i>Correlation between expression/splicing and EOD frequency</i>	94
<i>DHT suppresses levels of <math>\beta 1</math> mRNA</i>	96
<i><math>\beta 1</math> subunits modulate sodium channels in <i>Xenopus</i> oocytes</i>	97
<i><math>\beta 1S-181Y</math> has a reduced effect on <math>\alpha</math> subunits</i>	99
<i>Proline deletion does not affect the modulation of smNav1.4bL by <math>\beta 1L</math></i>	100
Discussion	101
<i><math>\beta 1</math> subunits modulate sodium channel kinetics</i>	101
<i>Alternative Splicing of the <math>\beta 1</math></i>	103
<i><math>\beta 1</math> expression levels correlate with EOD frequency</i>	105
<i><math>\beta 1</math> mRNA abundance, but not splicing, is regulated by androgens</i>	106
<b>Chapter 4</b>	
<b>General Discussion</b>	<b>122</b>
Two sodium channel $\alpha$ subunits in electrocytes of <i>Sternopygus</i>	123
Regulation of sodium channel mRNA abundance may determine cellular excitability	124
$\beta 1$ subunit expression: an independent regulation mechanism	125
Multiple levels of controls on multiple genes	127
Does expression of sodium channel subunits explain individual variation in sodium current?	129
<b>Appendices</b>	<b>134</b>
Appendix 1. cDNA sequence of smSCN4Aa(smNav1.4a)	134
Appendix 2. cDNA sequence of smSCN4Ab (smNav1.4b)	136
Appendix 3. Exon and intron sequences of SCN1B	138
Appendix 4. Intron 1L (between exon 1L and exon2) of smNav1.4b	140
Appendix 5. Genomic DNA sequence immediately upstream of exon1L of smNav1.4b (1202bp known, obtained by 5' RAGE)	140
Appendix 6. pNHE vector	142
<b>References</b>	<b>143</b>
<b>Vita</b>	<b>153</b>

## List of Tables

<b>Table 2.1</b> Primers Used in 3' RACE of sodium channels	27
<b>Table 2.2</b> Primers Used in 5' RACE of sodium channels	28
<b>Table 2.3</b> TaqMan PCR Primer/probe Sets and SYBR Green PCR Primers Used in Real-time Quantitative RT-PCR	32
<b>Table 2.4</b> Gene Structures of Nav1.4b in Zebrafish ( <i>Danio rerio</i> ) and Nav1.4 in Rat ( <i>Rattus norvegicus</i> )	42
<b>Table 2.5</b> Kinetic Properties of hNav1.4, smNav1.4bS and smNav1.4bL (wild-type and mutant) in <i>Xenopus</i> oocytes	50
<b>Table 3.1</b> Primers Used in Cloning $\beta$ 1 Subunit of <i>Sternopygus</i>	88
<b>Table 3.2</b> Primers and Probes Used in Real-time Quantitative RT-PCR	89
<b>Table 3.3</b> $\beta$ 1 subunits modulate the kinetic properties of sodium channels	98
<b>Table 3.4</b> $\beta$ 1S-181Y has a reduced effect on $\alpha$ subunits	99
<b>Table 3.5</b> Co-expression of $\beta$ 1L with mutant smNav1.4bL with a proline deletion	100

## List of Figures

<b>Figure 1.1</b> Relationship between the EOD and sodium current inactivation kinetics.	19
<b>Figure 2.1</b> One-step RT-PCR reactions with forward and reverse primers to confirm the open reading frames of Nav1.4a and Nav1.4b.	61
<b>Figure 2.2</b> Alignment of deduced protein sequences of hNav1.4, Nav1.4a and Nav1.4b(S) from <i>Sternopygus</i> .	62
<b>Figure 2.3</b> Secondary structure prediction in the N terminus of smNav1.4bL.	65
<b>Figure 2.4</b> Alignment of N-termini of human Nav1.4, smNav1.4a and smNav1.4bL.	66
<b>Figure 2.5</b> Alignment of C-termini of human Nav1.4, smNav1.4b and smNav1.4a.	67
<b>Figure 2.6</b> smNav1.4a and smNav1.4b have comparable abundance in electric organ.	68
<b>Figure 2.7</b> 5' RACE of Nav1.4b in <i>Sternopygus</i> , zebrafish ( <i>Danio rerio</i> ), and Nav1.4 in rat ( <i>Rattus norvegicus</i> ).	69
<b>Figure 2.8</b> Gene structure of Nav1.4b in <i>Sternopygus</i> (top), zebrafish (middle) and Nav1.4 in rat (bottom).	70
<b>Figure 2.9</b> Exon 1S, 1L and exon 2 of Nav1.4b in <i>Sternopygus</i> .	71
<b>Figure 2.10</b> Exon 1S, 1L of Nav1.4b in <i>Danio rerio</i> and the N-terminal sequences of Nav1.4bL in <i>Sternopygus</i> and <i>Danio rerio</i> .	72
<b>Figure 2.11</b> The distant exon of rNav1.4.	73
<b>Figure 2.12</b> Semi-quantitative RT-PCR of Nav1.4bL and Nav1.4bS in electric organ.	74
<b>Figure 2.13</b> Immunoprecipitation and western blot show the existence of the extra segment in the N-terminus of smNav1.4bL.	75
<b>Figure 2.14</b> Amplification of myosin light chain was used to screen total RNA samples from electric organ.	76

<b>Figure 2.15</b> Real-time quantitative RT-PCR showed mRNA level of smNav1.4b correlates with EOD frequency.	77
<b>Figure 2.16</b> Real-time quantitative RT-PCR showed mRNA level of smNav1.4a does not correlate with EOD frequency	78
<b>Figure 2.17</b> Real-time quantitative RT-PCR showed mRNA level of smNav1.4bL correlates with EOD frequency.	79
<b>Figure 2.18</b> Real-time quantitative RT-PCR showed mRNA level of smNav1.4bS does not correlate with EOD frequency.	80
<b>Figure 2.19</b> DHT lowered EOD frequency of <i>Sternopygus</i> .	81
<b>Figure 2.20</b> DHT lowered the mRNA levels of Nav1.4b (Nav1.4bL and Nav1.4bS) but not Nav1.4a in <i>Sternopygus</i> .	82
<b>Figure 2.21</b> Properties of hNav1.4, smNav1.4bL and smNav1.4bS.	83
<b>Figure 2.22</b> Proline deletion changes the inactivation kinetics of smNav1.4bL.	84
<b>Figure 3.1</b> Comparison of $\beta$ 1 subunit in <i>Sternopygus</i> and $\beta$ subunits in other species.	108
<b>Figure 3.2</b> Deduced amino acid sequence alignment between the sodium channel $\beta$ 1 subunit in <i>Sternopygus macrurus</i> (sm $\beta$ 1) and in rat (rat $\beta$ 1).	109
<b>Figure 3.3</b> The first exon of sodium channel $\beta$ 1 subunit gene (SCN1B) in <i>Sternopygus macrurus</i> .	110
<b>Figure 3.4</b> Alternative mRNA splicing of sodium channel $\beta$ 1 subunit in <i>Sternopygus</i> .	111
<b>Figure 3.5</b> Gene structure and alternative splicing of sodium channel $\beta$ 1 subunit.	112
<b>Figure 3.6</b> ClustalW alignment of the intracellular domains of $\beta$ 1 subunits in rat and <i>Sternopygus macrurus</i> .	113
<b>Figure 3.7</b> mRNA level of sodium channel $\beta$ 1 subunit correlates with EOD frequency.	114

<b>Figure 3.8</b> mRNA level of $\beta$ 1S splice form correlates with EOD frequency.	115
<b>Figure 3.9</b> mRNA level of $\beta$ 1L splice form does not correlate with EOD frequency.	116
<b>Figure 3.10</b> The mRNA splicing preference, represented by $\beta$ 1S/ $\beta$ 1L ratio, correlates with EOD frequency.	117
<b>Figure 3.11</b> DHT implants (n=8) lowered the mRNA level of $\beta$ 1 but did not change the splicing preference, compared to control group (n=4).	118
<b>Figure 3.12</b> Both $\beta$ 1 subunits of <i>Sternopygus</i> dramatically affect the kinetics of hNav1.4.	119
<b>Figure 3.13</b> Both $\beta$ 1 subunits affect the kinetics of smNav1.4bS.	120
<b>Figure 3.14</b> Both $\beta$ 1 subunits affect the kinetics of smNav1.4bL.	121
<b>Figure 4.1</b> Working model for the regulation of sodium channel subunits in the electric organ of <i>Sternopygus macrurus</i> .	131
<b>Figure 4.2</b> Schematic illustration of the relations of expression levels of multiple sodium channel subunits with EOD frequency.	132
<b>Figure 4.3</b> The expressions of smNav1.4b and $\beta$ 1S show compensation to each other.	133

---

## CHAPTER 1

### General Introduction

---

#### Voltage-gated sodium channel

Voltage-gated sodium channels are responsible for the initiation and propagation of action potentials in excitable cells. Thus, they play important roles in physiology and pathology of skeletal muscle, heart and nervous system. Since the first isolation of the sodium channels by tetrodotoxin and scorpion toxin labeling (Agnew et al., 1980; Beneski and Catterall, 1980), ten voltage-gated sodium channels have been identified in mammals. Among them, Nav1.4 is expressed in skeletal muscles, Nav1.5 is expressed in heart, the other eight channels are expressed in a variety of cell types in nervous system (Novakovic et al., 2001).

A voltage-gated sodium channel is usually composed of a large (>200kD), pore-forming  $\alpha$  subunit and one or two relative smaller (<40kD), auxiliary  $\beta$  subunits. The  $\alpha$  subunit contains four homologous transmembrane domains (I–IV), three intracellular loops (I-II, II-III and III-IV loop) connecting them and intracellular amino (N) and carboxy (C) termini. Each domain has six transmembrane segments (S1–S6). The ion selectivity filter is located at the outer pore and formed by four amino acids (DEKA), one from each domain and located between S5 and S6, while the inner pore formed by S6 segment from each domain is the receptor site of local anesthetics (Catterall, 2000).

Upon depolarization, voltage-gated sodium channels increase the conductance of

sodium ions, then quickly decrease the conductance within a few milliseconds. These two processes are referred to as activation and inactivation respectively. It has been proposed and experimentally supported that the rotational and outward movement of S4 segments is responsible for the activation (Catterall, 2000). The inactivation, more important in many physiological and pathological conditions, is controlled by a gate containing an IFM motif located in loop III-IV (Vassilev et al., 1988). Several regions act as inactivation gate receptors, including hydrophobic residues at the intracellular part of S6 in domain IV, intracellular regions linking S4 and S5 in domain III and IV (Mcphee et al., 1995; Smith and Goldin, 1997; Mcphee et al., 1998). Further evidences suggest that S4 in domain IV has a coupling effect between activation and inactivation (Chen et al., 1996).

The control of inactivation also involves the C terminus of sodium channel. Switching the C termini between Nav1.2 and Nav1.5 resulted in the exchange of their inactivation kinetics and voltage dependence, and deletion of the distal half of the C terminus of either Nav1.2 or Nav1.5 negatively shifted steady-state inactivation (Mantegazza et al., 2001). Structural analysis predicts six  $\alpha$  helices in the C terminus and the deletion of the last helix is sufficient for this negative shift (Cormier et al., 2002). Furthermore, two channelopathic mutations in the C termini of sodium channels have been identified recently. One mutation (D1866Y) in Nav1.1, responsible for inherited epilepsy, positively shifts the inactivation voltage dependence (Spampanato et al., 2004). The other one (F1705I) in Nav1.4 located in the fifth of the six helices in the C terminus (for details, see Fig. 2.5), associated with cold-aggravated myotonia, also positively shifts the voltage dependence and slows the rate of inactivation (Wu et al., 2005).

Despite the evidence suggesting the function of the C terminus in channel inactivation, the effect of the N terminus is still not known. However, several studies have provided thoughtful hints on this direction. Proteolysis analysis suggests the N terminus has a compact tertiary structure, resistant to proteases unless denatured. The C terminus, on the other hand, has an extended conformation, easily accessible for proteases (Zwerling et al., 1991). Furthermore, a pattern of competitive binding with steep concentration dependence was observed with specific antibodies against the beginning of the N terminus and the distal end of the C terminus (34 a.a. after the sixth helix), indicating a strong interaction between the two ends of Nav1.4 (Sun et al., 1995), of which the electrostatic nature has been shown by a further study (Zhang et al., 2000).

### **Regulation of voltage-gated sodium channels contributes to cellular excitability**

Phosphorylation and dephosphorylation of sodium channels can rapidly alter the conductance or kinetics of sodium channels and regulate cellular excitability. PKA has been shown to phosphorylate Nav1.2 in cultured neurons (Rossie and Catterall, 1987) and reduce the sodium current (Li et al., 1992; Smith and Goldin, 1996). Four cAMP dependent protein kinase (PKA) phosphorylation sites in loop I–II have been identified (Murphy et al., 1993) and one of them is involved in dopaminergic modulation of Nav1.2 in hippocampal neurons (Cantrell et al., 1997). Phosphatase 2A and calcineurin dephosphorylate sodium channels and reverse the effect of PKA (Chen et al., 1995). Another protein kinase, protein kinase C (PKC), also reduces sodium current and slows

the inactivation of Nav1.2 (Numann et al., 1991). Furthermore, activated receptor tyrosine kinase (RTK) rapidly inhibits sodium current and lowers the voltage dependence of inactivation through *src* signaling pathway (Hilborn et al., 1998). Dephosphorylation by receptor tyrosine phosphatase  $\beta$  slows sodium channel inactivation, positively shifting its voltage dependence, and increases whole-cell sodium current (Ratcliffe et al., 2000).

Transcriptional control of the sodium channel, by intracellular and extracellular signals or changes of electrical activity, remains an essential process for long-term functional regulation. During development, the expression of sodium channel (presumably Nav1.4) in rat skeletal muscle cells peaks on day 13 and decreases to about a half by day 18, in parallel with changes in sodium channel density. The mRNA level is upregulated by electrical activity and cAMP but downregulated by cytosolic calcium level (Offord and Catterall, 1989). Glial-derived growth factor modulates the expression of Nav1.9 substantially in some dorsal root ganglion (DRG) neurons (Fjell et al., 1999). Nav1.2 and  $\beta 1$  are both drastically downregulated in tufted cells in olfactory bulb after these cells were deafferentated (Sashihara et al., 1997).

Differential mRNA expression becomes especially crucial in cells expressing multiple sodium channels, as alteration of sodium channel constitution on membrane with kinetically different sodium channels may directly change the cellular excitability. One well-studied system, the small DRG neuron, contains three TTX-sensitive (Nav1.1, Nav1.6, Nav1.7) and two TTX-resistant sodium channels (Nav1.8 and Nav1.9). Following axotomy, small DRG neurons show a five-fold decrease of TTX-resistant current density, together with downregulation of Nav1.8 and Nav1.9 expression (Dib-Hajj et al., 1996; Dib-Hajj et al., 1998). Meanwhile, they also re-gain the expression of

Nav1.3, which is expressed in embryonic DRG neurons but lost during development (Waxman et al., 1994). On the contrary, in these neurons, Nav1.8 is upregulated and Nav1.3 is downregulated in response to nerve growth factor both *in vivo* (Dib-Hajj et al., 1998; Fjell et al., 1999) and *in vitro* (Black et al., 1997).

### **$\beta$ 1 subunit of voltage-gated sodium channels**

Four  $\beta$  subunits have been identified to date (Isom et al., 1992; Isom et al., 1995; Morgan et al., 2000; Yu et al., 2003). They are homologous in sequence, structure and some of the functions. They are all type-I membrane proteins, each with a large extracellular N terminal domain containing an immunoglobulin (Ig) fold, a single transmembrane domain and a short cytoplasmic C terminus (Isom and Catterall, 1996). Among these auxiliary subunits,  $\beta$ 1 and  $\beta$ 3 share more sequence similarity and so do  $\beta$ 2 and  $\beta$ 4.

Generally, the four  $\beta$  subunits have dual functions: to modulate the kinetics of  $\alpha$  subunits and to facilitate cell-cell interaction. Many studies co-expressed one or more  $\beta$  subunits with different  $\alpha$  subunits in several different expression systems and showed very complex, sometimes different, patterns of results. Several *in vivo* studies further highlighted the importance of these  $\beta$  subunits.  $\beta$ 1 knock-out mice exhibit a series of phenotypic change including expression pattern change of  $\alpha$  subunits, spontaneous seizure, reduction and disruption of nodes of Ranvier (Chen et al., 2004). A cysteine-to-tryptophan (C121W) mutation in  $\beta$ 1 subunit disrupts the Ig fold and causes generalized epilepsy with febrile seizures plus type 1 (GEFS+1), possibly by accelerating the recovery from fast inactivation or the disruption of homophilic cell adhesion (Wallace et al., 1998;

Meadows et al., 2002). Interestingly, a mutation in the C terminus of Nav1.1 (D1866Y) also causes a similar GEFS+ phenotype. Further study revealed that the mutation disrupts the interaction between  $\beta$ 1 subunit and the C terminus of Nav1.1 (Spampanato et al., 2004). Additionally, a recent study suggests that the intracellular domain of  $\beta$ 4 may be the endogenous open-channel blocker responsible for resurgent sodium current kinetics and high-frequency firing in Purkinje neurons (Grieco et al., 2005).

Despite the structural and functional similarities, however,  $\beta$  subunits are expressed in different tissue types.  $\beta$ 1 and  $\beta$ 3 show ubiquitous expression in brain, heart, kidney, liver and adrenal gland and they exhibit a complementary expression pattern in brain regions such as olfactory cortex and basal ganglia ( $\beta$ 3 rich), thalamic nuclei ( $\beta$ 1 rich) and individual layers of the neocortex (Morgan et al., 2000). Outside the nervous system,  $\beta$ 1 is expressed in muscle and heart (Isom et al., 1992).  $\beta$ 3 is not expressed in muscle or heart but abundant in kidney and adrenal gland (Morgan et al., 2000; Qu et al., 2001).  $\beta$ 4 and  $\beta$ 2 both exhibit neuronal expression in hippocampus, cerebellum, thalamus and dorsal root ganglion, but show differences in neuron types and subcellular localization as well (Yu et al., 2003).

Part of my dissertation is focused on the  $\beta$ 1 subunit. In humans, it is encoded by a single gene with five exons located on chromosome 19 (Makita et al., 1994). It has been co-expressed with multiple sodium channel  $\alpha$  subunits (Isom et al., 1992; Makita et al., 1994; Qu et al., 1995). It forms a non-covalent association with  $\alpha$  subunits and generally increases the membrane density of  $\alpha$  subunits and speeds the inactivation of sodium current. The intracellular domain is responsible for the association with  $\alpha$  subunit (Meadows et al., 2001), while the stand-alone extracellular domain can still modulate the

kinetics of  $\alpha$  subunit in *Xenopus* oocytes, though 10,000 fold of this mutant  $\beta 1$  is required to be as effective as full-length  $\beta 1$  (McCormick et al., 1998; Meadows et al., 2001).

Furthermore, The Ig fold structure in the extracellular domain and the negative charges within are both required for the modulatory function of  $\beta 1$  (McCormick et al., 1998). All these results suggest that the intracellular domain of the  $\beta 1$  subunit associates with  $\alpha$  subunit, while the Ig fold in the extracellular domain presents the negative charges to the  $\alpha$  subunit and the electrostatic interaction may affect the inactivation of the  $\alpha$  subunit.

In addition to its modulatory function on sodium current kinetics, sodium channel  $\beta 1$  subunit also functions as a cell adhesion molecule (CAM) and interacts with various molecules. It associates with extracellular matrix molecules such as tenascin-R and tenascin-C and causes cellular aggregation when  $\beta 1$  is expressed in *Drosophila* S2 cells. This association is independent of its cytoplasmic domain (Malhotra et al., 2000).  $\beta 1$  also interacts with contactin, another extracellular surface glycoprotein, and coexpression with contactin increases the sodium current density 3-4 times (Kazarinova-Noyes et al., 2001). Inside the cell, the cytoplasmic domain of  $\beta 1$  associates with ankyrin G, which also associate with  $\alpha$  subunits in loop I-II (Malhotra et al., 2002; Lemaillet et al., 2003; McEwen et al., 2004; Mohler et al., 2004). Furthermore, both the intracellular and extracellular domains of  $\beta 1$  interact with receptor tyrosine phosphatase  $\beta$  (Ratcliffe et al., 2000).

Recent studies showed that the modulation on sodium current kinetics by the  $\beta 1$  subunit may depend on its function as CAM. When a tyrosine ( $\beta 1Y181$ ) in the cytoplasmic domain is phosphorylated or mutated to glutamate to mimic its phosphorylated state ( $\beta 1Y181E$ ),  $\beta 1$  loses the interaction with ankyrin G, weakens the

association between ankyrin and Nav1.2 and does not modulate the function of Nav1.2 (Mcewen et al., 2004).

### **Alternative mRNA splicing of ion channels**

Alternative mRNA splicing allows a single gene to generate multiple mRNA transcripts and consequently produce multiple proteins, therefore it significantly increases the proteomic diversity. In the nervous system, multiple genes including some ion channels have been found to exhibit alternative mRNA splicing. The N-type calcium channel shows differential expression of a small cassette exon in brain, sympathetic and sensory ganglion neurons (Lin et al., 1997). The cassette exon causes the presence of a fragment of only two amino acids, ET (glutamic acid and threonine), which induces slower activation kinetics of the N-type calcium channel when expressed in *Xenopus* oocytes (Lin et al., 1999). Another example is Ca<sup>2+</sup>-activated K<sup>+</sup> (BK) channel. In the hair cells of turtle and chicken inner ear, at least eight splicing sites and multiple splice variants produced by the combination of these sites generate an extremely complex splicing pattern (Navaratnam et al., 1997; Rosenblatt et al., 1997). It is proposed that the translational products of different BK channel transcripts with different kinetics may account for the electrical tuning of the cochlea (Fettiplace and Fuchs, 1999).

Additionally, BK channel also contains two STREX exons in rat adrenal chromaffin tissue and the alternative splicing of these two exons may associate with the repetitive firings (Xie and Mccobb, 1998). Some ligand-gated channels are also under the regulation of alternative splicing. A cassette exon in GABA<sub>A</sub>  $\gamma$ 2 subunit adds a PKC phosphorylation site and may modulate channel function in response to ethanol (Whiting

et al., 1990; Krishek et al., 1994). Alternatively spliced dopamine D2 receptors show differential specificities to G-proteins coupling, which in turn result in differential effects on adenylyl cyclase activity (Guiramand et al., 1995).

The molecular mechanisms of alternative mRNA splicing are very complex and are largely unclear. Studies in several well-identified systems suggest that the mechanisms commonly involve both cis-acting specific sequence in the mRNA precursor and trans-acting RNA binding proteins, which together cause changes in the assembly of spliceosome and exon definition (Black, 2003). One protein involved in several neuron- or muscle-specific splicings is polypyrimidine tract binding protein (PTB, also called hnRNP I). It regulates a variety of genes including *c-src*,  $\alpha$ -actinin,  $\alpha$ -tropomyosin, GABA<sub>A</sub>  $\gamma$ 2, clathrin light chain B and NMDA R1 (Grabowski and Black, 2001; Wagner and Garcia-Blanco, 2001). It binds on specific sequences in intron(s), usually uracil and cytosine abundant, and represses the exon definition nearby.

Alternative mRNA splicing of voltage-gated sodium channels has started to draw attention recently. The mouse has three alternative 5'-splice variants of the untranslated exon1, and two 3'-splice variants in the 3' untranslated region (UTR) of Nav1.5 (Shang and Dudley, 2005). A cryptic splice site causes a shortened exon 27 and a truncation of segments 2 and 3 of domain IV in human Nav1.5, and accounts for 20% cases of Brugada syndrome, a cardiac arrhythmia (Hong et al., 2005). Nav1.6 has four mutually exclusive 5'-untranslated exons (Drews et al., 2005). Another study (Yang et al., 2004) suggests transcriptional regulation of sodium channel, including transcription initiation and variations in the 5' and 3' UTRs, may contribute to the translational efficacy and in turn to cellular excitability.

Furthermore, two mRNA splicing variants of  $\beta 1$  subunit have been identified in rat and human (Kazen-Gillespie et al., 2000; Qin et al., 2003). One splicing variant,  $\beta 1_A$ , retains the third intron and in turn extra 55 amino acids between the Ig loop and the transmembrane domain.  $\beta 1_A$  increases the level of Nav1.2 expression on plasma membrane, like  $\beta 1$ , but modulates the kinetics in a more subtle manner (Kazen-Gillespie et al., 2000). The other splice variant,  $\beta 1_B$ , has a novel exon 3A to replace exons 3~5 and may produce a hydrophobic transmembrane C terminus. Functional studies show  $\beta 1_B$  increases sodium current of Nav1.2 without changing the kinetics (Qin et al., 2003). The mechanisms of the splicing of sodium channel  $\alpha$  and  $\beta 1$  subunits are still not known.

### **Hormonal control of ion channels**

Steroid hormones play important roles in many biological functions and behaviors in vertebrates. The classic “genomic” mechanism involves multiple steps including diffusion across plasma membrane, binding and activation of specific intracellular receptors, translocation of activated receptors, interaction with co-factors and modulation of target gene transcription. The upregulation of gene expression usually requires steroid receptors to act as transcriptional factors to facilitate the recruitment of basal transcription machinery, while on the other hand, the repression of gene expression undergoes more complex mechanisms, such as nucleosome remodeling, competition with co-activators, RNA processing, etc (Dobrzycka et al., 2003). In the past two decades, “non-genomic” mechanisms of steroids have been identified. The steroids can participate in post-translational modifications of some proteins and alter their functions, directly or indirectly *via* their membrane or cytoplasmic receptors.

The transcription and splicing of ion channel genes are subject to hormonal controls. Cortisol increases the expressions of both sodium channel  $\beta 1$  subunit and one transcript (7.0kb) of Nav1.5 but not the other (8.5kb) to about 2.5 fold each in developing sheep heart, while fetal adrenalectomy prior the natural surge of cortisol greatly reduced the expressions (Fahmi et al., 2004). Pituitary removal causes a reduction of glucocorticoids and an abrupt decrease in the proportion of BK transcripts containing a “STREX” exon in rat (Xie and Mccobb, 1998). Hormones can also affect ion channels via non-genomic mechanism. Estradiol activates BK channel in smooth muscle by binding on the extracellular domain of its  $\beta 1$  subunit (Valverde et al., 1999; Dick et al., 2002). Notably, all these tissues consist of uniformed cells thus are easily accessed and studied. Besides their own important functions, they may also lead to more understandings of molecular events in more complex organs, such as brain.

### **Electric fish and electric organ**

Electric fish are generally categorized into strongly electric fish, which use electric discharge to attack their predators and preys, and weakly electric fish, which use electric discharge to locate objects around themselves and communicate. Weakly electric fish can be further grouped into pulse-type and wave-type fish, according to the timing of discharge. In parallel, electric fish are classified to two orders, Gymnotiformes of America and Mormyriiformes of Africa. They have convergently evolved electric organs. *Sternopygus macrurus* is the most widely distributed species of Gymnotiform fish, distributed in all hydrogeographical regions of tropical south America and most lowland aquatic habitats (Hulen et al. 2005).

*Sternopygus* emit a wave-type electric organ discharges (EOD) from 50 to 200 Hz for electrolocation and intra-species communication. The EOD is produced by a well-defined circuit in *Sternopygus* (Fig. 1.1B). A midline medullary nucleus, called pacemaker nucleus, controls the EOD frequency. The pacemaker nucleus contains two groups of electrically coupled neurons: pacemaker neurons and relay neurons. Pacemaker neurons initiate the rhythmic firings and drive the relay neurons. Relay neurons send axons out of the nucleus and synapse on electromotor neurons in spinal cord, which further synapse, through acetylcholine receptors, on electrocytes in the electric organ located in the tail of *Sternopygus*. Electrocytes are cells with polarized membranes. The posterior end of the membrane has acetylcholine receptors and all the voltage-gated channels, while the anterior end has no voltage-dependent channels but Na<sup>+</sup>-K<sup>+</sup> ATPase. When an electrocyte fires an action potential, the posterior end depolarizes but the anterior end remains at resting potential, thus generating a net potential along the electrocytes. Stacks of electrocytes are ensheathed in electrically resistive connective tissue and produce EOD of ~1 volt.

Developmentally and evolutionally, the electric organ in *Sternopygus* derives from muscle. However, these two tissues types differ significantly in both function and gene expression. Immunohistochemical studies showed that the electric organ does not express tropomyosin or myosin heavy chain, but expresses keratin, a protein not found in the muscle (Patterson and Zakon, 1996). On the other hand, electric organ also lacks sarcomeres or contractile function upon synaptic stimulation. Experimental manipulations can change these two phenotypes between one another. Amputation of the tip of fish tail induces the regeneration of the electric organ, arising from satellite cells

and going through certain stages with expression and then loss of typical muscular proteins (such as myosin heavy chain). Denervation of the electric organ partially reverts the phenotype back to muscle fiber, by re-expression of myosin and tropomyosin and the appearance of small sacromere clusters (Unguez and Zakon, 1998).

### **Electric organ discharge**

The EOD frequency of *Sternopygus*, set by pacemaker neurons, is individually unique, sexually dimorphic and under hormonal control (Zakon and Unguez, 1999). In response to different EOD frequencies, electrocytes produce action potentials with different shapes. In *Sternopygus*, the EOD frequency ranges from 30 Hz to 200 Hz with pulse durations that range from 3 msec to 12 msec (Mills and Zakon, 1991). Male fish tend to have lower EOD frequencies and longer pulse durations than female fish (Fig. 1.1C). The sexual dimorphism is believed to be important for gender recognition and as a component of the reproductive behaviors of this species (Hopkins, 1974).

Previous research has identified the ionic currents in electrocytes, including a TTX-sensitive sodium current, two potassium currents (an inward rectifier and a classical delayed rectifier), a large, presumably voltage-insensitive chloride current but no calcium current (Ferrari and Zakon, 1993). The sodium current activates at about -45mV, peaks at 5-10mV and reverses at about 50mV. The decay of the sodium current can be fit with a single exponential term, but includes a non-inactivating component at very depolarized potentials (Ferrari and Zakon, 1993). Furthermore, the inactivation kinetics of sodium current in electrocytes correlates with individual EOD frequency (Ferrari et al., 1995; Mcanelly and Zakon, 2000). The fast inactivation time constant of the peak sodium

current varies from 0.5 to 4.7 msec and systematically correlates with the EOD frequency (Fig. 1.1C). From low EOD frequency fish to high EOD frequency fish, a trend of negative shift in the voltage dependence of steady-state inactivation was also observed. The fine modulation of the sodium current kinetics is essential for the important behavior. However, the molecular sources of this variation and the regulation mechanisms remained unclear.

One hypothesis is that the sodium channels in the electric organs with different EOD frequencies are phosphorylated to different levels, since phosphorylation has been known to modulate sodium channel kinetics. However, the application of 8 bromo cyclic AMP, a membrane-permeant cAMP analog, on electrocytes only increased the sodium current magnitude but did not change the inactivation kinetics, suggesting that at least the PKA pathway is not involved in the regulation (Mcanelly and Zakon, 1996). Another hypothesis is that differential expression of sodium channel subunits or mRNA splice variants contribute to the regulation. This dissertation focuses on this hypothesis and reveals multiple levels of controls by a fairly complex mechanism.

### **Androgen modulates EOD and sodium current inactivation kinetics**

Previous studies showed chronic treatment with 5 $\alpha$ -dihydrotestosterone (DHT) lowered the EOD frequency and increased action potential duration in electrocytes (Mills and Zakon, 1991; Ferrari et al., 1995). Furthermore, the inactivation time constant of sodium currents was also significantly slower in DHT-implanted fish (Ferrari et al., 1995). The sodium current kinetics change in electrocytes seems independent of the change of EOD frequency by DHT treatment, since local implants of small doses of DHT

in electric organ had no effect on EOD frequency, but broadened EOD pulse duration (Few and Zakon, 2001).

### **Summary of this dissertation**

In this study, I cloned the full-length sequences of two Nav1.4 orthologs in *Sternopygus*, smNav1.4a and smNav1.4b (originally named Na6 and Na1), previously identified in the electric organ of *Sternopygus macrurus* (Lopreato et al., 2001). 5' rapid amplification of cDNA end (RACE) revealed two transcript forms of smNav1.4b, smNav1.4bL and smNav1.4bS, caused by alternative first exons (1L and 1S). A unique characteristic of this finding is that exon 1L contains a start codon while exon 1S does not, thus smNav1.4bL contains an extended N-terminal segment, which includes a predicted helical structure with multiple positively charged residues. Expression of smNav1.4bL and smNav1.4S in *Xenopus* oocytes showed this extended N terminal segment speeds the inactivation and negatively shifts the voltage dependence of inactivation. Using site-directed mutagenesis, I deleted a proline next to the helix to disorient the helix and found the effect of this segment on inactivation time constant was abolished and the effect on voltage dependence was partially reversed. This is the first evidence that the N terminus of sodium channel plays a role in channel function.

In addition, the identical pattern of alternative first exons is also seen in the zebrafish (*Danio rerio*) but not in rat (*Rattus norvegicus*), although a novel splice form of rNav1.4 was identified by 5'RACE as well.

In this study, I took advantage of two unique characteristics of this model system to study the correlation between gene expression and cellular excitability. First, the electric organ in *Sternopygus* contains a large number of cells with similar cellular excitability allowing me to harvest ample tissue with a uniform cellular phenotype from a single individual (Ferrari and Zakon, 1989; Ferrari et al., 1995). Secondly, in this species there is a strong correlation between a behavioral parameter set by the brain — EOD frequency— and sodium current kinetics in electrocytes (Ferrari et al., 1995), allowing me to bypass electrophysiological measurements, to maximize the RNA yield for multiple studies and directly correlate levels of gene expression with easily obtained EOD frequency.

In the electric organ of *Sternopygus*, smNav1.4a and smNav1.4b are expressed at comparable levels. However, in contrast to the comparable abundance of smNav1.4bL and smNav1.4bS in muscle, electric organ preferentially expresses smNav1.4bL than smNav1.4bS, suggesting the existence of tissue-specific transcriptional regulation on smNav1.4b gene. Furthermore, using quantitative real-time RT-PCR, I found the mRNA level of smNav1.4b, especially smNav1.4bL, correlated with individual EOD frequency, but smNav1.4bS and smNav1.4a did not.

The second half of my dissertation focuses on the sodium channel  $\beta 1$  subunit. I cloned this gene from *Sternopygus* and further identified two mRNA splicing variants: one ( $\beta 1L$ ) containing four exons and similar to mammalian  $\beta 1$ , and one novel transcript ( $\beta 1S$ ) lacking the third exon therefore translated to a different and shorter C terminus. The two splicing variants exhibit distinct pattern of differential expression in different tissue types.

In the electric organ, the mRNA levels of  $\beta 1$ , especially  $\beta 1S$ , and the splicing preference for  $\beta 1S$  correlate with the EOD frequency, but the mRNA level of  $\beta 1L$  does not.

In addition, we co-expressed either of the two splice forms of  $\beta 1$  with hNav1.4, smNav1.4bL, smNav1.4bS in *Xenopus* oocytes. Both splice forms of  $\beta 1$  drastically sped the rates of inactivation of the  $\alpha$  subunits, negatively shifted the inactivation voltage dependence of smNav1.4bS but not smNav1.4bL, and had no effect on activation voltage dependence of the  $\alpha$  subunits. In the region different in two  $\beta 1$  subunits, a tyrosine has been shown to interact with ankyrin G and affect the modulation on  $\alpha$  subunits (Malhotra et al., 2002; Mcewen et al., 2004). The tyrosine is conserved in  $\beta 1L$  but replaced by a threonine in  $\beta 1S$ . In order to examine if the subtle functional difference between the two  $\beta 1$  subunits is due to this change, I generated a mutant  $\beta 1ST181Y$ , and observed weakened functions, suggesting the threonine is not a mutation but instead better fit with the cytoplasmic domain of  $\beta 1S$  for its functions.

DHT can lower the EOD frequency and slow down the inactivation kinetics, as shown in previous studies (Mills and Zakon, 1991; Ferrari et al., 1995; Few and Zakon, 2001). In this study, DHT implants lowered the EOD frequency and also the mRNA levels of smNav1.4b (both smNav1.4bL and smNav1.4bS), but not smNav1.4a. Total  $\beta 1$  mRNA level, but not the splicing of  $\beta 1$ , is also lowered by DHT.

In conclusion, the results suggest that, in *Sternopygus*, multiple levels of mRNA control including expression abundance, alternative mRNA splicing and tissue-specific transcription initiation of sodium channel  $\alpha$  and  $\beta 1$  subunits may all contribute to the individual variation in cellular excitability. Hormones, such as DHT, may play important

roles to realize these controls. In addition, the discoveries of novel  $\alpha$  and  $\beta 1$  subunits and their extraordinary functions may lead to more understanding of the structure and function of sodium channels.

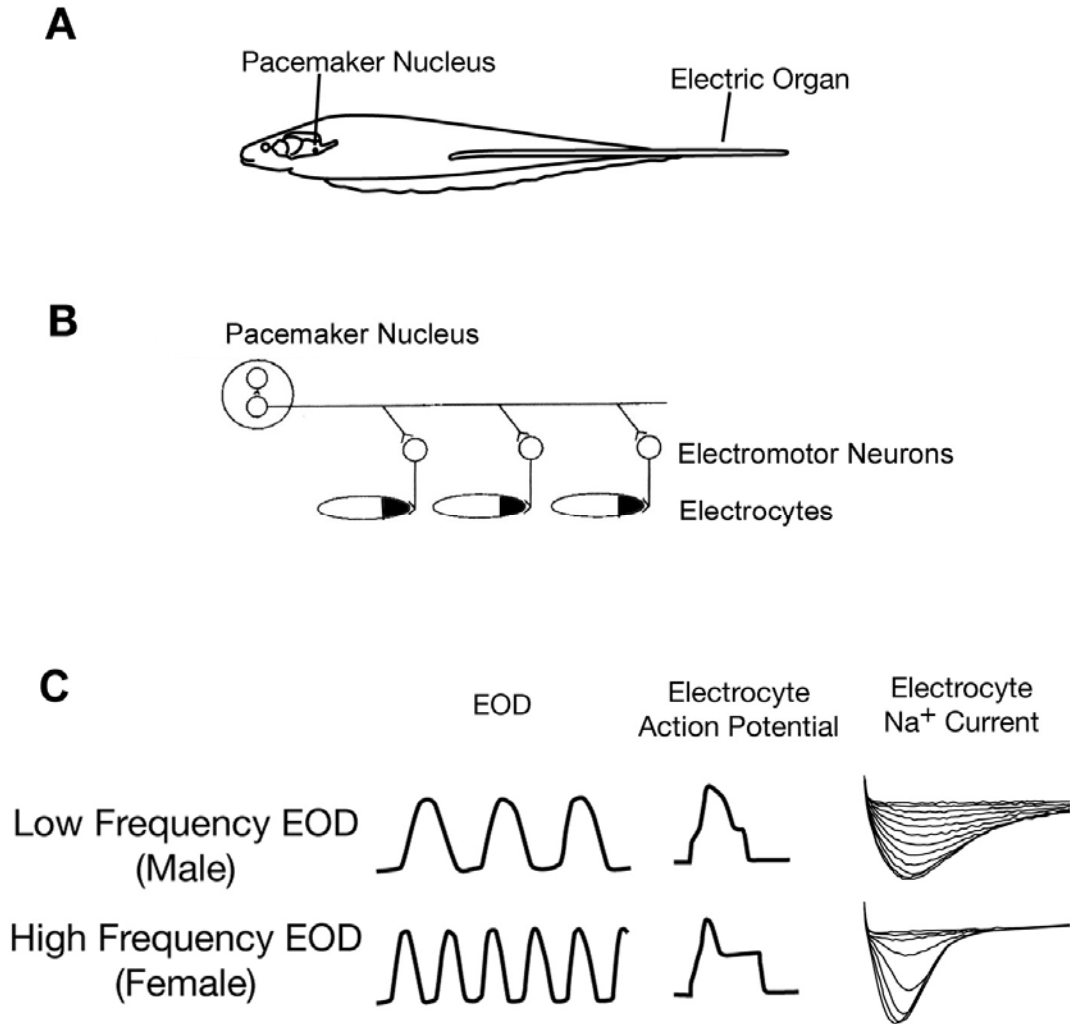


Figure 1.1. Relationship between the EOD and sodium current inactivation kinetics. (A) EOD frequency is determined by the firing rate of pacemaker neurons in the pacemaker nucleus. The ~50 pacemaker neurons are electrotonically coupled and fire simultaneously. Each action potential travels down to spinal motorneurons (not depicted) and these innervate the electrocytes, the cells of the electric organ. There is a 1:1 relationship between firing rate of the pacemaker neurons and EOD frequency as each descending action potential initiates a pulse from the electric organ. (B) The circuit to generate EOD. In the pacemaker nucleus located in ventral medulla, pacemaker neurons (upper) set the EOD frequency and couple with relay neurons (lower), then relay neurons synapsed on spinal electromotor neurons, which further synapse on the posterior end (filled) of electrocytes in the electric organ. (C) Each pulse of the EOD is determined by the membrane properties of the electrocytes. Males generate low frequency EODs with long duration pulses (left). The long pulses result from long duration action potentials (note stylized action potential riding on current injection, center), whose duration is partly determined by the rate of inactivation of the sodium current (right). Figure adapted from McAnelly and Zakon, 1996 and Ferrari et al., 1995.

---

## CHAPTER 2

### Regulation of sodium channel $\alpha$ subunit expression underlies cellular excitability of electrocytes

---

#### Abstract

The electric fish *Sternopygus macrurus* emits an electric organ discharge (EOD) composed of a series of pulses. Males emit long pulses at low frequencies, females emit short pulses at higher frequencies, and juveniles emit at intermediate values. Furthermore, EOD frequency and pulse duration are regulated by androgens. The EOD pulse is shaped by a sodium current whose rate of inactivation correlates with EOD frequency and pulse duration, and is modulated by androgens. In this study, I first cloned full-length sequences of the two sodium channel  $\alpha$  subunits expressed in the electric organ of *Sternopygus*, smNav1.4a and smNav1.4b. I also identified two smNav1.4b mRNA transcripts with alternative first exons. One exon, 1L, contains a start codon thus will translate into a longer protein, while the other, 1S, does not. Electric organ expresses smNav1.4a and smNav1.4b at comparable levels and preferentially express the smNav1.4b transcript containing exon 1L (smNav1.4bL). In the electric organ the mRNA level of smNav1.4bL correlates with EOD frequency, but the mRNA level of smNav1.4a does not. Androgen implants lowered smNav1.4bL mRNA levels but did not affect smNav1.4a. Expression of each splice form in *Xenopus* oocytes showed smNav1.4b, especially smNav1.4bL, has extraordinary properties of sodium current inactivation,

compared to smNav1.4bS and its human ortholog, hNav1.4. Deletion of a proline in the extended N terminal segment of smNav1.4bL partially eliminated the differences between smNav1.4bL and smNav1.4bS. These data suggest that the expressions of specific sodium channel  $\alpha$  subunits contribute to the cellular excitability of electrocytes in *Sternopygus*.

## Introduction

Weakly electric fish *Sternopygus macrurus* emit electric discharges for electrolocation and communication. The electric organ discharge (EOD) is generated by the electric organ, a novel organ that is evolutionally and developmentally differentiated from skeletal muscle (Zakon and Unguez, 1999). The EOD frequency of *Sternopygus*, set by the pacemaker nucleus in brain, is individually unique, sexually dimorphic, and under hormonal control (Zakon and Unguez, 1999). Previous research has shown that the kinetic parameters of sodium current inactivation in the electrocytes are correlated with EOD frequency and can be modulated by long-term androgen treatment (Ferrari et al., 1995; Mcanelly and Zakon, 2000). However, the molecular mechanisms of this variation are not known.

Three possible mechanisms for the variation of sodium current kinetics were hypothesized (Ferrari et al., 1995):

- 1) Different levels of phosphorylation of sodium channels by kinases.
- 2) Different expression of different sodium channel genes.
- 3) Regulation by auxiliary subunits such as sodium channel  $\beta$ 1 subunits.

Additional studies in the lab have shown that PKA activation increases sodium current magnitude without changing its inactivation parameters in the electric organ (McAnelly, 1996), and a treatment for a longer time (60min vs. 20min) causes a slight increase (~25%) of the EOD and electrocyte action potential duration (Mcanelly et al., 2003). Compared to the natural variation range of EOD durations (3 msec to 12 msec), the contribution of PKA to the sodium current kinetics seems minor. My dissertation focuses on the other two hypotheses and studies the expression pattern of multiple

sodium channel subunit and its regulation on the molecular level. This chapter addresses sodium channel  $\alpha$  subunits in the electric organ and Chapter 3 focuses on the  $\beta 1$  subunit of sodium channel.

In this study, I cloned the full-length sequences of two Nav1.4 orthologs, smNav1.4a and smNav1.4b (originally named Na6 and Na1), previously identified in the electric organ of *Sternopygus* (Lopreato et al., 2001). 5' rapid amplification of cDNA end (RACE) revealed two transcript forms of smNav1.4b, smNav1.4bL and smNav1.4bS, caused by alternative first exons (1L and 1S). A unique characteristic of this finding is that exon 1L contains a start codon while exon 1S does not, thus smNav1.4bL contains an extended N-terminal segment, which includes a predicted helical structure with multiple positively charged residues. Comparison between the kinetics of smNav1.4bL and smNav1.4S shows this segment greatly changes the channel kinetics, making Nav1.4bL a channel with distinctively faster inactivation and more negative voltage dependence. Deletion of a proline in this segment altered the kinetics of smNav1.4bL, towards the levels of smNav1.4bS.

Additionally, the identical pattern of alternative first exons is also seen in the zebrafish (*Danio rerio*) but not in rat (*Rattus norvegicus*), although a novel splice form of rNav1.4 was identified by 5'RACE as well.

In *Sternopygus*, electric organ expresses Nav1.4a and Nav1.4b at comparable levels. Between the two transcripts of smNav1.4b, electric organ preferentially expresses Nav1.4bL, but muscle expresses them both in comparable abundance, suggesting the existence of tissue-specific transcriptional regulation. Furthermore, using quantitative real-time RT-PCR, I found the mRNA level of Nav1.4b, especially Nav1.4bL – a channel

with fast inactivation kinetics, correlates with individual EOD frequency – a behavioral parameter set by the brain pacemaker and highly correlated with sodium current kinetics in electrocytes. On the other hand, the expression level of Nav1.4bS and Nav1.4a do not correlate with EOD frequency.

DHT can lower the EOD frequency and slow down the inactivation kinetics, as shown in previous studies (Mills and Zakon, 1991; Ferrari et al., 1995; Few and Zakon, 2001). In this study, DHT implants lowered the EOD frequency and also the mRNA levels of Nav1.4b (both Nav1.4bL and Nav1.4bS), but not Nav1.4a. These results suggest multiple levels of transcriptional control on sodium channel  $\alpha$  subunits underlie the regulation of cellular excitability of electrocytes in *Sternopygus*.

## **Materials and Methods**

### **Experimental Animals**

Gold-lined black knifefish (*Sternopygus macrurus*) were housed in aquaria in the laboratory at ~25°C and on a 12:12 light/dark cycle. All fish used in this study were sexually immature adults of both sexes. Fish were fed earthworms every other day. EOD frequencies of a fish was measured by immersing bipolar electrodes next to it in the tank, and sending its amplified (Grass P-15, Grass Corp., Quincey, MA) EOD to a multimeter (Fluke, Everett, WA) on frequency counter setting.

For harvesting electric organs only, each fish was removed from its aquarium, placed on a countertop in a net, and its tail was rapidly cut with scissors. The fish was immediately returned to its aquarium to recover. Recovery rate was 100%. When multiple tissues were taken, fish were euthanized with 1.0% phenoxyethanol, and brains,

muscle, and heart were removed.

Zebrafish (*Danio rerio*) were obtained from a local vendor and temporarily housed in the laboratory aquaria. Tissues (brain, muscle and heart) were taken after fish were euthanized with 1.0% phenoxyethanol.

Rat leg muscle was obtained from the laboratory of Dr. Hitoshi Morikawa at the University of Texas at Austin.

These procedures were in accordance with the University of Texas IACUC protocols.

### **RNA and DNA Isolation**

Tissues either freshly dissected or stored frozen at -80 °C were used for RNA isolation. Total RNA was extracted with RNA-STAT60 (TEL-TEST, Friendwood, TX) according to the manufacture's instructions. RNA samples were treated with DNase I (2U/50ul) for 30 min at 37°C, phenol-chloroform extracted and precipitated with 75% ethanol. The RNA quality was examined by Agilent Bioanalyzer 2100 (Agilent, Wilmington, DE) to ensure no DNA contamination or RNA degradation.

Genomic DNA was isolated as previously described (Lopreato et al., 2001).

### **RT-PCR, PCR and Cloning PCR products**

All Reverse Transcription Polymerase Chain Reactions (RT-PCRs) were carried out with the One-step RT-PCR kit (Qiagen, Valencia, CA) unless otherwise specified. Reaction mixture contained 0.4mM each dNTP, 1x buffer supplied with the kit, 1.2µM each primer, 50ng to 500ng total RNA and 1µl enzyme mix in every 25µl reaction.

Reactions were incubated at 50 °C for 30 min for reverse transcription and then heated at 95 °C for 10 min to inactivate reverse transcriptase and activate Taq polymerase. PCR reactions were usually run 40 cycles with denaturing at 95 °C for 30 sec, annealing at 53 °C for 30 sec and extension at 72 °C for one min per kilobasepair (kb).

PCR reactions with DNA templates were carried out with TAKARA Taq DNA polymerase (TAKARA, Shiga, Japan). Reactions mixture contained 0.4mM each dNTP, 10mM Tris-Cl, 50mM KCl, 1.5mM MgCl<sub>2</sub>, 1.2μM each primer. Thermocycler setting was the same as the PCR part of RT-PCR.

All PCR products were examined with electrophoresis in 0.8~3% agarose gel according to product length. Bands of interest were excised and PCR products were extracted with Gel Extraction Kit (Qiagen) and ligated into pCR2.1-TOPO, pCRII-TOPO or pCRXL-TOPO vectors (Invitrogen, Carlsbad, CA) according to their lengths. Ligation products were transformed with TOP10 competent cells (Invitrogen). *E.Coli* colonies were grown in LB medium or terrific broth for 16~18 hrs. Plasmid DNA was isolated with Qiagen Miniprep Kit (Qiagen), and further sequenced by the sequencing facility lab at the University of Texas at Austin. All sequences were analyzed with MacVector Software (Genetics Computer Group, San Diego, CA).

### **3' and 5' Rapid Amplification of cDNA Ends (RACE)**

In 3' RACE, total RNA as template and an anchor-T primer (see Table 2.1) were first used in a reverse transcription reaction with Superscript II reverse transcriptase (Invitrogen) at 42 °C for 1hr to produce non-specific cDNAs from mRNA molecules. Then two gene-specific forward primers 3RP1 and 3RP2 in a nested pattern and an

anchor reverse primer were used in two consecutive PCR reactions to selectively amplify the target sequence. The most prominent products were cloned.

Table 2.1 Primers Used in 3' RACE of sodium channels

Gene	Primer Name	Primer Sequence
smNav1.4a	3RP1	TAAAGTTTCTTGTAATAAGTTTTTGTC
	3RP2	CCCTCAAATTATGCCCTAAGTG
smNav1.4b	3RP1	AGGTTGGGATGGACTTCTAGGTCCTATG
	3RP2	AACATTTGTGAAGGGTGATTGTGGGAAC
Both	Anchor-T	GACCACGCGTATCGACTTTTTTTTTTTTTTTTTTV
	Anchor	GACCACGCGTATCGAC

5' RACE was carried out with FirstChoice RLM-RACE kit (Ambion, Austin, TX). 10µg total RNA was treated with calf intestine alkaline phosphatase (CIP) to remove free 5'-phosphates from nucleic acid molecules except Guanosine cap protected intact mRNA. Then tobacco acid pyrophosphatase (TAP) was used to remove the cap before a 45nt RNA adapter provided by the kit was ligated to the 5' ends of mRNA molecules by T4 RNA ligase. Reverse transcription was performed with M-MLV reverse transcriptase and random decamers. Two PCR reactions in a nested pattern were then performed with gene-specific reverse primers 5RP1, 5RP2 specifically designed for each species (Table 2.2), and outer and inner forward primers targeted at the 5'RACE adapter. Products of nested PCR were cloned and sequenced. The sequence immediately after the ligated RNA adaptor is considered the starting site of the mRNA transcript.

Table 2.2 Primers Used in 5' RACE of sodium channels

Species	Gene	Primer	Primer Sequence
<i>Sternopygus</i>	Nav1.4a	5RP1	TTCCTTCTCCCTGTTCCGCAGCTCGGTA
		5RP2	GGAACACATCGGGGCCTGGCGGAGAGAC
<i>Sternopygus</i>	Nav1.4b	5RP1	TGATGAGAGCAGAGCAGAGGTGTG
		5RP2	TCCTGTAGCAGTAGACCATCTCCAC
<i>Danio rerio</i>	Nav1.4b	5RP1	ACTCAGACAGTAACAGGCTGGTTCA
		5RP2	GTCTCCATAGATAAACGGCAGGACT
<i>Rattus norvegicus</i>	Nav1.4	5RP1	AGCCACCCTCCTGACGATGCTGAA
		5RP2	CAGGCGTGGCAGAGAATCGGAAGA

### Cloning intron and promoter sequences of smNav1.4b

Forward and reverse primers were designed in exon 1S and exon 2 respectively. PCR reactions were performed with genomic DNA. The intron sequence was identified by the removal of the 5' and 3' sequences overlapping with the two adjacent exons.

To identify the proximal promoter sequence, 5' RAGE (rapid amplification of genomic ends) was performed with the method previously described (Liu and Baird, 2001). 20 µg genomic DNA was partially digested with 0.5 unit *Nla III* (New England Biolabs, Boston, MA) in a 50 µl reaction at 37°C for 1hr, then heated at 85°C for 30min to inactivate the enzyme. Fragments larger than 2 kb were isolated by agarose gel electrophoresis and further purified with Qiagen Gel Extraction Kit (Qiagen). Purified fragments were poly-cytosine tailed with terminal transferase (New England Biolabs).

Then two rounds of PCR were performed in a similar manner to 3' RACE, but in the opposite direction.

### **Semi-Quantitative RT-PCR**

To examine the relative abundance of smNav1.4a and smNav1.4b in electric organ, one-step RT-PCR reactions were set up with 100ng total RNA isolated from three pooled fish and primers designed to amplify a region of the loop II-III in both genes (forward primer TCATMTTCCTGGGCTCCTTCTACCT and reverse primer TCCA KGGKGCACAGCAGTYCCACTT). Due to the different lengths of the amplicons, smNav1.4a and smNav1.4b generated two products with sizes of 519 and 450bp respectively. Reactions were stopped after every third cycle between 24 and 39 cycles. RT-PCR products were analyzed on a 2% agarose gel.

To examine the relative abundance of smNav1.4bL and smNav1.4bS, 90ng total RNA isolated from pooled (3 medium EOD frequency fish) electric organ and muscle was used in 20µl One-step RT-PCR reactions containing primers designed specifically for either exon (Table 2.3) were used to amplify exon 1L and exon 1S. Reactions were stopped after 24, 27, 30 and 33 cycles, analyzed on a 1.5% agarose gel and photographed for 2 seconds with UV light.

### **Immunoprecipitation and Western Blot**

A polyclonal rabbit antibody (Na1-NT) was generated by Sigma-Genosys (The Woodlands, TX) against the peptide NRTAHVKKSEKLLKLW. The antisera were affinity-purified for higher specificity.

Electric organ, brain and muscle from four *Sternopygus* were quickly dissected, pooled and homogenized in ice-cold lysis buffer (50 mM Tris-Cl, pH 8.0; 150mM NaCl; 10 mM EDTA; 1% Triton X-100) freshly mixed with protease inhibitors (Roche, Indianapolis, IN). Cell lysates were incubated for 2 hr, and centrifuged at 10,000 xg for 10 min to remove the insoluble fraction. Cell lysate containing 1mg solublized protein was cleared with 100µl protein A-agarose (Upstate, Lake Placid, NY) then mixed with 5µg affinity-purified Na1-NT antibody and incubated overnight. 50µl protein A-agarose was added again, incubated for 2 hours, collected by 1min centrifugation, washed 3 times with ice-cold lysis buffer and finally resuspended in 50ul 2X Laemmli sample buffer. All incubation and centrifugation steps were carried out at 4°C. Immunoprecipitated samples were boiled for 5 minutes before loaded on a 7.5% SDS-PAGE gel (Bio-Rad, Hercules, CA).

The protein in SDS-PAGE gel was transferred onto nitrocellulose membrane (Bio-Rad) overnight with a constant 20mA current in a transfer buffer containing 20% methanol. The membrane was blocked with T-TBS blocking buffer (Pierce, Rockford, IL) and blotted with 1:1000 dilution of pan-Na channel antibody (Upstate) at 4°C for 12 hours. The membrane was rinsed with TBS containing 0.05% Tween 20 and incubated with HRP-conjugated goat anti-rabbit IgG 1:20000 (Bio-Rad) at room temperature for 2 hours. After TBS rinse twice, the membrane was incubated with SuperSignal West Pico Chemiluminescent Substrate (Pierce) and exposed to CL-XPosure film (Pierce).

### **Differential Display RT-PCR**

Total RNA was isolated from 6 *Sternopygus* (3 males, 3 females) and reverse transcribed with an anchor-polyT primer. PCR reactions were set up with  $\alpha$ -[P<sup>33</sup>]-dATP and run in 6% denaturing polyacrylamide gel. The gel was dried and exposed to Kodak Omat-XAR film for 2 days. Differentially amplified bands were excised, extracted with boiling water and re-amplified with the same set of PCR primers. All other conditions followed the instruction of RNAimage kit (GenHunter, Nashville, TN).

The primers used to show differential expression of myosin light chain were H-AP25 AAGCTTTCCTGGA and H-T<sub>11</sub>G AAGCTTTTTTTTTTTG, both included in the RNAimage kit.

### **Real-time Quantitative RT-PCR**

Total RNA samples were extracted from 16 fish as described above. The RNA quality was examined with Agilent Bioanalyzer 2100 (Agilent, Wilmington, DE) to ensure no DNA contamination or RNA degradation. RT-PCRs with myosin light chain primers were performed to confirm minimal contamination from muscle tissue. RNA from 12 fish was eventually used in the real-time quantitative RT-PCR.

Primer/probe sets were determined by Primer Express software (Applied Biosystems, Foster City, CA), with criteria set by the program (amplicon <150bp, primer T<sub>m</sub> 59~60°C, probe T<sub>m</sub> ≥ 68°C, see Table 2.3). TaqMan® One-Step RT-PCR Master Mix Reagents Kit (Applied Biosystems) or Brilliant SYBR Green QRT-PCR Master Mix Kit (Stratagene, Cedar Creek, TX) were used for detection. All reactions were tested in triplets. Standard curves were produced by linear correlation of Ct values of 0.5x, 1x, 2x

4x or 0.50x, 0.70x, 1x, 1.41x, 2x. Each gene was examined for 2 to 4 times and repeated reactions can usually produce results with  $R > 0.90$ . 18S rRNA showed strong correlation ( $R = 0.87$ ,  $p < 0.002$ ) to total RNA measured by a spectrometer thus was used as the calibrator gene. The primer/probe set for 18S rRNA was supplied by TaqMan® Ribosomal RNA Control Reagents (Applied Biosystems). All values are presented as mean  $\pm$  S.E.M. Statistical significance was assessed using the Student's two-sample, two-tailed, independent t-test.

Table 2.3 TaqMan PCR Primer/probe Sets and SYBR Green PCR Primers Used in Real-time Quantitative RT-PCR

Transcript	Amplicon	Sequence	T <sub>m</sub>	
Nav1.4b(both)	70bp	Forward	AGAGAACGACCATGGAGACTTCA	59°C
		Reverse	GCTCTTCCCCTGAGTCCATGT	59°C
		Probe	CAGCAATGATCTTGTCATGA	69°C
Nav1.4a	72bp	Forward	G TTCAGTGGACTACGAGCTTCTACAA	59°C
		Reverse	TCTGGATCAACAGGCTCTTCCT	59°C
		Probe	TGTGAGGAAGAGGAGGAA	68°C
Nav1.4bS	183bp	Forward	GCCCAGGACTTAGACGAAAAGTAAC	57°C
		Reverse	GGCGTGAAGCGGCGGAAAACATC	63°C
Nav1.4bL	182bp	Forward	CTGGAGGTATGGCAGAGGAATCGTA	60°C
		Reverse	GGCGTGAAGCGGCGGAAAACATC	63°C

## **DHT treatment**

DHT was sealed in silicon capsules and implanted in the abdominal cavity. The EOD frequency of each fish was monitored every other day after the implant. Eighteen days after the implant, the tails of these fish were removed for RNA isolation, and fish were bled to determine the plasma concentration levels of DHT. Plasma was analyzed at the Endocrine Core Laboratory of the Yerkes National Primate Center (Atlanta, GA) using a commercially prepared kit (Diagnostics Systems Laboratory, Webster, TX) calibrated for *Sternopygus* plasma. The plasma DHT level of the DHT-implant group was significantly higher than that of the control group (DHT-implant: 9.8 +/-2.7 ng/ml; control: 0.52 +/- 0.50 ng/ml;  $p < 0.0001$ ).

## **Plasmid Construction of Nav1.4bL, Nav1.4bS full-length sequences**

To construct the plasmid containing the full-length sequence of smNav1.4bL, two-step RT-PCR was used to clone the two parts of this gene (98 to 3171 and 2570 to 5622 respectively) in pCRXL-TOPO vector. The two plasmids were digested with *KpnI* and *XbaI* and cross-ligated to construct a plasmid containing the full-length cDNA of smNav1.4bL in pCRXL vector, thus named smNav1.4bL-pCRXL.

pGEMHE vector (Liman et al., 1992) was used to add  $\beta$ -globin 5' and 3' UTRs to the two sides of this gene for higher translation efficacy in oocytes. For plasmid linearization in *in vitro* transcription procedure, the multi-cloning sites of pCR2.1 containing a *SpeI* site was inserted to the *NheI* site of pGEMHE vector. The modified plasmid was named pNHE (for sequence and digestion map, see Appendix 6). The full-length sequence of smNav1.4bL was cut from pCRXL and ligated into pNHE vector thus

named smNav1.4bL-pNHE.

The plasmid containing smNav1.4bS was constructed by the removal of the first start codon in the insert of smNav1.4bL-pNHE, as it shares the same ORF and therefore is translated into the same protein as smNav1.4bS. The sequence immediately after the first start codon (156bp) to 1791bp was amplified by a PCR reaction with a forward primer containing an *XmaI* site (CCCGGG) 5' overhang and further cloned in pCR2.1 TOPO vector. The plasmid insert was cut with *XmaI* and *EcoRV* and used to replace the corresponding sequence in Nav1.4bL-pNHE, to produce smNav1.4bS-pNHEKO (the 5' *EcoRI* site of the insert is knocked out by *XmaI* for detection of the successful replacement). Desired plasmid was screened by *EcoRI* digestion, which only linearized target plasmid, but cut twice on the original plasmid. The whole insert of selected plasmid was sequenced to ensure no mutation was induced in the insert during the procedure.

The human Nav1.4 plasmid cDNA in pSP64T was kindly provided by R.A.Harris (University of Texas at Austin, Austin, TX).

### **Site-directed Mutagenesis**

Similar to the construction of Nav1.4bS-pNHEKO, the sequence 110-1791 of the insert of smNav1.4bL-pNHE was amplified by a PCR reaction with a forward primer with an *Xma I* overhang CCCGGGCAGACATGCCCAAGCAAAAGATCAC and a reverse primer CTTTCCTGTTGTGTGGGTGGGGCTCTT. The PCR product was cloned in pCRXL-TOPO vector and sequenced to confirm the absence of mutation by PCR errors.

Site-directed mutagenesis was carried out with QuikChange XL Mutagenesis Kit (Stratagene, La Jolla, CA). Two primers with a proline codon deletion (primer1 CAGAAAACTCAAACCTATGGCATCAGGTGGAGCGGCTG and primer2 CAGCCGCTCCACCTGATGCCATAGTTTGAGTTTTTCTG) were used with 10ng the plasmid containing *XmaI*- smNav1.4b (110-1791) and *Pfu* DNA polymerase to amplify 18 cycles. The product was treated with *Dpn I* to remove the methylated parental DNA template and transformed into XL10-Gold Ultracompetent cells supplied with the kit. Plasmid DNAs from *E. Coli* colonies were sequenced to ensure the plasmid insert contains only the desired mutation.

The plasmid containing *XmaI*-smNav1.4bL (110-1791)-Proline deletion and plasmid smNav1.4bL-pNHE sequence was digested with *XmaI* (cut before the insert) and *EcoRV* (cut at 1687 of smNav1.4bL) and cross-ligated. Desired plasmid was screened by digestion with *EcoRI* , which only linearized target plasmid, but cut twice on the original plasmid). The whole insert of selected plasmid was sequenced to ensure no other mutation except the proline deletion. The plasmid was named smNav1.4bL-Pdel-pNHEKO.

### **Expression of Nav1.4 genes in *Xenopus* oocytes**

All plasmids constructed in this study were linearized by *SpeI*.

Linearized plasmids were used as templates to synthesize cRNA using T7 mMessage mMachine *in vitro* transcription kit (Ambion). The phenol-chloroform extracted and ethanol precipitated cRNA was examined with Bioanalyzer 2100 (Angilent) to confirm the proper length.

Oocytes were removed surgically from female *Xenopus laevis* frogs (Ann Arbor, MI) and digested with collagenase (type 1A, Sigma, St. Louis, MO) to remove the follicle membrane. Oocytes were injected with 20ng/40nl human or fish Nav1.4 cRNA to produce 1 to 5 uA sodium currents. Injected oocytes were maintained in modified Broth's solution (88mM NaCl, 1mM KCl, 2.4mM NaHCO<sub>3</sub>, 0.82mM MgSO<sub>4</sub>, 0.91mM CaCl<sub>2</sub>, 0.33mM Ca(NO<sub>3</sub>)<sub>2</sub>, 10mM HEPES, 220 mg pyruvate and 5 mg streptomycin) for 2–3 days.

Electrophysiological experiments were carried out in frog Ringer's solution (115 mM NaCl, 2.5mM KCl, 1.8mM CaCl<sub>2</sub>, 10mM HEPES) at 20–22 °C, 2–3 days post-injection. Electrodes were filled with 3 M KCl solution and had resistances of 0.5 and 1.0 MΩ. Macroscopic sodium currents in oocytes were measured in the two-electrode voltage clamp using oocyte clamp OC725B amplifier (Warner Instruments Inc. Hamden CT). pClamp 8.2 (Axon Instruments Inc. Sunnyvale, CA) was used to design and carry out all electrophysiological protocols.

Typical sodium currents were obtained by presenting a series of voltage clamp steps (-60 to +35 mV, 50ms) from a holding potential of -90 mV. Current-voltage (I-V) relationships were plotted. Conductance was calculated by  $G=I/(V_m-V_{rev})$  and normalized conductance-voltage curves were fit with a Boltzmann equation. Steady-state inactivation curves were obtained by presenting a test pulse (50 msec, -10 mV) following a series of conditioning pulses (-100 to 0 mV, 50 msec) with intervals of 1 sec for smNav1.4b and 10 sec for hNav1.4 at -90 mV to allow full recovery from inactivation. Currents were normalized and fit with a Boltzmann equation. The time constant of fast inactivation ( $\tau_h$ ) was tested by a depolarization step from -90 to -10 mV.  $\tau_h$  was extracted

from a single exponential fit over the range where the current decayed from 90% to 10%. Data analysis was performed using a combination of Clampfit 8.2 (Axon Instruments Inc.) and Origin 7.0 (OriginLab Corp., Northampton, MA).

## **Statistics**

All values are presented as mean +/- S.E.M. Statistical significance was assessed using the Student's two-sample, two-tailed, independent t-test. Linear correlation between gene expression and EOD frequency was done in Origin 7.0.

## **Results**

### **Cloning of Nav1.4 cDNA sequences in *Sternopygus***

Partial sequences of smNav1.4a and smNav1.4b were identified previously (Lopreato et al., 2001). In this study, more RT-PCRs, 5' and 3' RACE were performed to clone the last 2kb of smNav1.4b and the 5' and 3' UTRs of both genes. Cloning and sequencing errors in the previous partial sequences were corrected to identify the full-length open reading frames (ORFs) of both genes. To confirm the obtained fragments are from the same mRNA, one-step RT-PCR reactions with forward and reverse primers both located outside the ORFs were used to generate PCR products with expected sizes of ~5.5kb (Fig. 2.1).

The full-length cDNA of smNav1.4a is 7637 bp with the ORF from 280 to 5751. smNav1.4b full-length cDNA is 6029 bp, with the ORF from 114 to 5603. The complete sequences of these genes are listed in Appendix 1 and 2.

As shown in previous studies (Lopreato et al., 2001), smNav1.4a and smNav1.4b are duplicate orthologs of Nav1.4 in *Sternopygus*. Between these two genes and compared to hNav1.4 (GenBank, NP\_00325), all the transmembrane domains are well conserved, while the intracellular regions exhibit more variations, especially in I-II loops, II-III loops and the end of C termini (Fig. 2.2). Despite the difference in these regions, several important motifs are still well conserved (Fig. 2.2, Fig. 2.4 and Fig. 2.5), including ankyrin G binding domain at 924, IFM motif at 1310, EE &KK motifs at 1314 and CaM binding motif at 1735 (Fig. 2.2). In addition, most residues where mutations are known to be responsible for human channelopathies are conserved as well (Fig. 2.2).

However, F1705 (+ in Fig. 2.2) in hNav1.4, has been found associated with cold-aggravated myotonia possibly by causing a positive shift in voltage dependence and slowing the rate of inactivation (Wu et al., 2005), is conserved in smNav1.4b but changed to valine in smNav1.4a (Fig. 2.2 & Fig. 2.5). Whether this change affects any function is not clear.

### **Both sodium channels are expressed in electric organ at comparable levels**

To compare the relative expression levels of smNav1.4a and smNav1.4b in electric organ, one-step RT-PCR reactions were set up with primers designed to amplify a shared region, but with different lengths, in both genes. Reactions were stopped every third cycle between 24 and 39 cycles and loaded on an agarose gel (Fig. 2.6). The results showed smNav1.4a (upper band) and smNav1.4b (lower band) have comparable abundance. The upper band (smNav1.4a) is slightly stronger than the lower band (smNav1.4b). Given the slightly different PCR efficacy and the slightly different

mass:mole ratios due to the size difference, the experiment did not, and was not designed to, demonstrate accurate abundances of these two genes, but still showed that both genes are expressed in electric organ at comparable levels.

### **5' RACE revealed complex mRNA variation of smNav1.4b**

5' RACE revealed two transcripts of smNav1.4b in electric organ and muscle of *Sternopygus* (Fig. 2.7), and more interestingly, the longer band showed an extraordinary dominance in electric organ, in contrast to comparable abundances of the two transcripts in muscle. More experiments including 5'RAGE revealed the gene structure of Nav1.4b in *Sternopygus* (Fig. 2.8). This gene has two exclusive first exons named 1S and 1L according to their sizes, with a distance of at least 1.2kb. The most significant difference between the two alternative first exons is that exon 1L contains a start codon but exon 1S does not (Fig. 2.9), thus the two mRNA transcripts will be translated into two different proteins. One protein (smNav1.4bL, translated from exon 1L) has an extra 51 amino acid segment in the N terminus, which makes its N terminus ~ 50% longer than the other (smNav1.4bS), of which the translation starts in the second exon (Fig. 2.9). Structural analyses (Chou and Fasman, 1974; Garnier et al., 1978) predict a helix in the middle of the extended N terminal segment of Nav1.4bL and this helix contains six positively-charged amino acids (Fig. 2.3 and Fig. 2.4).

Additionally, sequencing multiple clones of the 5'RACE products revealed that transcripts of smNav1.4b start at multiple sites. Some sites are in close vicinity to each other (within only several basepairs), thus they are possibly controlled by the same promotor. Exon 1L exhibits four groups of starting sites (n= [1], [2,4,5], [3,3], [2], each

number indicates the number of clones starting from one site, each pair of square brackets include a group of sites close to each other, Fig. 2.9), making the exon size vary between 111bp and 211bp, though most products are ~180bp. Exon 1S has only two groups (n=[2], [4,2,1], Fig. 2.9) of starting sites in a short region. The size of exon 1S is between 129bp and 143bp. Interestingly, of the 7 clones of sequenced, exon 1S in the electric organ only start from the second group. The slight size difference of Nav1.4bS 5'RACE products in the electric organ and muscle (Fig. 2.7) might be the result of this. These results suggest multiple promoters may be involved and produce mRNA transcripts with different lengths. Different promoters may be under different regulation mechanisms and mRNA with different lengths may affect translation differently.

Since the method of 5'RACE keeps the 5' end of mRNA intact, it is unlikely that these sites are artifacts. In fact, I noticed that, even though these sites cover more than 100bp, all sequenced clones include the start codon. Also, these sites were repeatedly found in separate experiments, even in different tissues in a non-random pattern. Moreover, not all 5'RACE products (for example, a first exon in zebrafish Nav1.4bL, see next paragraph) exhibit multiple starts, further confirming this is not an experimental error.

### **5' RACE of Nav1.4b in zebrafish and rat**

I also examined Nav1.4b in the muscle of the zebrafish, *Danio rerio*, with 5'RACE and found two transcripts too (Fig. 2.7, Fig. 2.8 and Fig. 2.10A). More importantly, exon 1L also contains a start codon. The extra segment of N terminus translated from exon 1L in *Danio rerio* and the helical structure in this segment show

high similarities to those in *Sternopygus* (Fig. 2.10B). The predicted helix in zebrafish Nav1.4bL contains even more positively charged residues (Fig. 2.10B). Multiple transcription initiation sites are also seen in exon 1S (n=11) of *Danio rerio*, but not in exon 1L (n=4).

Furthermore, I performed 5'RACE carefully on rat (*Rattus norvegicus*) muscle and also identified two rNav1.4 transcripts (Fig. 2.7), but in a different pattern from Nav1.4b transcripts in the two fish species: both transcripts include a distant exon1 but one transcript splices out a proximal exon1A (Fig. 2.8 and Table 2.4). Neither the distant first exon nor the proximal cassette exon contains a start codon, thus, the two transcripts will be translated into identical protein products, though the presence of the cassette exon may still affect the translation process. Six starting sites (n=1, 1, 7, 2, 7, 3) were identified in the distant exon1 (Fig. 2.11). The transcript containing the cassette exon is novel. Its abundance seems very low in the leg muscle. The abundance in other tissues and its functional significance are not clear.

The exact locations of the exons and introns in zebrafish and rat were identified in their genomes (Table 2.4). Notably, the distance of between exon 1S and 1L is 34.4kb, far longer than the average intron size in zebrafish (0.2kb) and other animals (Vinogradov, 1999; Mattick and Gagen, 2001).

Table 2.4 Gene Structures of Nav1.4b in Zebrafish (*Danio rerio*) and Nav1.4 in Rat (*Rattus norvegicus*)

Gene	Chromosome	Exon	Start	End
Nav1.4b in zebrafish	3	Exon 1S	15191571	15191426
		Exon 1L	15157039	15156886
		Exon 2	15154608	—
Nav1.4 in rat	10	Distant exon 1	95760402	95760273
		Cassette exon	95744799	95744619
		Exon 2	95744537	—

\* Blast search was done at <http://www.ensembl.org>

### Tissue distribution pattern of smNav1.4 transcripts

5' RACE of Nav1.4b in *Sternopygus* showed a preferential expression of exon 1L in the electric organ, despite the longer size of its amplicon and therefore presumably less amplification efficacy in PCR reactions (Fig. 2.7). To further compare the expression level of each transcript between electric organ and muscle, semi-quantitative RT-PCR was performed with primers specifically designed for 1L and 1S. The same amount of total RNA from each tissue was used in RT-PCR reactions and amplified for 24, 27, 30 and 33 cycles. Due to possibly different amplification efficacies of different primer pairs, comparisons can only be made on the same transcript between tissue types, but not on different transcripts in the same tissue. The result (Fig. 2.12) shows that smNav1.4bL is expressed in electric organ and muscle at comparable levels, while smNav1.4bS is strongly repressed in electric organ.

### **Immunoprecipitation and western blot confirmed the existence of smNav1.4b protein**

The extra 51 amino acid N terminal segment in smNav1.4bL is composed of 41% non-polar and 59% polar and charged residues. Structural predictions suggest that this segment is located inside the cell. To confirm the existence of this novel N terminus, I had a polyclonal antibody generated against the  $\alpha$ -helix in this region and used it to immunoprecipitate solublized proteins from electric organ and muscle. I ran the precipitated protein on a SDS-PAGE gel and probed with a pan-Na channel antibody (epitope identical to smNav1.4b sequence) in western blot. The detection of a band at ~280kD (Fig. 2.13) confirms that the smNav1.4bL splice form is indeed translated in electric organ and muscle.

### **Correlation between gene expression and EOD frequency**

I used real-time quantitative RT-PCR to examine the mRNA levels of smNav1.4a, smNav1.4b and each splice variant of smNav1.4b in the electric organ of *Sternopygus*. Cautions were taken to ensure the accuracy of the measurements. First, total RNA samples were examined on Bioanalyzer 2100 to confirm no DNA contamination or RNA degradation. Secondly, I used RT-PCR for myosin light chain, which is abundant in muscle but negligible in electric organ (Fig. 2.14A), to screen the RNA samples to ensure that minimum muscle contamination. Only samples with minimal myosin light chain expression (<1% of muscle) were accepted in our study (Fig. 2.14B). Thirdly, 18S rRNA was used as the calibrator gene and its level strongly correlates with the total RNA readings of a spectrometer, indicating 18S rRNA is at fairly constant levels in electric organ across individuals and suitable to be a calibrator gene. The standard curve method

of real-time quantitative RT-PCR was used with 0.5x, 1x, 2x, 4x or 0.50x, 0.70x, 1x, 1.41x, 2x in later experiments to generate standard curves usually with  $R > 0.95$  in linear regressions.

First, the amplification of the most variable region in these two sodium channels—domain II-III loop was examined to assay mRNA levels of smNav1.4b and smNav1.4a. As shown in Fig. 2.15A, mRNA level of smNav1.4b was significantly ( $p < 0.01$ ) higher ( $1.39 \pm 0.13$ ) in high EOD frequency fish ( $> 100$  Hz,  $n = 4$ ) than the level ( $1.00 \pm 0.05$ ) in low frequency fish ( $< 80$  Hz,  $n = 8$ ). The normalized mRNA level of smNav1.4b in each individual fish positively correlated with its EOD frequency (Fig. 2.15B,  $R = 0.63$ ,  $p = 0.03$ ). On the other hand, mRNA level of smNav1.4a showed no significant difference (Fig. 2.16A,  $p = 0.84$ ) between the same groups of high EOD frequency fish ( $0.96 \pm 0.14$ ) in and low EOD frequency fish ( $1.00 \pm 0.13$ ). The normalized mRNA level of smNav1.4a in each individual fish did not correlate with its EOD frequency (Fig. 2.16B,  $R = -0.08$ ,  $p = 0.81$ ).

I also assayed individual forms of smNav1.4b for confirmation. Two major changes of the real-time quantitative RT-PCR method were made. First, the only difference between these two transcripts is the first exon, each about 150bp, and the sequences are GC rich, thus it is not applicable to design TaqMan primer and probe set with appropriate  $T_m$  within this region. Instead, SYBR Green was used to measure the amplified DNA amount of smNav1.4bL and smNav1.4bS. Secondly, because the abundance of Nav1.4bS is very low, one-step real-time quantitative RT-PCR failed to amplify it to reach measurable concentration, thus the reaction was reversed transcribed

and pre-amplified in the real time quantitative RT-PCR mixture for 15 cycles, then 5 $\mu$ l product of the first reaction was used in 50 $\mu$ l second relay reaction with the same buffer condition but fresh enzyme to be further amplified and measured. The linear standard curve was well maintained (Fig. 2.18C, R = -0.97), and all test samples were included in the range of standard curve, therefore the measurement remained quantitative.

The group of low EOD frequency fish showed lower mRNA level of smNav1.4bL than the high EOD frequency fish (Fig. 2.17A, low:  $1.00 \pm 0.13$ , n=8; high:  $2.71 \pm 0.49$ , n=4; p=0.001), while there was no significant difference observed with Nav1.4bS (Fig.2.18A, low:  $1.00 \pm 0.18$ , n=8; high  $1.33 \pm 0.24$ , n=4; p=0.30). Furthermore, the mRNA level of Nav1.4bL in each individual fish positively correlated with the EOD frequency (Fig. 2.17B, R=0.83, p<0.001.), but Nav1.4bS did not (Fig. 2.18B, R=0.41, p=0.18).

All numbers of real-time quantitative PCR results above are relative values, normalized by the low EOD frequency group average, thus don't indicate the absolute abundance of any transcript.

### **DHT affects expression of sodium channels in electric organ**

DHT has been known to not only lower the EOD frequency of *Sternopygus*, but also broaden the action potential duration and slow down the inactivation of sodium current in electrocytes (Ferrari et al., 1995). In this study, I implanted fish with DHT capsules and saw the plasma DHT level of the DHT-implant group significantly elevated, compared to that of the control group (DHT-implant:  $9.8 \pm 2.7$  ng/ml; control:  $0.52 \pm$

0.50 ng/ml;  $p < 0.0001$ ).

As seen in Fig. 2.19, compared to the control group implanted with empty capsules, the EOD frequency of DHT-implanted fish started to decrease three days after the implant and the difference became statistically significant after seven days (Control group:  $123.15 \pm 8.96$ , DHT group:  $100.86 \pm 3.90$ , t-test  $p=0.03$ ). We dissected the fish tails 18 days after the implant when the EOD frequency of the DHT group stabilized and significantly differed from the control group (Control group:  $125.00 \pm 9.94$ , DHT group:  $83.92 \pm 1.88$ ,  $p=0.0004$ ). We used real-time quantitative RT-PCR to quantify the mRNA levels in two groups and found the mRNA of total smNav1.4b was lowered (Fig. 2.20, Control group:  $1.00 \pm 0.13$ , DHT group:  $0.55 \pm 0.05$ ,  $p=0.003$ ) and each transcript form was lowered too (smNav1.4bL: Control group:  $1.00 \pm 0.21$ , DHT group:  $0.53 \pm 0.05$ ,  $p=0.01$ , smNav1.4bS: Control group:  $1.00 \pm 0.23$ , DHT group:  $0.29 \pm 0.04$ ,  $p=0.001$ ). The mRNA level of smNav1.4a was not affected by DHT (Control group:  $1.00 \pm 0.16$ , DHT group:  $0.91 \pm 0.04$ ,  $p=0.46$ ).

In order to locate the acting point of DHT on genomic DNA, the intron between exon 1L and exon 2 and the genomic DNA sequence 1.2kb upstream of exon 1L were cloned by PCR and 5' RAGE (see Appendix 4 & 5 for sequences). Transcriptional factor analysis on a bioinformatics server (<http://www.genomatix.de>) identified a putative androgen receptor binding site at 702-720 bp in the intron between exon1L and exon 2.

### **Expression of smNav1.4bL, smNav1.4bS and hNav1.4 in *Xenopus* oocytes**

The correlations between the mRNA level of smNav1.4b especially smNav1.4bL and EOD frequency found in this study, and between the kinetic parameters of sodium current inactivation and EOD frequency shown in a previous study (Ferrari et al., 1995), suggest that smNav1.4bL contributes to a faster speed and more negative voltage dependence of inactivation. In order to confirm this hypothesis, I constructed plasmids containing full-length sequences of smNav1.4bL and smNav1.4bS and injected cRNA into *Xenopus* oocytes. Currents were recorded with the two-electrode voltage clamp method. The results are presented with the most commonly used parameters,  $\tau_h$ , the time constant extracted from a single exponential fit over the decaying current, and  $V_{1/2}$ , the membrane potential where the membrane conducts half maximum current during activation and inactivation. Comparisons were made between smNav1.4bL and smNav1.4bS, and also to their human ortholog hNav1.4.

Indeed, as shown in Figure 2.21 and Table 2.5 on page 48, I observed a rapid inactivating current with smNav1.4bS ( $\tau_h = 2.63 \pm 0.10$  msec, n=14) and an even faster current with smNav1.4bL ( $\tau_h = 1.31 \pm 0.05$  msec, n=14), compared to hNav1.4 ( $\tau_h = 9.21 \pm 0.24$  msec, n=26). Both smNav1.4bS and smNav1.4bL showed no difference in activation voltage dependence ( $V_{1/2} = -28.53 \pm 1.51$  mV, n=10 and  $-28.75 \pm 1.18$  mV, n=16 respectively) from hNav1.4 ( $V_{1/2} = -28.66 \pm 3.3$  mV, n=8), but the two smNav1.4b channels differ greatly in the voltage dependence of inactivation. smNav1.4bS is inactivated at a slightly depolarized voltage ( $V_{1/2} = -43.01 \pm 1.48$  mV, n=21) compared to hNav1.4 ( $V_{1/2} = -48.35 \pm 2.37$  mV, n=11), but smNav1.4bL is inactivated at a negative

membrane potential ( $V_{1/2} = -58.97 \pm 0.93$  mV,  $n=15$ ). Since the only difference between Nav1.4bS and Nav1.4bL is the extended N terminal segment, thus the increase in the speed and the negative shift in voltage dependence of inactivation must be caused by this N-terminal segment, but it has little effect on activation voltage dependence. (All hNav1.4 data were done for an independent study by Mingming Wu and used in this dissertation as reference only).

Notably, even though all of these channels are expressed in muscle, hNav1.4 exhibits a much slower inactivation than smNav1.4bS and smNav1.4bL in *Xenopus* oocytes. However, little phenotypic difference is seen in the sodium currents in muscles of fish and human (Kirsch and Sykes, 1987; Coutts et al., 2006). This extraordinary slow inactivation  $\tau_h$  of hNav1.4 has been seen in multiple studies using *Xenopus* oocytes. One explanation is that there are two current components as the result of two hypothetical gating modes of the channel and oocytes stabilize the slow component (Ji et al., 1994). Another untested explanation is the incompatibility between mammalian genes and amphibian cells (Qu et al., 1995). The two sodium channels from *Sternopygus macrurus* inactivate much faster than hNav1.4, suggesting either they have less difference between the two hypothetical gating modes, or fish sodium channels are more compatible with the molecular environment in *Xenopus* oocytes. Future study on the difference between fish and mammalian sodium channels will provide a new angle to reveal more general properties of sodium channels.

I also studied the kinetic properties of these channels with the two alternative spliced sodium channel  $\beta 1$  subunits of *Sternopygus macrurus*. The details will be discussed in Chapter 3.

### **Deletion of a proline strongly affects the inactivation kinetics**

Because proline lacks a hydrogen thus cannot donate a hydrogen bond to stabilize an  $\alpha$  helix, therefore, proline often disrupts a helix and is located at the end of the  $\alpha$  helix. Also, its rigid structure usually forms a sharp bend in the peptide chain. Several prolines are located between the two predicted  $\alpha$  helices in the N terminus of smNav1.4bL, including a proline (P30) immediately after the helix in the extended N terminal segment of smNav1.4bL (Fig. 2.3 and Fig. 2.4). As an initial attempt to understand the function of the extended N terminal sequence, this proline was deleted from smNav1.4bL by site-directed mutagenesis and this mutation is expected to sharply divert the orientation of this positively charged helix (Fig. 2.22A). Not surprisingly, the deletion of this proline has no effect on activation voltage dependence ( $p=0.37$  and  $0.76$ , compared to smNav1.4bL and smNav1.4bS respectively, Table 2.5). However, this deletion causes changed the inactivation kinetics (Fig. 2.22, Table 2.5). First, the proline deletion makes the inactivation speed of smNav1.4bL almost two-fold slower, and indistinguishable from smNav1.4bS, suggesting the removal of the sharp bend of proline totally abolishes the effect of the extended N terminal segment on inactivation speed. Secondly, the voltage-dependence of inactivation is also changed by this mutation, to a level in the middle of smNav1.4bS and wild-type smNav1.4bL, suggesting the negative shift of inactivation voltage-dependence by this extended N terminal segment is affected, but not solely determined, by the position of the helix, or the deletion of the proline does not sufficiently displace the helix to cause a complete loss of the negative shift.

Table 2.5 Kinetic Properties of hNav1.4, smNav1.4bS and smNav1.4bL (wild-type and mutant) in *Xenopus* oocytes

	hNav1.4	smNav1.4bS	smNav1.4bL	smNav1.4bL (P30 deletion)
Activation	28.66 ±3.3	-28.53 ± 1.51	-26.86 ± 0.70	-27.99 ± 0.99
$V_{1/2}$ (mV)	n=8	n=10	n=15	n=17
		p1= 0.97	p1= 0.49	p1=0.80,
			p2= 0.28	p2=0.76
				p3=0.37
Inactivation	-48.35 ±2.37	-43.01± 1.48	-58.97 ± 0.93	-53.91 ± 0.78
$V_{1/2}$ (mV)	n=11	n=21	n=15	n=21
		p1=0.05	p1=0.0001	p1<0.01
			p2=1 x 10 <sup>-9</sup>	p2=1 x 10 <sup>-7</sup>
				p3=0.0002
Inactivation	9.04 ± 0.18	2.63± 0.10	1.31 ± 0.05	2.45 ± 0.19
$\tau_h$ (msec)	n=26	n=14	n=14	n=24
		p1< 1x 10 <sup>-24</sup>	p1< 1x 10 <sup>-27</sup>	p1< 1x 10 <sup>-28</sup>
			p2< 1x 10 <sup>-11</sup>	p2=0.50
				p3 <0.0001

\* t-tests, p1:compared to hNav1.4, p2: compared to smNav1.4bS, p3: compared to smNav1.4bL

## Discussion

### Variations in the ends of ion channels may allow functional diversity

Our lab started the study of these channels by cloning their partial cDNAs (Lopreato et al., 2001). In this study, I further identified the full-length sequences of these two Nav1.4a and Nav1.4b in *Sternopygus macrurus*. ClustalW alignments with hNav1.4 (Fig. 2.2) show that most of the residues where mutations are related to channelopathies are conserved in these genes, suggesting they are likely to function as normal sodium channels. But on the other hand, any functional differences between these two channels may be caused by important residues, motifs or structures not identified in previous studies in the field.

Careful examinations of 5'RACE products revealed two alternative first exons of smNav1.4b, which are differentially expressed in muscle and electric organ. Exactly the same pattern of exons is also found in the muscle of the zebrafish, *Danio rerio*, suggesting it may be common to other teleost fish species. The sequence of sodium channel is highly conserved for functions, suggesting any disturbance within mRNA sequence may cause serious defect, such as the loss of channel function and Brugada syndrome caused by a splice site change of Nav1.5 (Hong et al., 2005). Therefore, the mRNA ends might be the only likely places permissive for flexibility. In fact, recent studies show variations in the mRNA ends are indeed common to sodium channels. mNav1.5 has three alternative 5'-splice variants of the exon1 and two 3'-splice variants in untranslated regions (UTRs) (Shang and Dudley, 2005). Nav1.6 has four mutually exclusive 5'-untranslated exons in mouse and human (Drews et al., 2005). Although these variations only occur in the untranslated regions thus do not affect protein

sequences, they might still under regulations of different promoters or affect translational events. In addition to the possibility of being involved in these regulations in similar ways, the translatable exon 1L in *Sternopygus* directly changes the protein sequence and results in a functionally distinct sodium channel, Nav1.4bL.

Another channel, calcium-activated potassium channel (*slo*) in *Drosophila* shares some characteristics with smNav1.4b. Multiple alternative first exons of *slo* (C0, C1, C1b, C1c and C2) have been identified, and one of them (C2) has a start codon to generate an extra 17 a.a. segment in the N terminus (Becker et al., 1995; Bohm et al., 2000). Furthermore, these exons show tissue-specific expression pattern, controlled by multiple upstream regulatory elements in the introns (Brenner et al., 1996). The introns of smNav1.4b before the second exon may contain regulatory elements in a similar manner (for example, hormone receptor binding sites).

### **N terminus of sodium channel affects inactivation**

Multiple studies have shown the C terminus of sodium channel contributes to the control of inactivation. Switching the C termini between Nav1.2 and Nav1.5 resulted in the exchange of their inactivation kinetics and voltage dependence (Mantegazza et al., 2001). Deletion of the distal half of the C terminus of either Nav1.2 or Nav1.5, or even only the last helix, negatively shifted steady-state inactivation (Mantegazza et al., 2001; Cormier et al., 2002). Furthermore, two channelopathic mutations in the C termini of sodium channels have been identified recently. One mutation in Nav1.1 (D1866Y, equivalent to D1680 in hNav1.4, see Fig 2.2), causing inherited epilepsy, positively shifts the inactivation voltage dependence, by disrupting the interaction with  $\beta 1$  subunit

(Spampanato et al., 2004). The other mutation (F1705I) in Nav1.4, associated with cold-aggravated myotonia, also positively shifts the voltage dependence and slows the rate of inactivation (Wu et al., 2005).

The start codon in exon 1L of smNav1.4bL results in an extended N terminal segment, which makes its N terminus 50% longer than the N termini of mammalian Nav1.4 and smNav1.4bS. The addition of the extended N terminus causes a drastic change in the inactivation kinetics (50% faster, -16mV shift in voltage dependence). So far, many residues in the inter-domain loops and the C terminus have been studied but few studies have focused on the N terminus of voltage gated sodium channels. Given it is known that the N terminus interacts with C terminus by electrostatic forces with two helices at 13-30 and 1716-1737 in rNav1.4 (Zhang et al., 2000), and the C terminus affects the inactivation of sodium channel, one possible mechanism is that the extended N terminus may interfere with this electrostatic interaction and in turn affect the inactivation kinetics. Basic residues are condensed in the predicted  $\alpha$ -helical region (6 out of 17 a.a. between 14 to 31), thus may compete with the basic residue-rich region in the C terminus (6 out of 22, 1716-1737 in hNav1.4). Several prolines located between the two helices of the N terminus may act as hinges to facilitate the movement of N terminus into the position. As an initial attempt to understand the function of the extended N terminal sequence, I deleted the proline closest to the helix from the smNav1.4bL by site-directed mutagenesis and this mutation is expected to sharply divert the positively charged helix. The mutant smNav1.4bL exhibited inactivation kinetics very different from smNav1.4bL, but more similar to smNav1.4bS (Table 2.5), suggesting the N terminal helix and its proper orientation significantly account for the function of smNav1.4bL. This is the first

evidence showing the N terminus of a sodium channel can affect its inactivation.

Although the difference in the N terminus of smNav1.4b is identified in this study, it does not rule out the possibility of other alternative splicing sites downstream of the second exon and the possibility that these splicing events are co-regulated. However, a brief survey of RT-PCR in the electric organ at different regions of smNav1.4b didn't reveal any more splicing variants (data not shown), suggesting the presence of other splicing sites is unlikely, or the splicing products only produce subtle difference (<100bp) in transcript size.

### **Expression of sodium channels in the electric organ**

Evidently, between the two first exons of smNav1.4b, exon 1L is predominant in the electric organ, whereas the two exons are expressed at roughly equal levels in muscle. By what tissue-specific mechanism the expression of 1L is upregulated, or more likely, the expression of 1S is repressed, remains unclear but an intriguing question. One possibility is tissue-specific transcriptional factors are involved to regulate transcription initiation. I observed multiple transcription initiation sites of smNav1.4b transcripts, which might be the downstream targets for tissue-specific regulations. However, search for promoter sites on a bioinformatics server ([http://www.fruitfly.org/seq\\_tools/promoter.html](http://www.fruitfly.org/seq_tools/promoter.html)) revealed only one putative promoter at 850bp upstream of exon 1L, probably due to the limited accumulation of fish specific promoter sequences in the database. Further bioinformatics study and quantitative measurements are needed to address this question.

Changes in the expression of ion channels have been reported to contribute to the

regulation of cellular excitability in multiple systems. In dorsal root ganglion (DRG) neurons, the expression of a TTX-sensitive sodium channel Nav1.3 is general low, but rapidly upregulated following axotomy (Waxman et al., 1994). On the contrary, the expression of two TTX-resistant sodium channels Nav1.8 and Nav1.9 are downregulated in injured neurons (Dib-Hajj et al., 1996; Dib-Hajj et al., 1998). In the neighbouring DRG neurons and sciatic nerve, Nav1.8 is upregulated and re-distributed (Gold et al., 2003). These changes may contribute to the axotomy-induced change in excitability, although proofs for such a direct correlation are still needed (Flake et al., 2004).

In this study, smNav1.4b mRNA level correlates with cellular excitability of electrocytes, represented by EOD frequency. However, the consequential relation between them is not clear. One likely possibility, as my working model (Fig. 4.1), is that the differential expression of smNav1.4a and smNav1.4bL contributes to the cellular excitability. Another study (Zakon et al., 2006) showed smNav1.4b is the sole voltage gated sodium channel in the skeletal muscle of *Sternopygus*, which therefore needs to be fast to meet the requirements of muscle function, as a study shows the sodium inactivation time constant  $\tau_h$  in the skeletal muscle of zebrafish is only 0.1~0.3msec (Coutts et al., 2006). On the other hand, smNav1.4a is only expressed in the electric organ, presumably bringing this novel tissue type its characteristic slower sodium current inactivation and in turn broader action potential. RT-PCR proved these two genes are expressed in electric organ at comparable levels. My hypothesis is that smNav1.4a, presumably a channel with slow inactivation and expressed at a fairly constant level across individuals, sets the baseline of kinetics, but smNav1.4b (especially Nav1.4bL), a fast channel as seen in *Xenopus* oocytes, varies in its expression level and provides the

fine tuning of the cellular excitability. To prove this hypothesis, one key hurdle I encountered is that smNav1.4a seems to contain lethal sequences to *E. Coli* thus the construction of full-length clones failed many times. Future efforts will be focused on this. Although the kinetic measurements of smNav1.4a are not available now, however, it is hard to imagine its inactivation is as fast as, or faster than, the inactivation of smNav1.4bL and the inactivation of sodium current in electrocytes is still as slow as seen in previous studies. Furthermore,  $\beta 1$  subunit may also play a role in the regulation, by speeding the inactivation, negatively shifting the voltage dependence of inactivation and varying the expression level or differential affinities with  $\alpha$  subunits. This will be addressed in next chapter.

Notably, a previous study (Ferrari et al., 1995) showed that, from high frequency to low frequency fish, fast inactivation of electrocytes  $\tau$  varied between 0.5 to 4.7msec and steady-state inactivation  $V_{1/2}$  varied between -60mV to -38.5mV. Despite the difference between *Xenopus* oocytes and *Sternopygus* electrocytes, the recorded kinetic properties of smNav1.4bL, the main smNav1.4b channel expressed in electrocytes, and smNav1.4bS, behaving more like hNav1.4 thus presumably like smNav1.4a as well, falls in the same range. Furthermore, as observed previously (Ferrari et al., 1995), even though no quantitative measurements were made, the activation appeared slower in low EOD frequency fish, it is consistent with the observation in this study the fast activation of smNav1.4bL and its lower expression in low EOD frequency fish (Fig. 2.21). Therefore, the change from smNav1.4bS to smNav1.4bL, and the upregulation of smNav1.4bL in high EOD frequency fish (or repression of smNav1.4bL in low EOD frequency fish) are consistent with the trend of inactivation kinetics and may explain the individual variation

of the sodium current in electrocytes.

An alternative possibility is the expression of smNav1.4b in electrocytes is regulated directly or indirectly by the synaptic input from spinal electromotor neurons or the firing activity of electrocytes, similar to Nav1.2 that is abolished in some neurons after deafferentation (Sashihara et al., 1997). This seems less likely to be the case, as a previous study (Few and Zakon, 2001) showed that local administration of DHT on electric organ did not change EOD frequency thus the synaptic input from electromotor neurons, but altered cellular excitability (EOD duration), suggesting the cellular excitability of electrocytes is regulated with a mechanism at least partially independent of synaptic input. Previous studies also suggest some intracellular molecules are not likely to be involved in this regulation. cAMP increased the current amplitude but did not change the inactivation kinetics in electrocytes (Mcanelly and Zakon, 1996). Calcium current was not detected in voltage clamp recordings (Ferrari and Zakon, 1993). Thus the expression of Nav1.4b may have a different mechanism from the  $Ca^{2+}$  dependent regulation found in mammalian muscle development (Offord and Catterall, 1989).

However, innervation or denervation on electrocytes may have an effect on smNav1.4a instead. A previous study (Unguez and Zakon, 1998) showed the elimination of electrical activity or all synaptic input of electrocytes resulted in a partial reversal phenotype toward its myogenic lineage and re-expression of proteins such as myosin heavy chain and tropomyosin. Thus, expression of smNav1.4a, the electric organ specific sodium channel, is presumably downregulated or even lost after denervation, although experimental confirmation is needed.

### **Hormonal regulation of sodium channel expression**

The mRNA levels of both the transcripts of smNav1.4b are repressed by global administration of DHT (Fig. 2.20). Steroid hormones can act as ligands for either nuclear transcriptional factors or membrane receptors. Although non-genomic mechanisms exist on ion channels, as some studies have shown estrogen can modulate BK channel *via* mechanisms independent of intracellular signals (Valverde et al., 1999) and this modulation acts through the  $\beta 1$  subunit of BK channel (Dick et al., 2001; Dick and Sanders, 2001; Dick et al., 2002), more studies have shown steroids either enhance or repress gene expression *via* nuclear receptors by a more common “genomic” mechanism (Chew and Gallo, 1998; Walters and Nemere, 2004).

In this study, DHT showed a slowly induced (>2 days) and long-lasting (>3 weeks) effect, thus it seems more likely to act as a co-repressor of smNav1.4b gene and the accumulative effects changed the cellular excitability. Interestingly, although smNav1.4bS and smNav1.4bL are far away from one another (at least 1.2kb) and are likely to be transcribed from different starting sites, they are both repressed by DHT. smNav1.4bS only accounts for a small percentage of sodium channels in electrocytes, thus the DHT repression on smNav1.4bS probably has little functional effect and might be the side effect of the repression of smNav1.4bL, since its transcription initiates in the middle of smNav1.4bS thus the repression of smNav1.4bL may abort the transcription elongation process.

The steroid repression of gene expression can involve several complex mechanisms (Dobrzycka et al., 2003). One possibility is DHT-androgen receptor (AR) complex may bind on the vicinity of smNav1.4b gene and recruit histone deacetylase and

nucleosome remodeling complexes, thus represses the gene expression. A bioinformatics tool (<http://www.genomatix.de>) suggests a putative AR binding site in the intron between exon 1L and exon 2. Since this intron is contained in transcription products of both smNav1.4bL and smNav1.4S, histone deacetylation in this intron may abort both transcriptions. Notably, this putative AR binding site is not found in the 2.3kb intron in zebrafish. Specific antibody against AR of *Sternopygus* is needed for further experimental confirmation (such as Chromatin Immunoprecipitation) of the association between AR and this site, which may help reveal the mechanism of DHT repression on smNav1.4b gene.

### **Evolution of sodium channels in electric fish**

Nav1.4, the voltage gated sodium channel in mammalian skeletal muscle, has two orthologs in teleost fish, presumably caused by a genome duplication at the origin of teleosts (Jaillon et al., 2004). A “redundant” sodium channel may relax the selection pressure on these genes and allow one gene to lose expression in muscle but gain expression in another tissue, such as the evolutionally novel tissue – electric organ. Several lines of evidences suggest that, in *Sternopygus*, smNav1.4b is constrained in muscle and thus should maintain its properties for fast firing action potentials required for muscle function. On the other hand, smNav1.4a lost its expression in muscle, thus may accumulate mutations and be positively selected for slow inactivation, allowing long duration action potentials in the electric organ (Zakon et al., 2006). In fact, the EOD duration in electric fish shows 100-fold variation across species from 200  $\mu$ sec to 20 msec (Hopkins, 1999). Their muscles express Nav1.4b and do not show obviously

different phenotypes, thus presumably the function of smNav1.4b should be conserved. On the other hand, Nav1.4a, is lost in muscles but expressed in electric organs of four electric fish sampled (Zakon et al., 2006). Therefore, its expression may contribute to the variation of cellular excitability and in turn EOD duration in electric fish species.

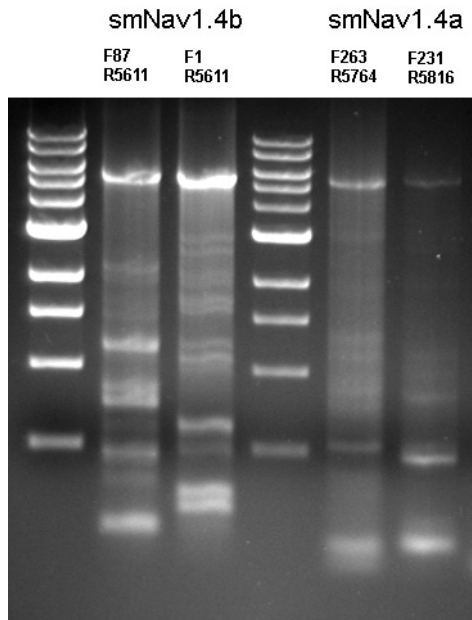


**Figure 2.1 One-step RT-PCR reactions with forward (F) and reserve (R) primers to confirm the open reading frames of Nav1.4a and Nav1.4b.**

Primers used are located outside the ORFs were used to generate PCR products about 5.5kb, which cover both ORF regions of the two genes.

Lane 1 and 4: New England Biolabs 1kb Ladder, from bottom to top: 0.5, 1, 1.5, 2, 3, 4, 5, 6, 8, 10kb.

Lane 2 and 3: RT-PCR of smNav1.4b, the starting positions of primers are marked on top of each lane. The major PCR product size is ~5.5kb, as expected.

Lane 5 and 6: RT-PCR of smNav1.4a, the starting positions of primers are marked on top of each lane. One of the major PCR products is ~5.5kb, as expected.





**Figure 2.2 Alignment of deduced protein sequences of hNav1.4, Nav1.4a and Nav1.4b(S) from *Sternopygus*.**

Full length sequences include Domain I (marked between ↓), domain II (between ↓↓), domain III (between ↓↓↓) and domain IV (between ↓↓↓↓) show higher homology than the inter-domain loops, N- and C- termini. Conserved motifs are labeled above the sequences including ankyrin G binding domain at 924, IFM motif at 1310, EE &KK motif at 1314 and CaM binding motif at 1735 (Figure 2.2). In addition, residues where mutations are responsible for human channelopathies are all conserved as well, including R669, R672, R675, L689, T704, M1360, M1370, M1592, F1589, N1584 responsible for periodic paralysis (PP, ▼), V445, S804, I1160, G1306, V1589 for potassium aggravated myotonia (PAM, ● in Figure 2.2), I693, V1293, T1313, L1433, R1448, G1456, F1473 for paramyotonia congenital (PMC or PC) (■) and L266 for sodium channel myotonias (▲). Others include two local anesthetic receptor sites F1589 and N1584 (↘), D1680 involved in the interaction with β1 subunit (\*). A serine close to the IFM motif (marked with “C”), which is subject to the phosphorylation of PKC and affect inactivation kinetics, is also conserved. F1705 in hNav1.4 is conserved in smNav1.4b but changed to valine in smNav1.4a (marked with +).

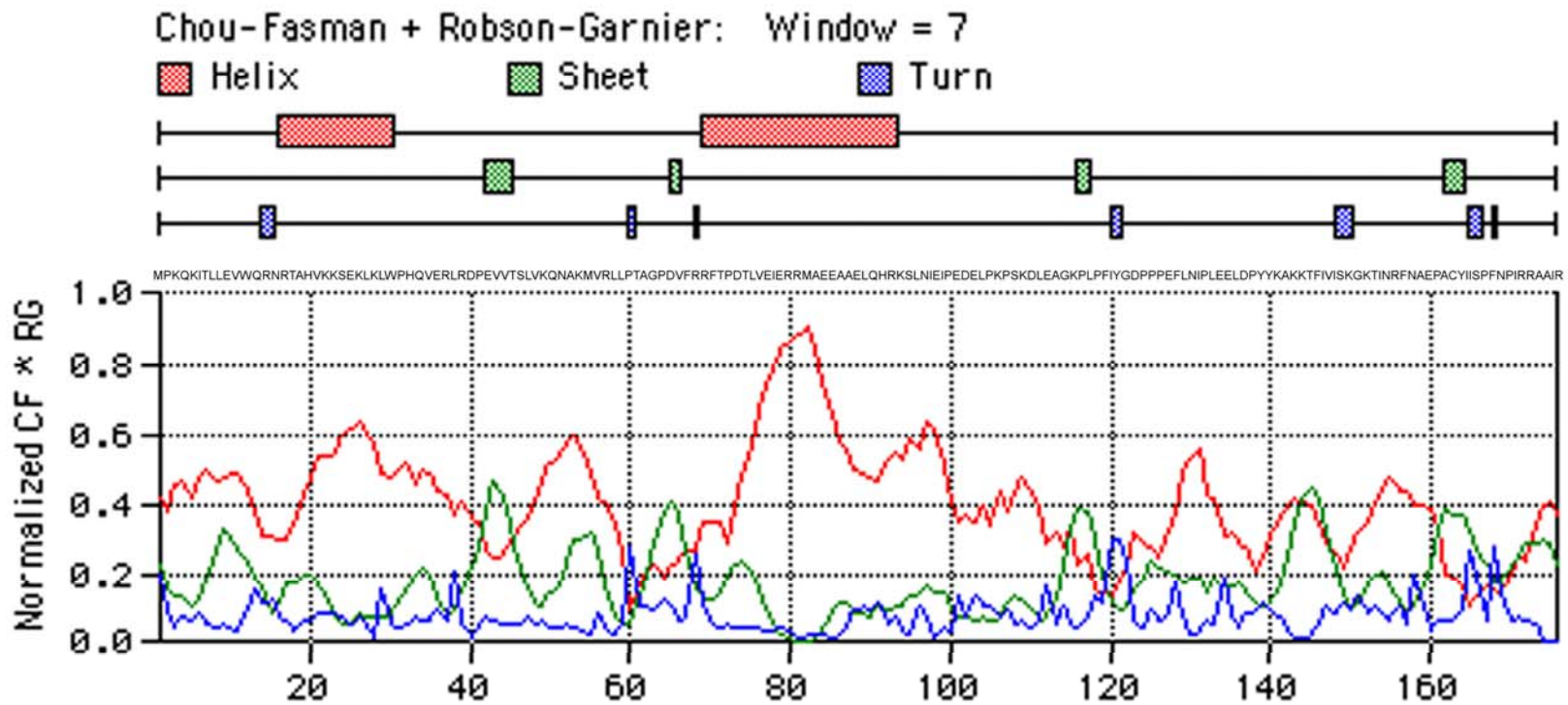


**Figure 2.3 Secondary structure prediction in the N terminus of smNav1.4bL.** Chou-Fasman and Robon Garnier prediction methods were used in MacVector software, the secondary structure prediction is accepted only where both the two methods agree.

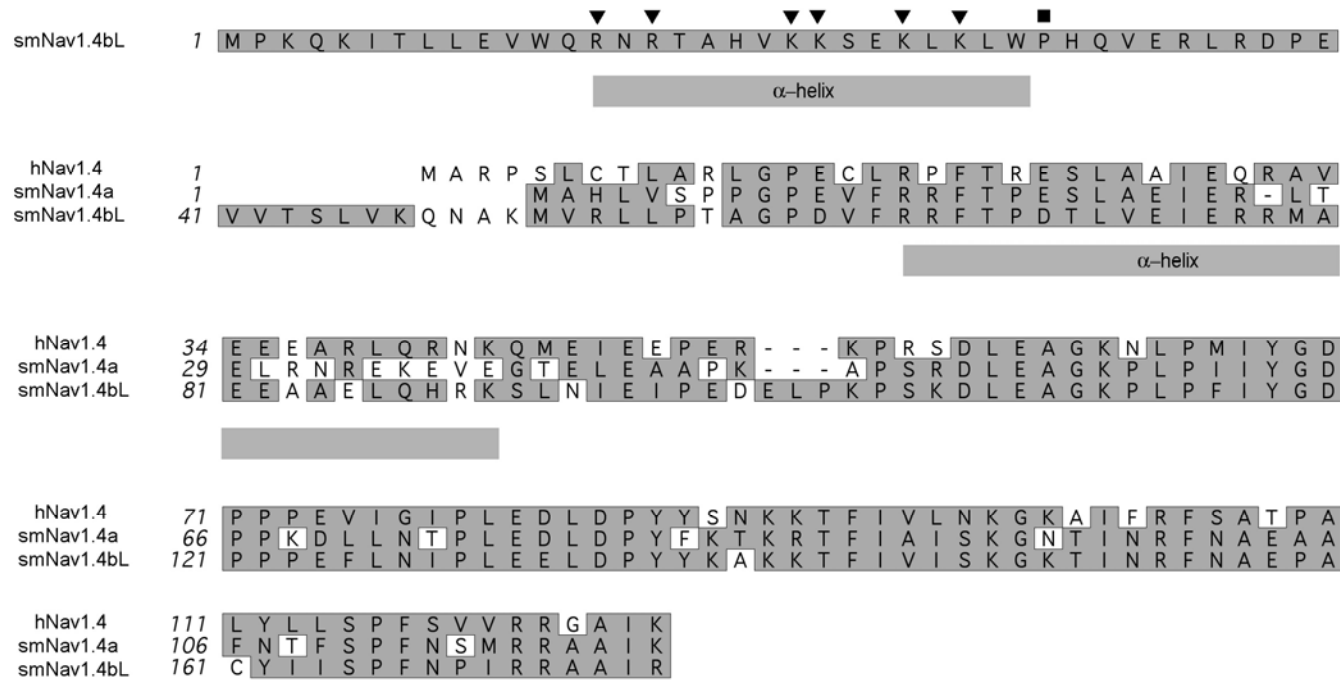


**Figure 2.4 Alignment of N-termini of human Nav1.4, smNav1.4a and smNav1.4bL.**

The predicted  $\alpha$ -helical regions are marked with rectangle bars below the sequence. In the first helix, positively charged amino acids are marked with reverse triangles ( $\blacktriangledown$ ). Predicted helices are marked with bars below the sequence. Deletion of the proline (marked with  $\blacksquare$ ) next to the helix showed a significant effect on channel kinetics.



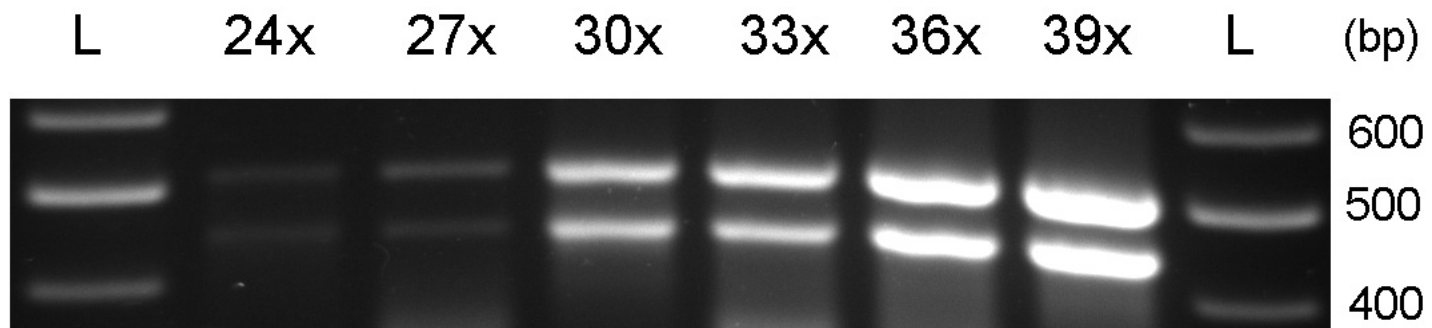


**Figure 2.6 smNav1.4a and smNav1.4b have comparable abundance in electric organ.** One-step RT-PCR reactions were set up identically but stopped at different time (cycle number on top of each lane). Products with expected sizes (519bp from smNav1.4a and 450bp from smNav1.4b) were separated and shown in a 2% agarose gel.

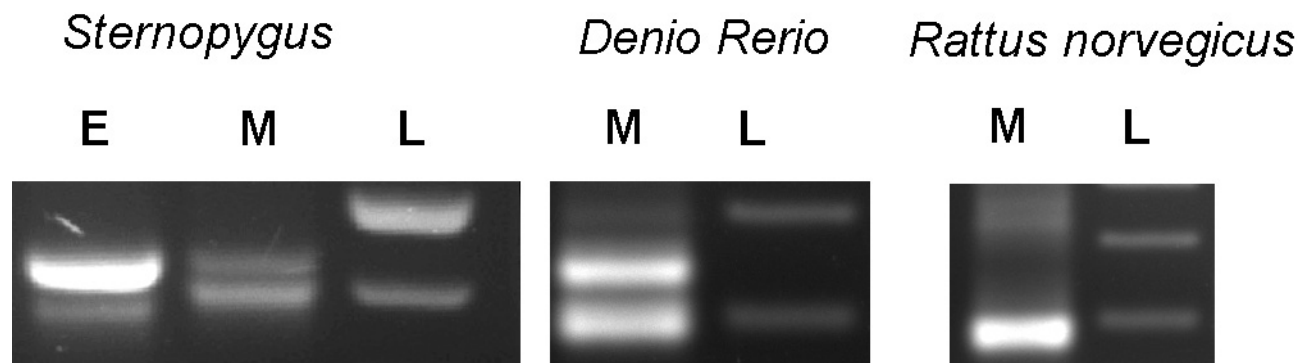


**Figure 2.7 5' RACE of Nav1.4b in *Sternopygus* , zebrafish (*Danio rerio*), and Nav1.4 in rat (*Rattus norvegicus*).** Gel pictures of 5' RACE products show two transcripts of the gene in each tissue type. The abundances of the two transcripts are comparable in the muscle of *Sternopygus* and zebrafish, but very different in the electric organ of *Sternopygus* and muscle of rat.

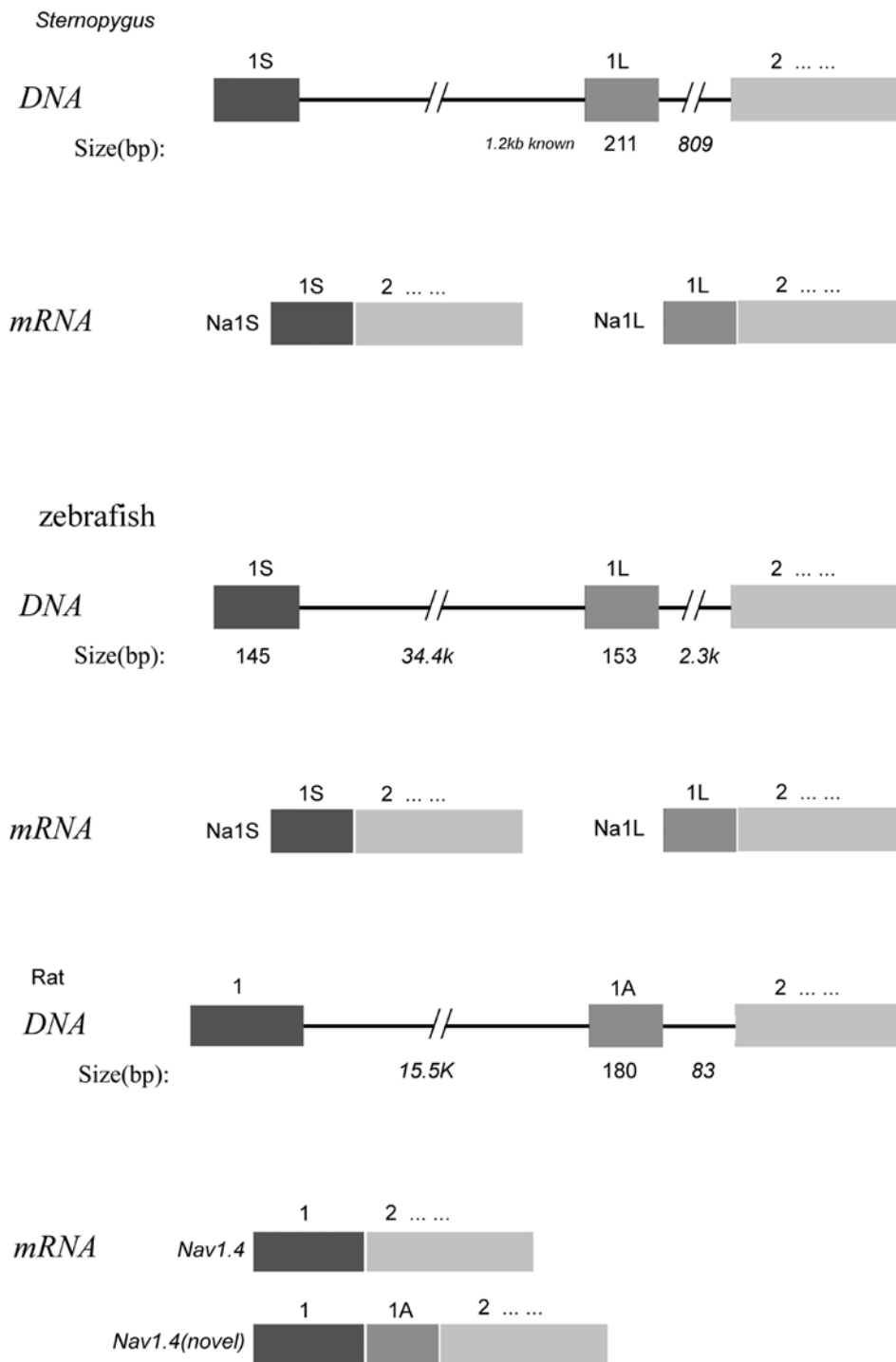


**Figure 2.8** Gene structure of Nav1.4b in *Sternopygus* (top), zebrafish (middle) and Nav1.4 in rat (bottom).



**A** Exon1S

```

1 * ggtttcattcaagacacccgtgcgtaagcgacagctgcccgagcctggactttctcca 60
61 * gagcagcaaaactttcggcttgatttgaaggaacactaaccttcggacctaggataaaa 120
121 ggaaatcttttctcctggctgagaaaagggttgtggaaagcttttacagtaactgtctgga 180
181 gaaactgagaagcgagcc

```

Exon1L

```

1 * gtttgtggaagcttttacagtaactgtctggagaaactgagaagcgagcc 52
53 ▼ atgaaagccaaagatcaacctgatagattttggagaaagaaccgatctgctcac 106
M K P K I N L I D F W R K N R S A H
107 ccaagcagagctaagaaaaccaaacaaaagctatcgcctcgacaactg 154
P S R A K K T K Q K L S P R Q L

```

**B**



**Figure 2.10 Exon 1S, 1L of Nav1.4b in *Danio rerio* and the N-terminal sequences of Nav1.4bL in *Sternopygus* and *Danio rerio*.**

A. Upper, exon1S of Nav1.4b in *Danio rerio*. Asterisks indicate the transcription initiation sites seen in 5' RACE.

Lower: exon1L of Nav1.4b in *Danio rerio*. The reverse triangle marks the start codon.

B. Alignment of the Nav1.4b N-termini in *Sternopygus* and *Danio rerio*. Filled triangles (▼ and ▲) mark positively charged amino acids. Three prolines are conserved between the two helices (■ and □).

```
1  * atcagcggcagcagctgtccttgccggccccggccccccagccaagt*cccccagagctcca 60
61  gccccagcctgaggtgggcacggcaccgccccgggctcgtcgccaccgctcttctctgcttc 120
121  tggccaacag
```

**Figure 2.11 The distant exon of rNav1.4. Asterisks indicate transcription initiation sites.**

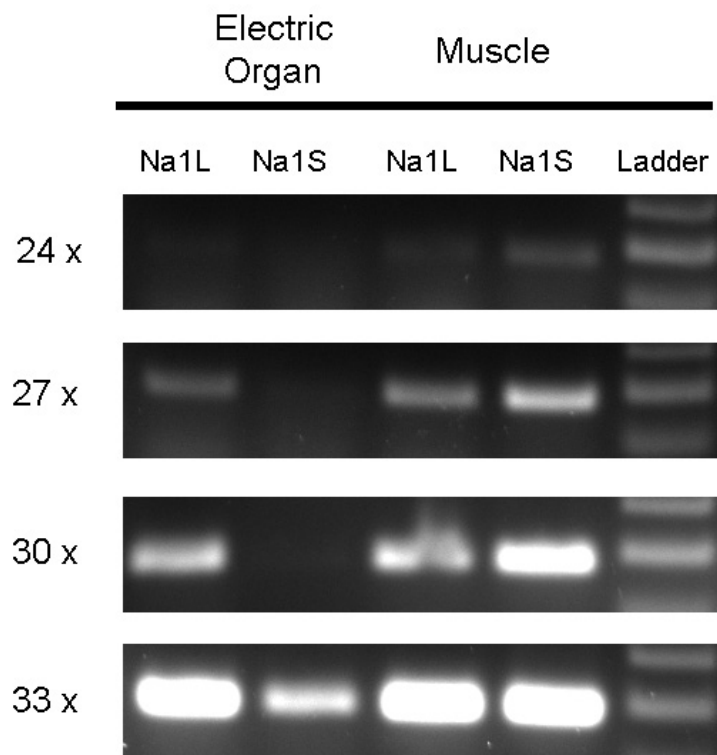


**Figure 2.12 Semi-quantitative RT-PCR of Nav1.4bL and Nav1.4bS in electric organ.** From top to bottom, PCR reactions with cycle number 24x, 27x, 30x and 33x. From left to right, Lane 1 and 2: PCR reactions targeted on exon 1L and 1S respectively, both with total RNA from electric organ as template. Lane 3 and 4: PCR reactions targeted on exon 1L and 1S respectively, both with total RNA from skeletal muscle as template.

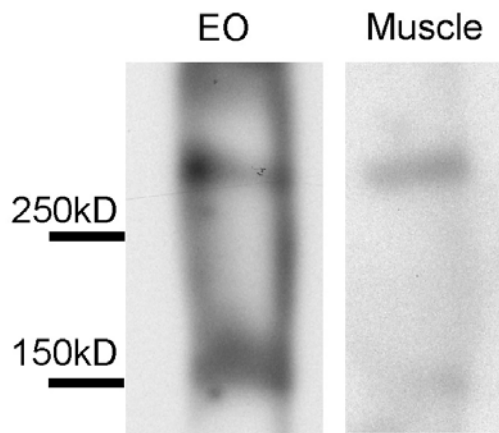


**Figure 2.13 Immunoprecipitation and western blot show the existence of the extra segment in the N-terminus of smNav1.4bL.**

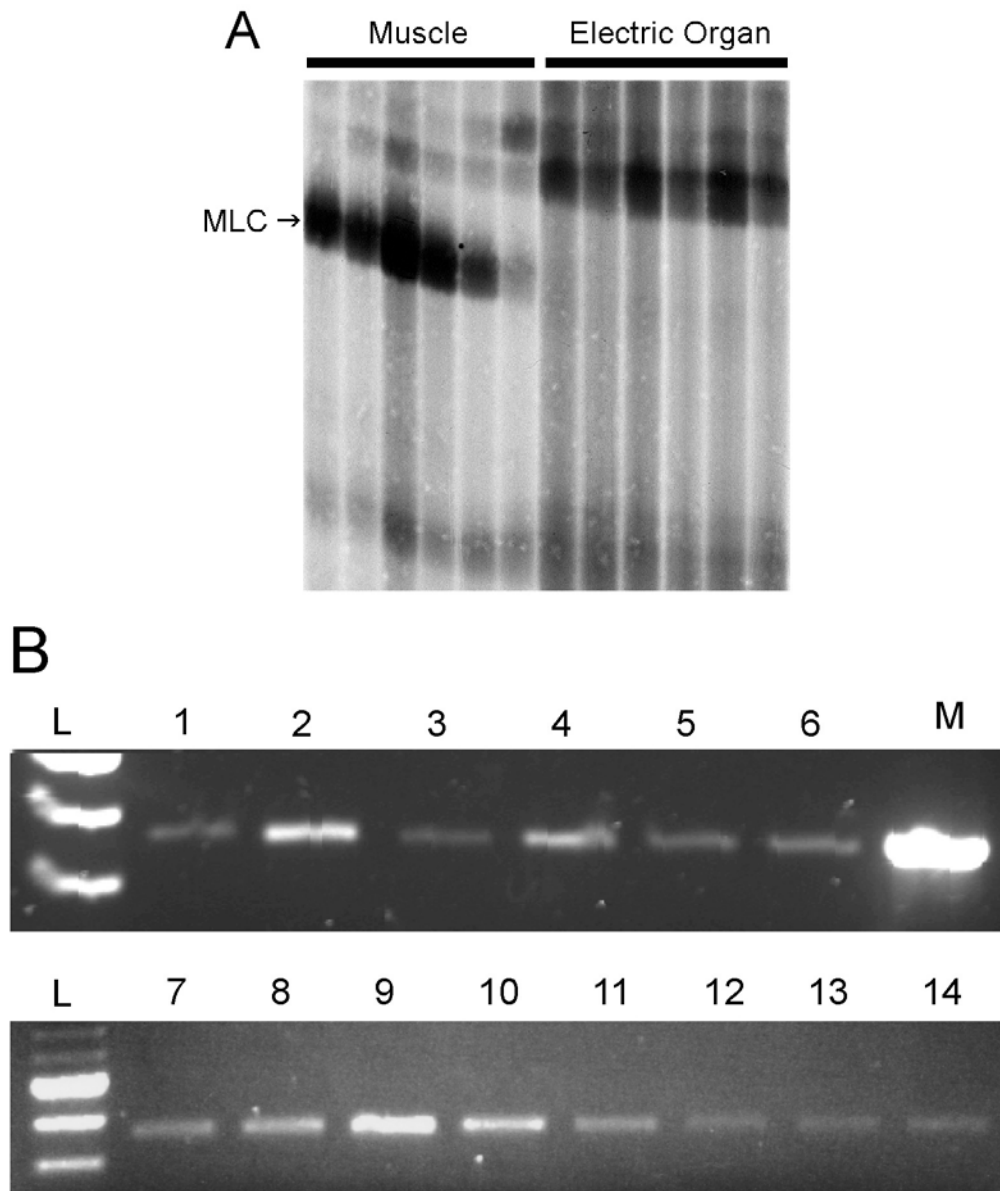


**Figure 2.14 Amplification of myosin light chain was used to screen total RNA samples from electric organ.** **A:** Differential display RT-PCR showed myosin light chain (MLC) is strongly expressed in the muscles of 6 individual fish, but not in the electric organs from the same group of fish. **B:** RT-PCRs with MLC primers were used to screen electric organ total RNA samples. 1 to 14 are 14 individual fish. M is muscle. Samples with visually higher MLC expression (fish #2 and #9) were removed from further real time quantitative RT-PCR tests.

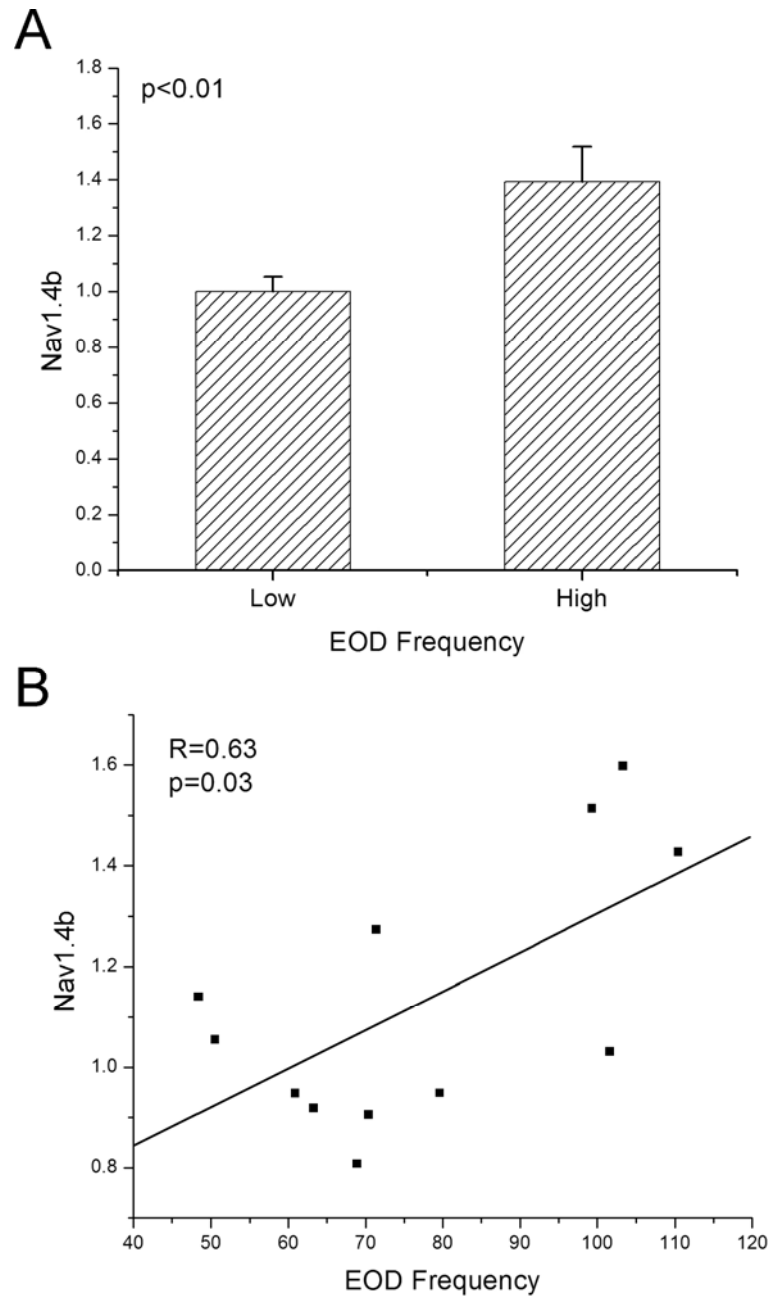


**Figure 2.15 Real-time quantitative RT-PCR showed mRNA level of smNav1.4b correlates with EOD frequency. A.** mRNA of smNav1.4b is at a significantly ( $p < 0.01$ ) higher level ( $1.39 \pm 0.13$ ) in high frequency fish ( $> 100$  Hz,  $n = 4$ ) than the level ( $1.00 \pm 0.05$ ) in low frequency fish ( $< 80$  Hz,  $n = 8$ ). **B.** The normalized mRNA level of smNav1.4b in each individual fish positively correlates with its EOD frequency ( $R = 0.63$ ,  $p = 0.03$ ).

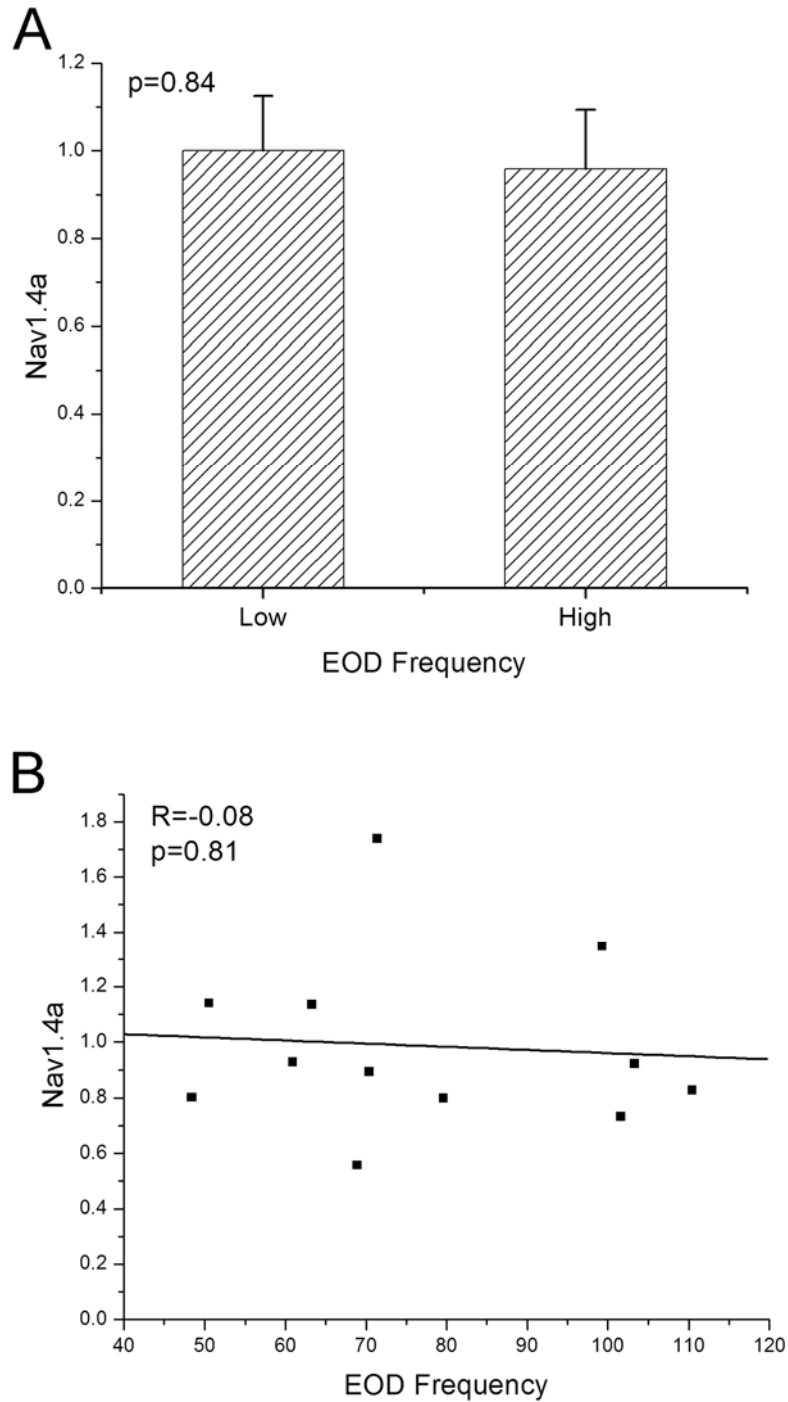


**Figure 2.16 Real-time quantitative RT-PCR showed mRNA level of smNav1.4a does not correlate with EOD frequency** **A.** mRNA level of smNav1.4a shows no significant difference ( $p=0.84$ ) between the same groups of high frequency fish ( $0.96 \pm 0.14$ ) in and low frequency fish ( $1.00 \pm 0.13$ ). **B.** The normalized mRNA level of smNav1.4a in each individual fish does not correlate with its EOD frequency ( $R = -0.08$ ,  $p = 0.81$ ).

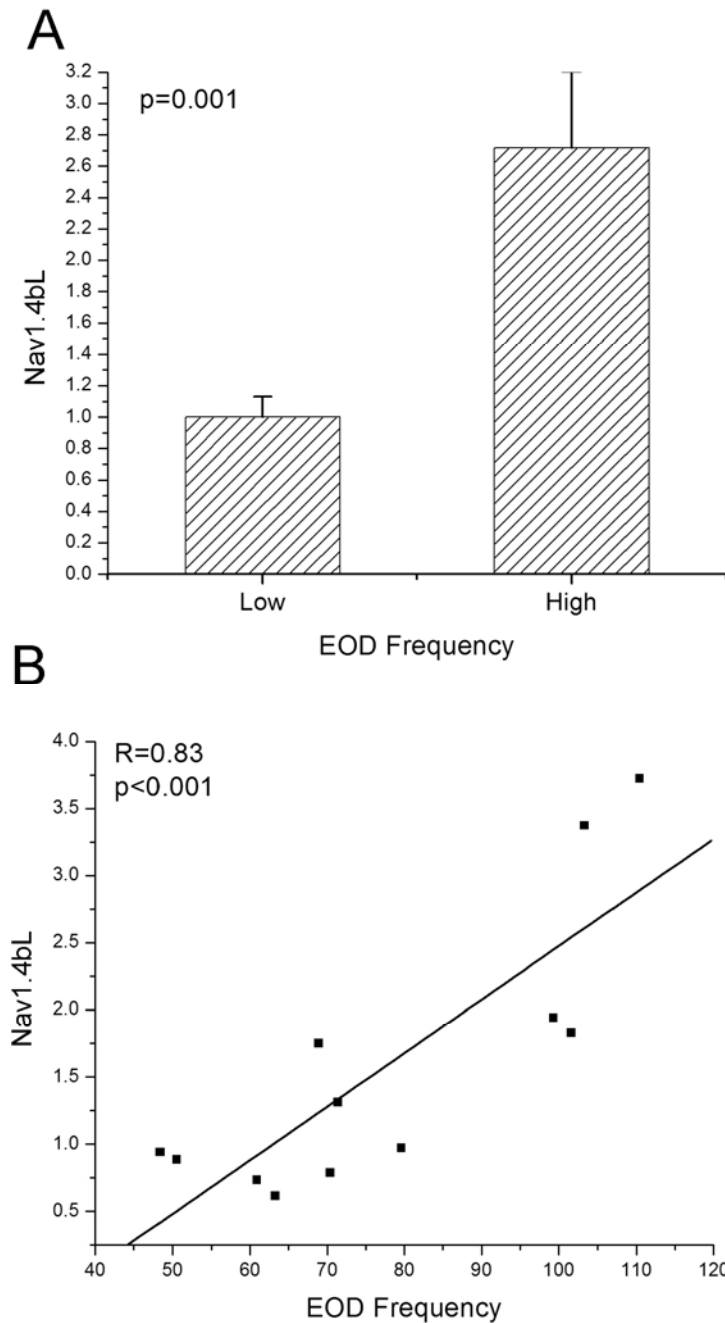


**Figure 2.17 Real-time quantitative RT-PCR showed mRNA level of smNav1.4bL correlates with EOD frequency. A.** The group of low frequency fish shows lower mRNA level of the smNav1.4bL than the high frequency fish (low:  $1.00 \pm 0.13$ ,  $n=8$ ; high:  $2.71 \pm 0.49$ ,  $n=4$ ;  $p=0.001$ ) **B.** the mRNA level of smNav1.4bL in each individual fish positively correlates with the EOD frequency ( $R=0.83$ ,  $p<0.001$ .)

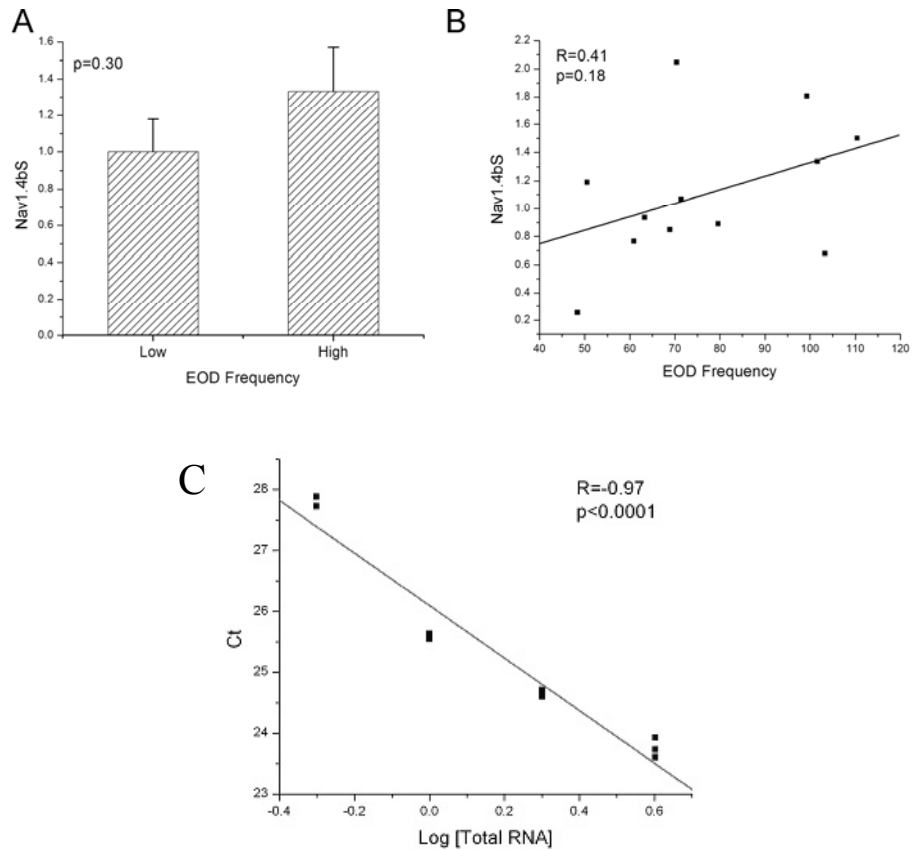


**Figure 2.18 Real-time quantitative RT-PCR showed mRNA level of smNav1.4bS does not correlate with EOD frequency. A.** No significant difference is observed with smNav1.4bS (low:  $1.00 \pm 0.18$ ,  $n=8$ ; high  $1.33 \pm 0.24$ ,  $n=4$ ;  $p=0.30$ ). **B.** The mRNA level of smNav1.4bS in each individual fish does not correlate with the EOD frequency ( $R=0.41$ ,  $p=0.18$ ) **C.** Standard curve in real time quantitative RT-PCR, showing the method remains quantitative after modification.

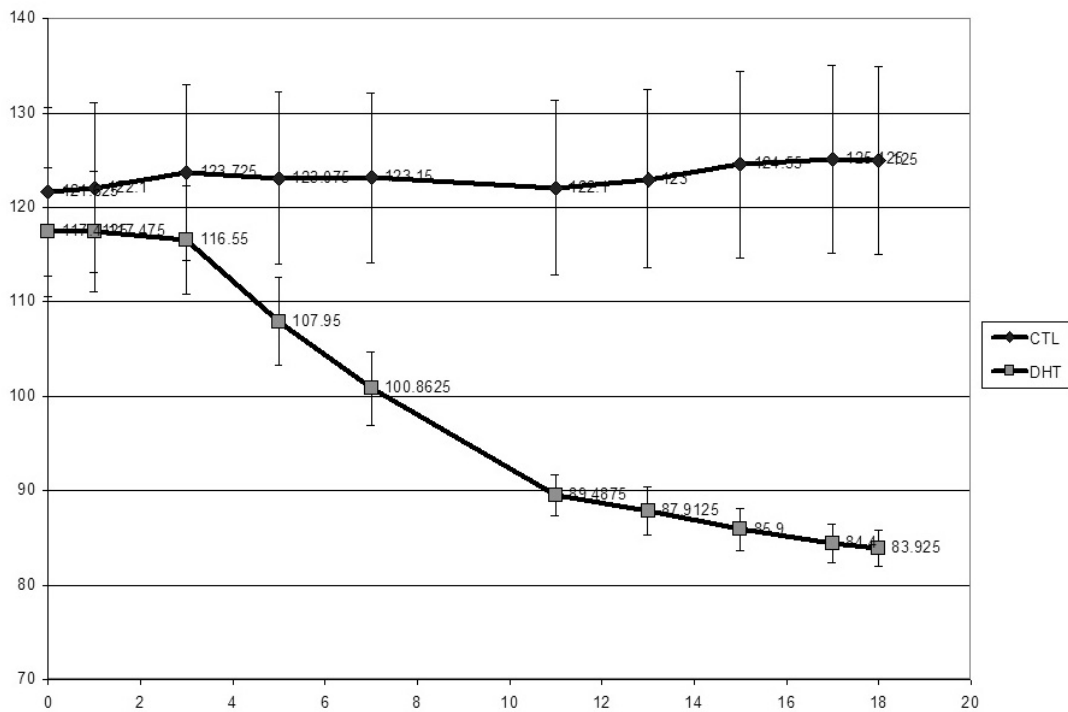


**Figure 2.19 DHT lowered EOD frequency of *Sternopygus*.**

Capsules containing DHT or empty capsules were implanted on day 0. EOD frequency was monitored the day after and every other day after. The EOD frequency was dropped a statistically significantly lower level on day 7.

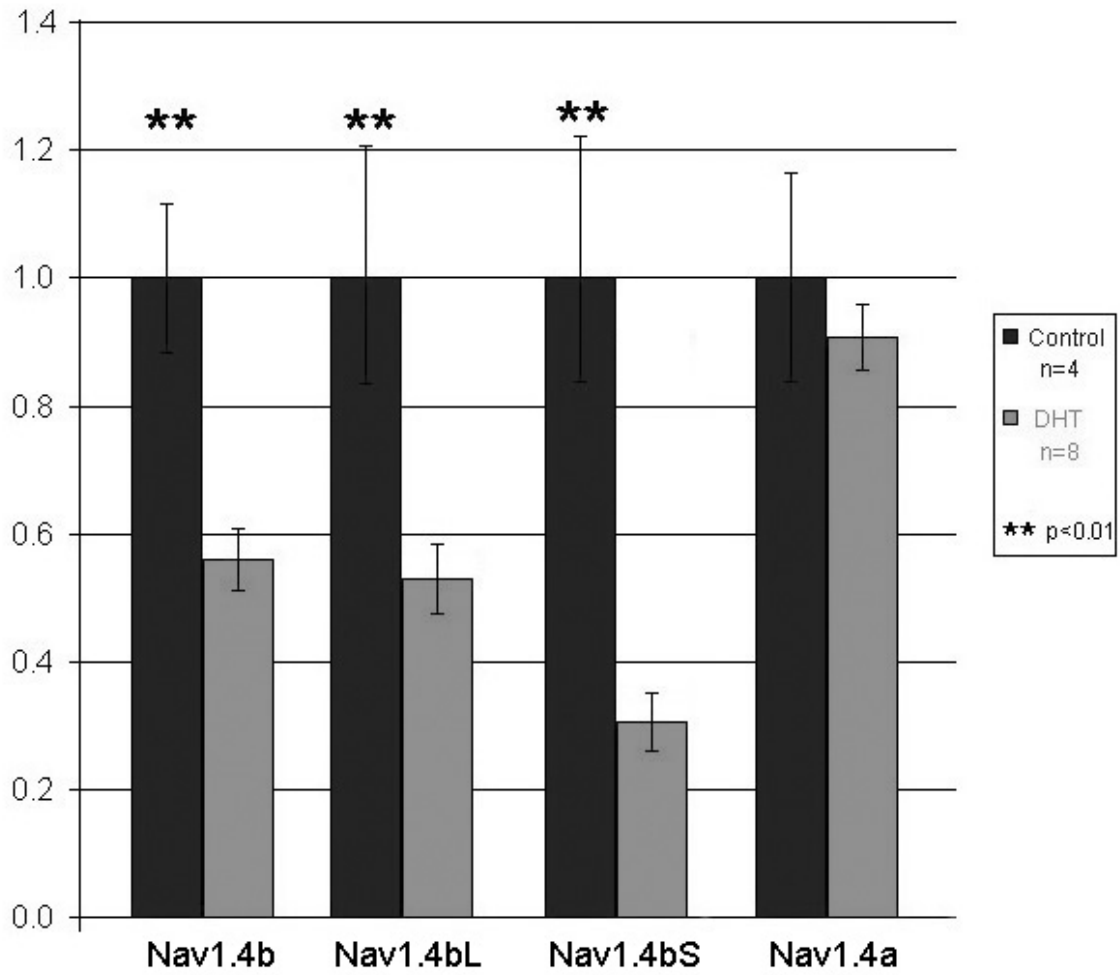


**Figure 2.20 DHT lowered the mRNA levels of Nav1.4b (Nav1.4bL and Nav1.4bS) but not Nav1.4a in *Sternopygus*.**

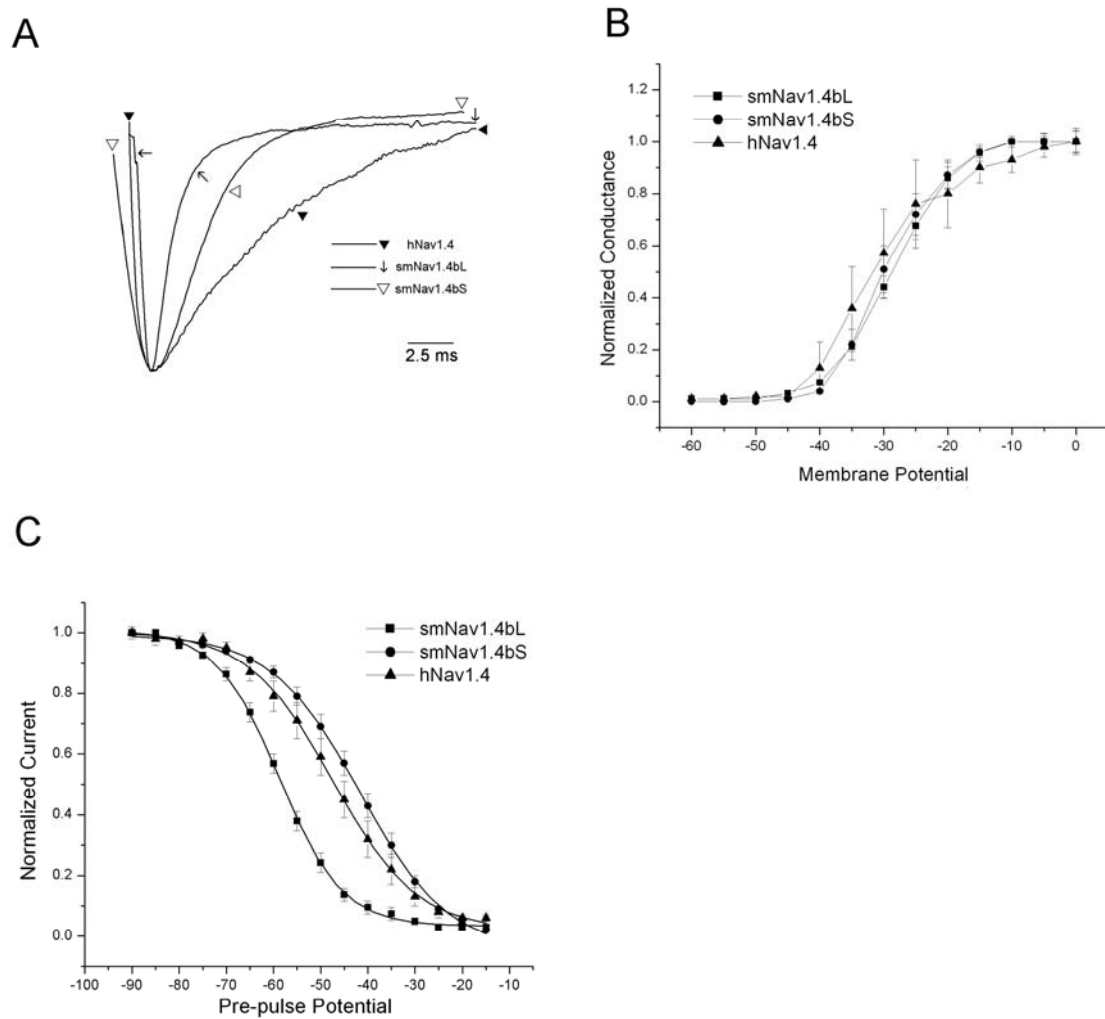


**Figure 2.21 Properties of hNav1.4, smNav1.4bL and smNav1.4bS.**

A. Representative normalized currents of these three sodium channel  $\alpha$  subunits.

B. Voltage-dependence of activation of these channels.

C. Steady-state inactivation curves of these channels.

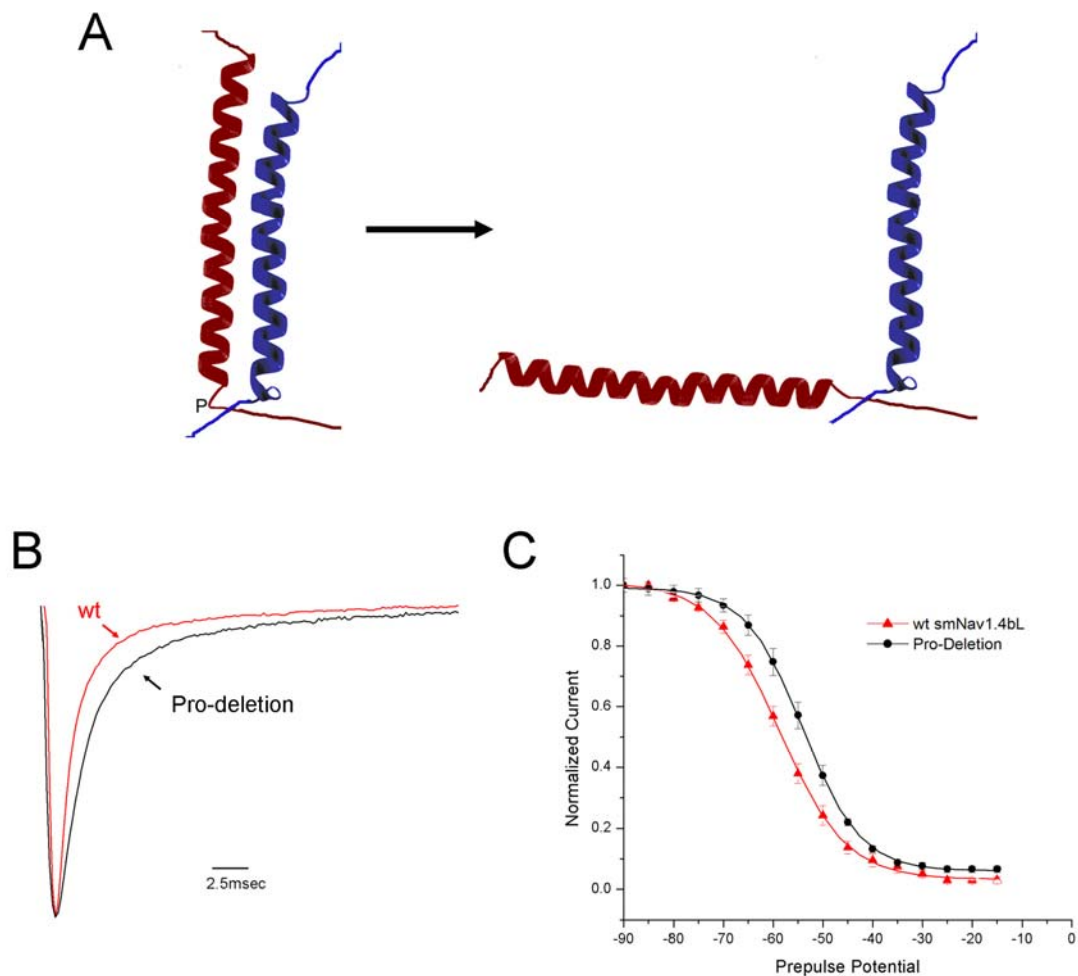


**Figure 2.22 Proline deletion changes the inactivation kinetics of smNav1.4bL.**

A. Schematic hypothetical illustration shows the deletion of a proline (P) next to a helix may bend the direction of the helix thus affects its interaction with other protein structures.

B. Deletion of the proline slows the inactivation of smNav1.4bL.

C. Deletion of the proline positively shifts the inactivation voltage dependence.

---

## CHAPTER 3

# Expression and alternative splicing of sodium channel $\beta 1$ subunit contribute to the individual variation of cellular excitability of electrocytes

---

### Abstract

The electric fish *Sternopygus* emits an electric organ discharge (EOD) composed of a series of pulses. Males emit long pulses at low frequencies, females emit short pulses at higher frequencies, and juveniles emit at intermediate values. Furthermore, EOD frequency and pulse duration are regulated by androgens. The EOD pulse is shaped by a sodium current whose rate of inactivation correlates with EOD frequency and pulse duration, and is modulated by androgens. In this study we tested whether the gradient in sodium current inactivation across EOD frequency might be due to graded regulation by a  $\beta$  subunit. We cloned the sodium channel  $\beta 1$  subunit in *Sternopygus*. We found a novel splice form of this gene and differential expression of  $\beta 1$  splice forms in different tissues. In the electric organ the mRNA levels of this gene and the splicing preference for one form correlate with EOD frequency. Androgen implants decreased the total  $\beta 1$  mRNA levels but did not affect splicing. Co-expression of each splice form in *Xenopus* oocytes with either the human muscle sodium channel gene, hNav1.4, or a *Sternopygus* ortholog, smNav1.4b, sped the rate of inactivation of the sodium current and shifted the steady-state inactivation leftward. The behavior of the fish  $\alpha$  and co-expressed  $\beta 1$  subunits in the oocyte replicate most of the properties of the electric organ's endogenous sodium current. These data highlight the role of ion channel  $\beta$  subunits in regulating cellular excitability.

## Introduction

Voltage-gated sodium channels initiate and propagate the action potential in excitable cells. A sodium channel is usually composed of a large (>200kD), pore-forming  $\alpha$  subunit and one or two relative smaller (<40kD), auxiliary  $\beta$  subunits. Four  $\beta$  subunits have been identified to date (Isom et al., 1992; Isom et al., 1995; Morgan et al., 2000; Yu et al., 2003). Among them, the  $\beta 1$  subunit was the first to be identified, most commonly distributed, and best characterized. The  $\beta 1$  subunit has been cloned from several mammalian species and it exhibits similar structures and functions. In addition, two mRNA splicing variants of  $\beta 1$  subunit have been identified in rat and human (Kazen-Gillespie et al., 2000; Qin et al., 2003).

The  $\beta 1$  subunit generally increases the density of  $\alpha$  subunits on the cell membrane and speeds the inactivation of the sodium current (Isom et al., 1992). It also interacts with various molecules such as contactin, tenascin-R and tenascin-C, neurofascin, receptor tyrosine phosphatase  $\beta$ , and ankyrin (Srinivasan et al., 1998; Xiao et al., 1999; Malhotra et al., 2000; Ratcliffe et al., 2000; Kazarinova-Noyes et al., 2001; Malhotra et al., 2002; Mcewen et al., 2004).  $\beta 1$  knock-out mice show a series of phenotypic changes including spontaneous seizures and disrupted nodal architecture, suggesting important roles of  $\beta 1$  subunit in the sodium channel localization and cellular excitability (Chen et al., 2004).

Weakly electric fish emit electric discharges for electrolocation and communication. The electric organ discharge (EOD) is generated by the electric organ, a novel organ that is evolutionally and developmentally differentiated from skeletal muscle (Zakon and Unguez, 1999). The EOD frequency of a sine-wave producing species called the gold-lined knifefish (*Sternopygus macrurus*) is individually unique, sexually

dimorphic, and under hormonal control (Zakon and Unguez, 1999). Previous research has shown that the inactivation kinetics of sodium current in the electrocytes of this species are correlated with individual and sex differences in the EOD frequency and can be modulated by long-term androgen treatment (Ferrari et al., 1995; Mcanelly and Zakon, 2000). However, the molecular mechanisms of this variation are not known.

Because graded expression of  $\beta 1$  subunit with a sodium channel  $\alpha$  subunit results in graded inactivation kinetics (Meadows et al., 2002), we tested the possible role of the  $\beta 1$  subunit in regulating the *Sternopygus* electrocyte sodium current. We found that  $\beta 1$  is expressed in a gradient with EOD frequency, regulated by androgens, and influences steady-state and fast inactivation of co-expressed sodium channels in a manner consistent with the natural variation of the endogenous current.

## **Materials and Methods**

### **Cloning $\beta 1$ subunit in *Sternopygus***

RNA isolation and RT-PCR procedures followed the same protocol as described in Chapter 2. The two degenerate primers used initially to clone the transmembrane domain of  $\beta 1$  subunit are listed in Table 3.1.

The sequence was extended with 5' and 3' RACE with the methods described in Chapter 2. The primers used are listed in Table 3.1.

Table 3.1 Primers Used in Cloning  $\beta$ 1 Subunit of *Sternopygus*

Primer Name	Target Domain	Sequence
BetaF1	Transmembrane	GAGGGCCGYSTGGHGTGGMAGGGCAG
BetaR1	Transmembrane	ATCTTCYTGTAGCAGTACACCATCTC
3RP1	3' end	GAGGGCCGYSTGGHGTGGMAGGGCAG
3RP2	3' end	TGTTACTTTGACCGAACGCTCAC
5RP1	5' end	TGATGAGAGCAGAGCAGAGGTGTG
5RP2	5' end	TCCTGTAGCAGTAGACCATCTCCAC

### Cloning introns of $\beta$ 1 subunit

Genomic DNA was isolated as previously described (Lopreato et al., 2001) . Six forward primers and four reserve primers were designed and used in 12 PCR reactions to cover the full span of the mRNA. Six most prominent bands were cloned and further sequenced. The intron sequences were identified by the comparison with cDNA sequences.

### Tissue distribution of the $\beta$ 1 subunit splicing forms

Total RNA was isolated from brain, electric organ, heart and muscle of three medium frequency fish as described above. RT-PCR was performed with primers NBF1 (GGATGGGCAGCAAGAACACA) and NBR1 (CGTAGAAGTCCATACCTCAACACACA), or NBF2 (CAGGAGAGGAGGCACTGAGAGA) and NBR2 (AATAAGCTCAA

TGTTTCAGGGATGA). The annealing temperature was 59 °C for higher specificity. The products were separated in 2% and 3% agarose gels.

### Real-time Quantitative RT-PCR

Real-time Quantitative RT-PCR followed the same procedure as described in Chapter 2. Primer/Probe sets were designed with Primer Express software (Applied Biosystems) and listed in Table 3.2.

Table 3.2 Primers and Probes Used in Real-time Quantitative RT-PCR

Transcript	Amplicon	Sequence	T <sub>m</sub>	
β1	84bp	467F	CGCACCAACACCACCAAGTA	59 °C
		551R	TCATCACCTCTGACAGGATCGA	59 °C
		P508	TAAGGCATCGCGTGGCA	70 °C
β1L	85bp	644F	AGAGAGCGCGGCTGAGTATT	60 °C
		729R	GGCTCTGCGTTATTCTGCTACTG	60 °C
		P678	CCGAGAGCAAAGAT	70 °C
β1S	74bp	626F	CAGGAGAGGAGGCACTGAGAGA	60 °C
		699R	AATAAGCTCAATGTTCAGGGATGA	60 °C
		P694	AGCGCAGCCAAAAC	71 °C

### DHT treatment

Same as described in Chapter 2.

### **Plasmid construction**

Plasmids containing full-length sequences of the two  $\beta 1$  subunits were constructed. First, specific primers were designed before the start codon in the first exon and after the stop codon in the fourth exon to amplify both splice variants in one RT-PCR reaction. The RT-PCR products were ligated in pCR2.1-TOPO vectors (Invitrogen). The clones were sequenced to separate the plasmids containing the cDNA of  $\beta 1L$  or  $\beta 1S$ . Then, the insert of these plasmids were cut out with *EcoRI* and ligated with pGEMHE vectors linearized with *EcoRI* too.

### **Site-directed mutagenesis**

Site-directed mutagenesis was carried out with QuikChange XL Mutagenesis Kit (Stratagene, La Jolla, CA). Two primers containing T to Y codon changes (primer1 GAG AGAGAGCGCAGCCAAATACCCTCTCAAGCTTCATCCC and primer2 GGGATGAGCTTGAGAGGGTATTTGGCTGCGCTCTCTCTC) were used with 10ng  $\beta 1S$ -pGEMHE vector and *Pfu* DNA polymerase to amplify 18 cycles. The product was treated with *Dpn I* to remove the methylated parental DNA template and transformed in XL10-Gold Ultracompetent cells supplied with the kit.

### **Co-expression of $\beta 1$ subunits with Nav1.4 in oocytes**

All followed the same procedures described in Chapter 2.

## Results

### Cloning of sodium channel $\beta$ 1 subunits in *Sternopygus*

An initial fragment of a  $\beta$  subunit was cloned by a one-step RT-PCR with total RNA isolated from the electric organ of *Sternopygus*. The two degenerate primers were based on the highly conserved transmembrane domain of mammalian voltage gated sodium channel  $\beta$ 1 subunits and zebrafish (*Danio rerio*) genomic sequences ([http://www.sanger.ac.uk/Projects/D\\_rerio/](http://www.sanger.ac.uk/Projects/D_rerio/)). Using 5'RACE and 3'RACE, we cloned the full-length cDNA of a sodium channel  $\beta$  subunit in *Sternopygus*, and confirmed the sequence by RT-PCR with primers outside the ORF (data not shown). We used the *Sternopygus* sequence to search the zebrafish, green spotted pufferfish (*Tetraodon nigroviridis*: <http://www.genoscope.cns.fr/externe/tetranew/>), and Fugu (*Takifugu rubripes*: <http://fugu.biology.qmul.ac.uk/>) genome and EST databases for other putative fish  $\beta$  subunits, and aligned them with those of human and *Xenopus*  $\beta$  subunits. A phylogenetic analysis indicates that fish have orthologs of  $\beta$ 1-3; we were unable to locate  $\beta$ 4 in any of the fish genome or EST databases (Fig. 3.1).

Alignment of the *Sternopygus*  $\beta$ 1 subunit and its rat ortholog (Fig. 3.2) shows that, despite the highly conserved transmembrane and intracellular domains, the extracellular domain only has limited similarity to the rat  $\beta$ 1 subunit (46% identity and 9% similarity). Nevertheless, it retains almost all the important amino acids studied to date which confirms the importance of these residues (McCormick et al., 1998; McCormick et al., 1999; Mcewen et al., 2004).

In addition, the first exon cloned by 5' RACE showed various lengths (Fig. 3.3),

suggesting multiple ( $\geq 3$ ) transcription initiation sites may exist. Nevertheless, all the first exons include the first start codon and, thus, would be translated into the same N terminal end. The C terminus varied due to alternative splicing (see next section).

### **Tissue distribution, gene structure, and alternative splicing of sodium channel $\beta 1$ subunit**

An RT-PCR performed to investigate the expression pattern in brain, electric organ, heart, and skeletal muscle revealed a distinct tissue distribution pattern (Fig. 3.4). A long product (~630bp) was expressed in brain, while a shorter product (~560bp) was expressed in muscle. Interestingly, the electric organ, and to a lesser extent the heart, expresses both forms. This expression pattern was confirmed with another pair of primers (Fig. 3.4) that gave smaller PCR products (145bp and 73bp) allowing for better resolution on the gel. This suggested the possibility of alternative splicing at the 3' end of the transcript.

To investigate the possibility of splicing, we identified the structure of this gene in genomic DNA. It consists of four exons and three introns (Fig. 3.5). The first start codon is located at 55bp of the first exon and the third exon contains the first stop codon. The gene structure is very different from its mammalian ortholog with six exons (Makita et al., 1994). By comparison with the gene structure of the human sodium channel  $\beta 1$  subunit, we found that exon2 and exon3 of *Sternopygus* correspond to human exon4 and exon5 respectively, while exon 1 of *Sternopygus* corresponds to the first three exons together in human. The sequence homology between the translational products of *Sternopygus* exon1 and the first three human exons is only 44% identity and 9%

similarity, but 68% identity and 15% similarity after that. It suggests there are greater changes in the first three exons, which cover most of the extracellular domain. The exon/intron structure of  $\beta 1$  in zebrafish is identical to that of *Sternopygus*. Since the exon/intron organization of the human  $\beta 1$  subunit gene is shared with the  $\beta 1$  gene of tetraodon as well as the human, zebrafish, and tetraodon  $\beta 3$  genes (data not shown), this must be the ancestral pattern.

The two RT-PCR products result from alternative splicing. The longer mRNA transcript containing all the four exons, can be translated into a protein (as shown in Fig. 3.2) comparable to mammalian  $\beta 1$ ; because the protein is longer, we refer to it as  $\beta 1$ Long ( $\beta 1L$ ). The shorter mRNA transcript, named  $\beta 1$ Short ( $\beta 1S$ ), lacks the third exon in the spliced mRNA and ends the open reading frame in the fourth exon; thus, it is translated into a shorter protein with a very different sequence at the end of the intracellular domain (Fig. 3.6). In this region, a tyrosine interacts with ankyrin and sodium channel  $\alpha$  subunit (McEwen et al., 2004). This tyrosine is replaced with a threonine in  $\beta 1S$ . This splicing pattern and the replacement of the C terminus including the tyrosine in  $\beta 1S$  are also found in zebrafish (Hobson and Isom, 2003).

Using real-time quantitative RT-PCR, I quantified the expression level of each splice form in different tissues. Because there is no other known gene that is expressed at constant levels across tissues and can be used as a calibrator gene, we used the ratio of  $\beta 1S$  to total  $\beta 1$  ( $\beta 1L + \beta 1S$ ) to represent the splicing pattern in each tissue. In different individuals, brain consistently shows exclusive expression of  $\beta 1L$  with no detectable  $\beta 1S$ . Muscle has a fairly stable but low ratio of about 5%. Heart and electric organ have

relatively higher percentage (~20% and ~35%) of the longer splice form, but on the other hand show greater individual variation. Due to the individual variation, which will be focused on later in this report, these quantitative results are only representative estimations but are consistent with the expression pattern seen in Figure 3.4.

### **Correlation between expression/splicing and EOD frequency**

I used real-time quantitative RT-PCR to examine the correlation between the mRNA levels of the  $\beta 1$  gene and each splice variant in the electric organ and the fish's EOD frequencies. Same TaqMan real-time quantitative RT-PCR as the method in Chapter 2 was used.

The amplification of exon1 and 2 of the  $\beta 1$  gene, which are common to both splice forms, was used to assay the total  $\beta 1$  mRNA level. As shown in Figure 3.7A, levels of total  $\beta 1$  mRNA were higher ( $1.68 \pm 0.36$ ) in fish with high EOD frequencies ( $> 100$  Hz,  $n = 4$ ) and lower ( $1.00 \pm 0.11$ ) in fish with low EOD frequencies ( $< 80$  Hz,  $n = 8$ , t-test  $p=0.05$ ). The normalized mRNA level of each individual fish positively correlated with its EOD frequency (Fig. 3.7B,  $R = 0.62$ ,  $p = 0.03$ ).

I also assayed each form of  $\beta 1$  with splice form-specific primers. The group of fish with low EOD frequencies had lower expression of  $\beta 1S$  than fish with high EOD frequencies (Fig. 3.8A, low:  $1.00 \pm 0.13$ ,  $n=8$ ; high:  $1.62 \pm 0.31$ ,  $n=4$ ;  $p=0.05$ ), while there was no significant difference observed with  $\beta 1L$  (Fig. 3.9A, low:  $1.00 \pm 0.10$ ,  $n=8$ ; high:  $0.81 \pm 0.15$ ,  $n=4$ ;  $p=0.31$ ). Furthermore, the mRNA level of  $\beta 1S$  in each individual fish positively correlated with the EOD frequency (Fig. 3.8B,  $R= 0.66$ ,  $p=0.02$ .), while  $\beta 1L$

did not (Fig. 3.9B,  $R = -0.42$ ,  $p = 0.17$ ). Conceptual addition of the values for two splice forms is consistent with the pattern of total mRNA using common primers.

I then asked whether splicing preference (the ratio of  $\beta 1S/\beta 1L$ ) correlates with EOD frequency. The  $\beta 1S/\beta 1L$  ratio was positively correlated with EOD frequency (Fig. 3.10B,  $R = 0.72$ ,  $p = 0.01$ ). The average ratio was  $1.00 \pm 0.21$  in low EOD frequency ( $< 80$  Hz,  $n = 8$ ) fish and  $1.80 \pm 0.31$  in high frequency ( $> 100$  Hz,  $n = 4$ ) fish (Fig. 3.10A,  $p = 0.05$ ).

All values of real-time quantitative PCR result above are relative numbers, (normalized by the average of low frequency fish group), thus don't indicate the absolute abundance of any transcript.

Several characteristics of the  $\beta 1$  subunit splicing in *Sternopygus* directed my attention to polypyrimidine tract binding protein (PTB, also known as hnRNP I), a repressor of exon definition well identified in several other studies. PTB is responsible for the splicing of several genes with differential expression in neurons and non-neuronal cells, such as  $\alpha$ -tropomyosin, GABAA, c-src, NMDAR1, clathrin, BK channel (Wagner and Garcia-Blanco, 2001; Black, 2003). For instance, PTB represses the splicing for a cassette exon of c-src gene in non-neuronal cells, but not neurons (Wagner and Garcia-Blanco, 2001), exactly matching the splicing pattern of  $\beta 1$  in *Sternopygus*. Furthermore, the exon/intron sequence of  $\beta 1$  contains two characteristic regions regulated by PTB: upstream of the regulated exon, CU rich region (68~76%, in *Sternopygus*  $\beta 1$ , 68% CU) and at least two "CUCUCU" elements. I tested whether levels of PTB co-vary with the extent of splicing. I cloned PTB in *Sternopygus* and found four homologous transcripts

encoded by two genes. But the mRNA level of neither of the two PTB gene transcripts in electric organ correlated with EOD frequency (data not shown), suggesting this splicing process is either PTB-independent, or that further post-transcription regulation of PTB occurs.

### **DHT suppresses levels of $\beta 1$ mRNA**

Chronic treatment of *Sternopygus* with DHT lowers EOD frequency, broadens electrocyte action potential duration, and slows the inactivation time constant of sodium current in electrocytes. In this study, I implanted the fish with DHT capsules to test whether androgen treatment affected levels or splicing of  $\beta 1$  subunit mRNA. Compared to the control group which was implanted with empty capsules, the EOD frequency of the DHT-treated fish started to decrease three days after the implant and the difference became statistically significant after seven days (Control:  $123.15 \pm 8.96$  Hz, DHT:  $100.86 \pm 3.90$  Hz,  $p=0.03$ ). We dissected the fish's tails 18 days after the implant when the EOD frequency of the DHT group had stabilized and significantly differed from the control group (Control:  $125.00 \pm 9.94$  Hz, DHT:  $83.92 \pm 1.88$  Hz,  $p=0.0004$ ). I used real-time quantitative RT-PCR to quantify the mRNA levels in the two groups and found the total mRNA level of  $\beta 1$  is lowered by about 20% (Control:  $1.00 \pm 0.07$ , DHT:  $0.82 \pm 0.10$ ,  $p<0.03$ ), while the splicing preference is not significantly changed (Control:  $1.00 \pm 0.14$ , DHT:  $1.19 \pm 0.14$ ,  $p=0.47$ ) (Fig. 3.11).

## **$\beta$ 1 subunits modulate sodium channels in *Xenopus* oocytes**

I examined the functional difference between the two splice variants, to test whether the  $\beta$ 1 subunit speeds up inactivation of fish sodium currents as in mammals, and determine whether fish  $\beta$ 1 subunits are effective in modulating a mammalian  $\alpha$  subunit. I constructed plasmids containing each variant and co-injected cRNAs of either  $\beta$ 1S or  $\beta$ 1L with hNav1.4 cRNA or the *Sternopygus* orthologs (smNav1.4bL and smNav1.4bS) into *Xenopus* oocytes and recorded sodium currents with two-electrode voltage clamp.

The effects of expression of  $\beta$ 1: $\alpha$  subunits in a ratio of 6:1 or 20:1 were statistically indistinguishable. This verified that the  $\beta$ 1 subunits were present in saturating concentrations and also allowed us to pool these data for subsequent analyses.

Co-expression of the  $\beta$ 1 subunit had no effect on the activation voltage of either sodium channel  $\alpha$  subunit. Similar to the effect of mammalian  $\beta$ 1 subunits on mammalian sodium channels when co-expressed in oocytes or CHO cells (Isom et al., 1992; Bennett et al., 1993; Patton et al., 1994; Isom et al., 1995; Qu et al., 1995) except one report (Qu et al., 2001), both  $\beta$ 1L and  $\beta$ 1S shifted the steady-state inactivation of hNav1.4 to slightly more hyperpolarized values, and significantly sped up  $\tau_h$  (Fig. 3.12, Table 3.3).

When co-expressed with smNav1.4bS,  $\beta$ 1L and  $\beta$ 1S both shifted the steady-state inactivation curve strongly leftward by -20 mV (Fig. 3.13, Table 3.3). They also significantly sped up  $\tau_h$ . Since smNav1.4bS alone inactivates more rapidly than hNav1.4, the effect of  $\beta$ 1 on its  $\tau_h$  was less dramatic than it was for hNav1.4; but the rates of  $\tau_h$  for both  $\alpha$  sodium channel types co-expressed with the  $\beta$ 1 were similar. There was no

significant difference in the ability of  $\beta 1L$  and  $\beta 1S$  to influence fast or steady-state inactivation of smNav1.4bS.

Interestingly, both inactivation  $\tau_h$  and voltage dependence of smNav1.4bL alone are unique, even exceeding the state of smNav1.4bS modulated by  $\beta 1$  subunits (Table 3.3). Like the other two  $\alpha$  subunits, when co-expressed with  $\beta 1$  subunits,  $\tau_h$  of smNav1.4b was further sped up by both  $\beta 1$  subunits, although much less dramatically. However, unlike the obvious effect on the other two  $\alpha$  subunits, the steady-state inactivation of smNav1.4bL was not shifted significantly by  $\beta 1L$  or  $\beta 1S$ .

Table 3.3  $\beta 1$  subunits modulate the kinetic properties of sodium channels

		hNav1.4		smNav1.4bS		smNav1.4bL	
Activation $V_{1/2}$ (mV)	$\alpha$ only	-28.66±3.3	n=8	-28.53 ± 1.51	n=10	-26.86 ± 0.70	n=15
	$\alpha + \beta 1L$	-24.60±1.35	n=24	-30.30 ± 0.99	n=14	-28.07 ± 1.42	n=8
		p1=0.18		p1=0.32		p1=0.40	
	$\alpha + \beta 1S$	-25.69±1.17	n=16	-31.16 ± 1.38	n=9	-28.74 ± 1.18	n=16
		p1=0.3		p1=0.22		p1=0.18	
Inactivation $V_{1/2}$ (mV)	$\alpha$ only	-48.35±2.37	n=11	-43.01± 1.48	n=21	-58.98 ± 0.94	n=15
	$\alpha + \beta 1L$	-52.76±0.92	n=24	-59.22± 1.33	n=10	-61.85 ± 1.15	n=7
		p1=0.04		p1=1x 10 <sup>-7</sup>		p1=0.08	
	$\alpha + \beta 1S$	-52.02±0.93	n=16	-56.18± 1.19	n=24	-61.03 ± 1.31	n=13
		p1=0.12 p2=0.59		p=1x 10 <sup>-8</sup> , p2=0.15		p=0.20 , p2=0.69	
Inactivation $\tau_h$ (msec)	$\alpha$ only	9.04± 0.18	n=26	2.63± 0.10	n=14	1.31± 0.05	n=14
	$\alpha + \beta 1L$	1.23± 0.08	n=23	1.81± 0.15	n=12	0.78 ± 0.03	n=7
		p1<1x 10 <sup>-31</sup>		p1<0.0001		p1<1 x 10 <sup>-6</sup>	
	$\alpha + \beta 1S$	2.09± 0.14	n=21	1.95± 0.11	n=22	1.08± 0.08	n=23
		p1<1x 10 <sup>-26</sup> p2<1x10 <sup>-5</sup>		p1=0.0003, p2=0.46		p1=0.04, p2=0.05	

\*p1 compared to “ $\alpha$  only”, p2 compared to  $\alpha + \beta 1L$

### **$\beta$ 1S-181Y has a reduced effect on $\alpha$ subunits**

A tyrosine Y181 (equivalent position using the amino acid numbering system originally proposed in Isom *et al.* 1992) in the  $\beta$ 1 subunit plays an important role in  $\beta$ 1-ankyrin interactions and modulation of  $\beta$  subunit (Mcewen *et al.*, 2004), but in  $\beta$ 1S, this tyrosine is replaced by a threonine (Fig. 2). To examine if this replacement influences  $\beta$ 1S function, we changed the threonine to tyrosine in  $\beta$ 1S by site-directed mutagenesis and examined its functions with smNav1.4 and hNav1.4 in *Xenopus* oocytes. Mutant  $\beta$ 1S showed a reduced ability to shift the steady-state inactivation of smNav1.4b and the  $\tau_h$  of both  $\alpha$  subunits (Table 3.4).

Table 3.4  $\beta$ 1S-181Y has a reduced effect on  $\alpha$  subunits

		hNav1.4	smNav1.4bS
Inactivation $V_{1/2}$ (mV)	$\alpha$ only	-48.35±2.37 n=11	-43.01± 1.48 n=21
	$\alpha + \beta$ 1S	-52.02±0.93 n=16 p1=0.12	-56.18± 1.19 n=24 p1=1x 10 <sup>-8</sup>
	$\alpha + \beta$ 1S-181Y	-51.07±1.63 n=19 p1=0.26, p2=0.54	-48.20 ±1.21 n=8 p1=0.05, p2=0.001
Inactivation $\tau_h$ (msec)	$\alpha$ only	9.04± 0.18 n=26	2.63± 0.10 n=14
	$\alpha + \beta$ 1S	2.09± 0.14 n=21 p1<1x 10 <sup>-26</sup>	1.95± 0.11 n=21 p1=0.0003
	$\alpha + \beta$ 1S-181Y	4.61±0.31 n=15 p1<1x 10 <sup>-12</sup> , p2<1x 10 <sup>-8</sup>	2.32±0.16 n=11 p1=0.09, p2= 0.07

p1 compared to “ $\alpha$  only”, p2 compared to  $\alpha + \beta$ 1S

### Proline deletion does not affect the modulation of smNav1.4bL by $\beta$ 1L

smNav1.4bL and smNav1.4bS only differ in an extended N terminus of 51 residues, but respond differently to the modulation of  $\beta$ 1 subunits, especially  $\beta$ 1L. As the initial effort to understand this difference, I generated a mutant construct with the deletion of a proline (P30) immediately after the predicted positively-charged helix in the extended N terminal segment. The voltage dependence of this mutant lies between smNav1.4bL and smNav1.4bL, but  $\tau_h$  is slowed close to smNav1.4bS (see Chapter 2 for details). Similar to the co-expression of  $\beta$ 1L and wild-type smNav1.4, co-expression of  $\beta$ 1L with this mutant sped  $\tau_h$ , but had no significant effect on voltage dependence of activation and inactivation (Table 3.5).

Table 3.5 Co-expression of  $\beta$ 1L with mutant smNav1.4bL with a proline deletion

		smNav1.4bL		smNav1.4bL (Pro30 deletion)	
Activation $V_{1/2}$ (mV)	$\alpha$ only	-26.86 $\pm$ 0.70	n=15	-27.99 $\pm$ 0.98	n=17
	$\alpha$ + $\beta$ 1L	-28.07 $\pm$ 1.42	n=8 p=0.40	-26.90 $\pm$ 0.80	n=7 p=0.51
Inactivation $V_{1/2}$ (mV)	$\alpha$ only	-58.98 $\pm$ 0.94	n=15	-53.91 $\pm$ 0.78	n=21
	$\alpha$ + $\beta$ 1L	-61.85 $\pm$ 1.15	n=7 p=0.08	-53.56 $\pm$ 1.73	n=11 p=0.83
Inactivation $\tau_h$ (msec)	$\alpha$ only	1.31 $\pm$ 0.05	n=14	2.45 $\pm$ 0.19	n=26
	$\alpha$ + $\beta$ 1L	0.78 $\pm$ 0.03	n=7 p < 1 x 10 <sup>-6</sup>	1.72 $\pm$ 0.16	n=15 p = 0.03

p compared to “ $\alpha$  only”,

## Discussion

Beta subunits influence sodium channel gating and insertion (Isom et al., 1992; Makita et al., 1994; Catterall, 2000; Isom, 2001; Isom, 2002), they are developmentally regulated (Sutkowski and Catterall, 1990; Sashihara et al., 1995), and mutations in the  $\beta 1$  subunit are implicated in GEFS+ epilepsy (Spampanato et al., 2001). Nevertheless, little is known about the factors that control their regulation or participation in physiological plasticity. In this study, we used a weakly electric fish, *Sternopygus*, to investigate sodium channel  $\beta 1$  subunit regulation because of several advantages of this model system. First, the electric organ contains a large number of cells with similar cellular excitability allowing us to harvest ample tissue with a uniform cellular phenotype from a single individual (Ferrari and Zakon, 1989; Ferrari et al., 1995). Secondly, in this species there is a strong correlation between a behavioral parameter — EOD frequency—and a sodium current parameter—inactivation time constant (Ferrari et al., 1995). Thus, we are able to compare an easily derived measure of cellular excitability with accurate measures of mRNA levels in a homogenous tissue on an individual basis. Finally, steroid hormones, such as DHT, modulate EOD frequency and sodium current kinetics (Mills and Zakon, 1991; Ferrari et al., 1995), providing a powerful tool for examining modulation of  $\beta 1$  subunits as an agent of cellular plasticity.

### **$\beta 1$ subunits modulate sodium channel kinetics**

Multiple studies have shown  $\beta 1$  subunit modulates the kinetics of different sodium channels in different expression systems (Isom et al., 1992; Makita et al., 1994;

Isom et al., 1995; Qu et al., 2001; Meadows et al., 2002), but the mechanism is largely unclear. One study (McCormick et al., 1998) showed that the intracellular domain is needed for the association with  $\alpha$  subunits but the extracellular domain is required for the functional modulation. The Ig fold may serve as a scaffold to present the negatively charged residues to the  $\alpha$  subunit. However, even though the modulation may be initiated outside of the membrane, it does not rule the possibility the effect will be transduced inside the membrane, where the inactivation gate and its receptor sites are located.

In this study, the variation of  $\alpha$  subunits provides additional understandings on the modulation of sodium channel kinetics by  $\beta 1$  subunits ( $\beta 1L$  and  $\beta 1S$  in *Sternopygus macrurus*).  $\beta 1$  subunits have no significant effects on the activation voltage dependence of any  $\alpha$  subunit co-expressed in our experiments (hNav1.4, smNav1.4bS, smNav1.4bL and smNav1.4bL-P30-deletion). The extended N terminal segment of smNav1.4bL makes its inactivation faster than smNav1.4bS. Regardless of the presence of this segment (smNav1.4bL vs. smNav1.4bS), or the status of this segment (wild-type smNav1.4bL vs. proline deletion mutant), the  $\beta 1$  subunit always speeds up  $\tau_h$ , thus suggesting the modulations on  $\tau_h$  by the N-terminal segment and  $\beta 1$  subunit are additive and independent.

On the other hand, when given to smNav1.4bS, the extended N terminal segment, as well as the  $\beta 1$  subunits, negatively shifts the voltage dependence. But when they co-exist (smNav1.4bL and  $\beta 1$ ),  $\beta 1$  doesn't cause any further shift. This suggests the modulations on voltage dependence by the N terminal segment and  $\beta 1$  subunits are competitive or exclusive. Deletion of the proline in the segment partially reversed its

effect, but still does not allow any further modulation by  $\beta 1$  subunits. The data of  $\tau_h$  and voltage dependence together suggest that these two kinetic parameters may undergo independent mechanisms of modulations.

### **Alternative Splicing of the $\beta 1$**

Alternative mRNA splicing increases the diversity and flexibility of gene expression and regulation. One splice product of the sodium channel  $\beta 1$  subunit affects the extracellular domain and may be developmentally important in rats (Kazen-Gillespie et al., 2000). In addition, a novel  $\beta 1$  subunit with an extended exon 3 has been identified in human. It is widely expressed and, although incapable of modulating channel kinetic and steady-state properties, it increases the ionic current conducted by Nav1.2 in *Xenopus* oocytes (Qin et al., 2003).

I cloned the sodium channel  $\beta 1$  subunit from *Sternopygus* and identified two splice variants. One transcript exhibits a high similarity in deduced protein sequence to its mammalian homologues. The other one, a novel splice form, has a different intracellular domain. In this region, an important amino acid identified in previous studies (McEwen et al., 2004), tyrosine181, is replaced by a threonine and the C terminus is also changed in both size and sequence. This splicing pattern is confirmed by an independent study in zebrafish (Hobson and Isom, 2003), suggesting that this pattern is common in teleosts.  $\beta 1L$  is expressed in the brain of adult zebrafish whereas  $\beta 1S$  is only expressed in the brain in early development (Hobson et al., 2004), I observed in adult *Sternopygus* that  $\beta 1L$  is also expressed in brain, and  $\beta 1S$  is expressed in myogenic tissues (muscle, heart, EO). The *Sternopygus* electric organ, and to a lesser extent heart, also express the  $\beta 1L$ .

splice variant.

Developmentally, electric organ derives from the fusion of differentiated muscle fibers (Zakon and Unguez, 1999). As it develops from muscle, the electric organ down-regulates some muscle-specific genes and activates some genes not normally expressed in muscle (Patterson and Zakon, 1996; Unguez and Zakon, 1998). This study shows the gain of mRNA splicing of the  $\beta 1$  subunit. The addition of  $\beta 1L$  in the electric organ may be caused by the induction of neuronal splicing regulators. On the other hand, the splicing for  $\beta 1S$  is still retained and perhaps even actively regulated, suggesting either the neuronal splicing regulator is controlled at certain level or there are two sets of splicing regulators in competition.

Functionally,  $\beta 1L$  is more effective than  $\beta 1S$  in speeding  $\tau_h$  of hNav1.4 although the significance of this is unclear since this is a heterospecific mixing. There was no significant difference in the splice variants' ability to modify steady-state or fast inactivation of smNav1.4b. It is possible that differences between these splice forms would become apparent when the  $\beta 1$  subunits are expressed in non-saturating concentrations or in their native tissues. Specifically, two sodium channel genes are expressed in the electric organ of *Sternopygus* (see below) and it is possible that  $\beta 1L$  and  $\beta 1S$  differentially associate with or modulate these two channel genes in the context of the electrocyte.

A major difference between the two splice forms is the replacement of a functionally critical tyrosine by a threonine in the truncated C terminus of the  $\beta 1S$ . Unlike the complete loss of modulatory functions exhibited when this conserved tyrosine is replaced with glutamate in the mammalian  $\beta 1$  (Mcewen et al., 2004),  $\beta 1S$  modulates

the sodium current kinetics even without a tyrosine at this site suggesting the alternative splicing product retains its essential functions. We tested whether tyrosine and threonine are functionally interchangeable at this site in  $\beta 1S$  by site-directed mutagenesis.  $\beta 1S$ -T181Y had a reduced effect on both hNav1.4 and smNav1.4b suggesting that threonine fits better in the microenvironment of the C terminus of  $\beta 1S$ . However,  $\beta 1S$ -T181Y retained some modulatory function suggesting either tyrosine can replace some of the function of threonine or that residual function results from the rest of the  $\beta 1$  C terminus.

### **$\beta 1$ expression levels correlate with EOD frequency**

The amount of total  $\beta 1$  mRNA correlates with EOD frequency and EOD frequency is correlated with the inactivation rate of the electrocyte sodium current (Ferrari et al., 1995). Levels of smNav1.4bL mRNA also correlate with EOD frequency. Thus, there is a coordinated up-regulation of a sodium channel with fast inactivation kinetics and  $\beta$  subunits which speed inactivation rates further, in fish with rapidly inactivating sodium currents. The contributions from these two genes may be additive or parallel.

Both the differential splicing of the  $\alpha$  subunit of large-conductance calcium-activated potassium (BK) channel and the differential expression of its auxiliary  $\beta 1$  subunit contribute to the electrical tuning of hair cells in the chicken cochlea (Ramanathan et al., 1999). Reminiscent of what we see in the electric organ of *Sternopygus*, the BK channel's  $\beta 1$  subunit shows a gradient of expression in the cochlea along the frequency-tuning axis. The  $\beta$  subunits of the BK channel are molecularly

unrelated to the  $\beta$  subunits of sodium channels (Behrens et al., 2000), suggesting that regulation of the expression of auxiliary channel subunits might be a common means of tuning cellular excitability.

### **$\beta$ 1 mRNA abundance, but not splicing, is regulated by androgens**

In this study, levels of  $\beta$ 1 mRNA were repressed by DHT. DHT implant lowered  $\beta$ 1 expression to about ~80%, which is less than the natural difference between low and high EOD frequency fish (~1.7 fold). In our experiment we used fish with EOD frequencies (~125 Hz) in the middle of the species range (50-200 Hz). DHT lowered the EOD to ~ 80 Hz, a 45Hz drop, which is approximately one third of the total EOD frequency range of this species. Nevertheless, this suggests that the suppression of  $\beta$ 1 by androgens only partially accounts for the regulation of  $\beta$ 1 levels in the population. In this species, EOD frequency is raised by treatment with estrogen and human chorionic gonadotropin (hCG) (Zakon et al., 1990; Dunlap et al., 1997). It is possible that these hormones enhance, rather than suppress, the abundance of  $\beta$ 1.

DHT had no effect on  $\beta$ 1 splicing. Activity-dependent splicing regulation is seen in the BK channel (Xie and Black, 2001). Since each electric fish emits EOD at a unique frequency within the species EOD frequency range, it is possible that the rate at which the electrocytes are being driven influences  $\beta$ 1 splicing. This, however, seems unlikely in that DHT administration, which lowers the EOD frequency, had no effect on splicing.

Steroid hormones can act as ligands for either nuclear transcriptional factors or membrane receptors. Although several studies showed estrogen can modulate subunits of

ion channel, such as the  $\beta 1$  subunit of BK channel (Valverde et al., 1999; Dick et al., 2001; Dick and Sanders, 2001; Dick et al., 2002), *via* intracellular signal independent mechanism, more studies have shown that steroids can enhance or repress gene expression *via* nuclear receptors (Chew and Gallo, 1998; Walters and Nemere, 2004). In our study, DHT showed a slowly induced ( $>2$  days) and long-lasting ( $\sim 3$  weeks) effect, not concurrent with the diffusion time of the implanted steroid, thus it is more likely to act as a co-repressor of the  $\beta 1$  gene and to change cellular excitability in an accumulative way. The steroid repression of gene expression can involve several complex mechanisms (Dobrzycka et al., 2003). Further study on the promoter region of  $\beta 1$  gene and its interaction with androgen receptor and co-repressors may reveal the mechanism.

Beta1 subunits in the heart are developmentally up-regulated by corticosteroids (Fahmi et al., 2004) reinforcing the idea that  $\beta$  subunits may be commonly utilized for fine regulation of electrical responses.

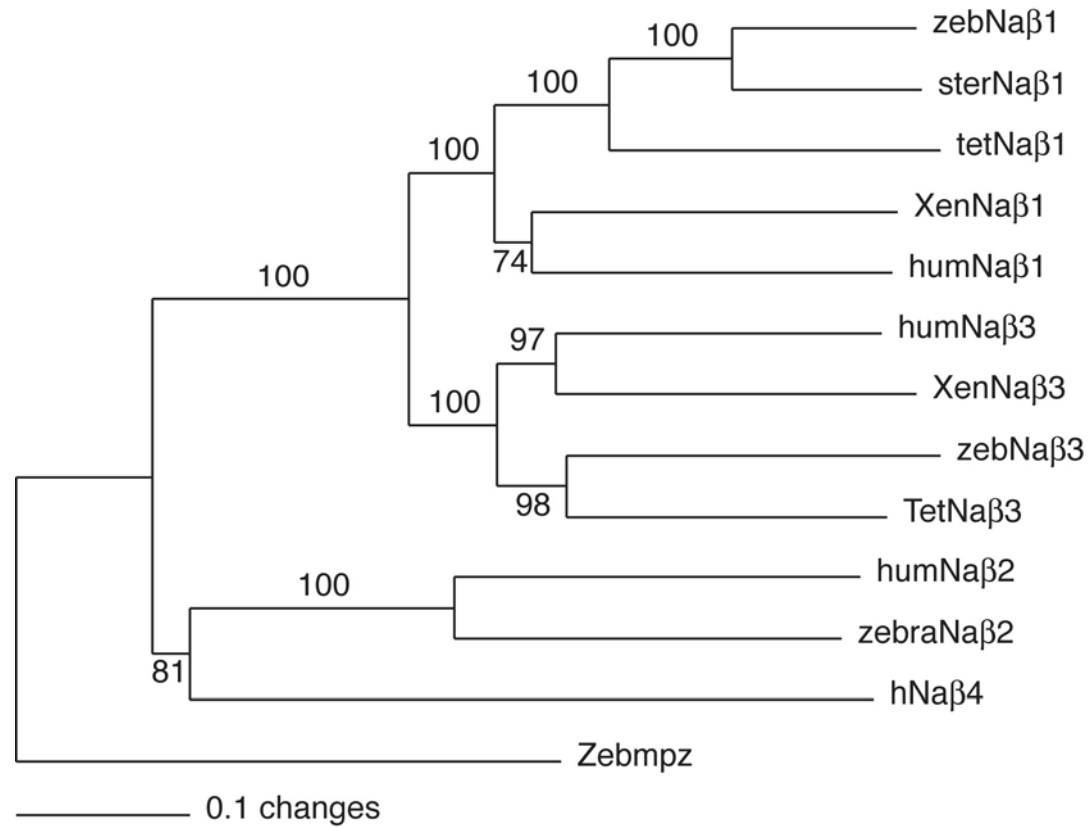


**Figure 3.1 Comparison of  $\beta$ 1 subunit in *Sternopygus* and  $\beta$  subunits in other species.**

Amino acid sequences from human, zebrafish, *Tetraodon*, and *Xenopus* were aligned in ClustalX, imported into PAUP\* (1998) and analyzed by the neighbor joining method. The tree was rooted with a zebrafish myelin P<sub>0</sub> sequence, a distantly related member of the immunoglobulin family. The data were resampled one thousand times to generate bootstrap values, which strongly support the tree.

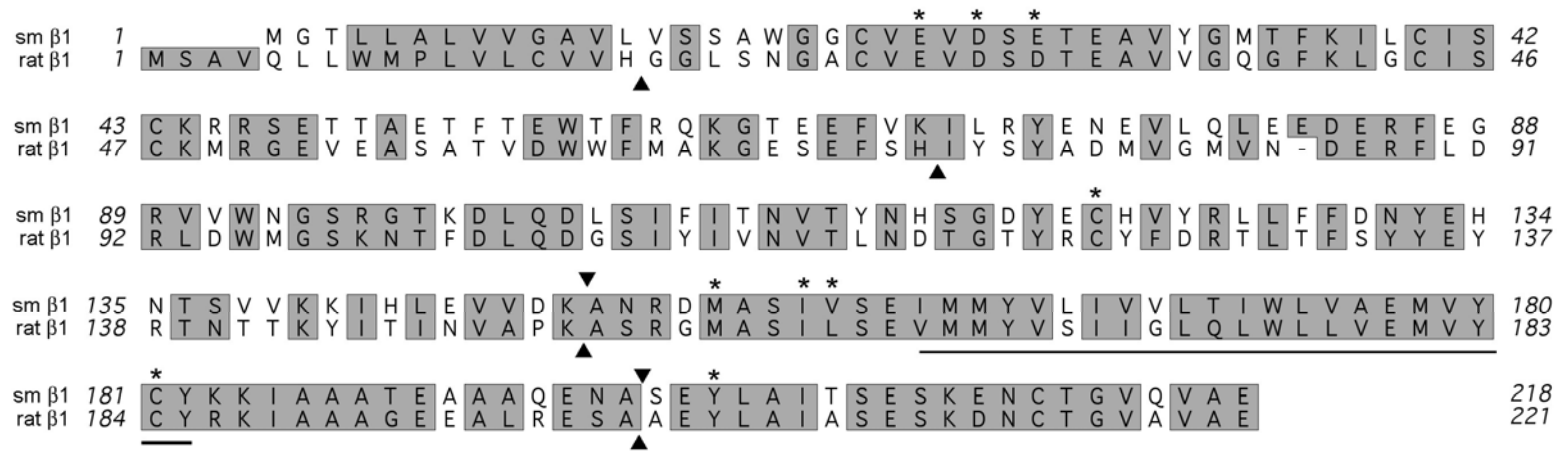


**Figure 3.2 Deduced amino acid sequence alignment between the sodium channel β1 subunit in *Sternopygus macurus* (smβ1) and in rat (rat β1).** The transmembrane domain is underlined. Amino acids identical or functionally similar are shaded with the residues studied previously marked by asterisks above. Triangles (▲) and reverse triangles (▼) indicate the exon boundaries in rat β1 and smβ1 respectively.

```

1  *      *
   gtgCGcgtgagagtgTgcttGtGtGcttgagacgcgaagggacgc
46  tgctcctcagTgaagatgtctgcagTgcagctgctgtggatgccg
      M S A V Q L L W M P
91  ttggTgctgtgtgtggTgcacggTgggctcagcaatggggcatgt
   L V L C V V H G G L S N G A C
136  gtggaggtggactcggacacagaggcggTcgtgggccaaggcttc
   V E V D S D T E A V V G Q G F
181  aaactgggttgcatctcctgtaagatgaggggggaggtagaggcc
   K L G C I S C K M R G E V E A
226  tccgccactgtggactggtggttcatggccaaaggggagagcgag
   S A T V D W W F M A K G E S E
271  tttagccacatctacagttatgctgatatggtgggcatggttaat
   F S H I Y S Y A D M V G M V N
316  gacgaacgcttcctggaccgctggactggatgggcagcaagaac
   D E R F L D R L D W M G S K N
361  acattcgacctgcaagacggctccatctacatcgtcaacgttacc
   T F D L Q D G S I Y I V N V T
406  ttaaatgacacgggcacctaccgctgttactttgaccgaacgctc
   L N D T G T Y R C Y F D R T L
451  accttcagctactacgagtaccgcaccaacaccaccaagtacatc
   T F S Y Y E Y R T N T T K Y I
496  accattaatgtggcacctaag
      T I N V A P K

```

**Figure 3.3** The first exon of sodium channel  $\beta 1$  subunit gene (SCN1B) in *Sternopygus macrurus*. Deduced amino acid sequence is under the nucleotide sequence. Asteroids mark the transcript starting sites revealed by 5' RACE.

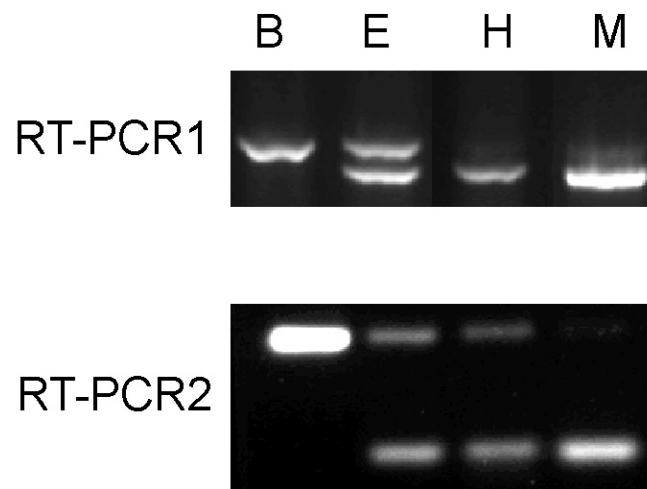


**Figure 3.4 Alternative mRNA splicing of sodium channel  $\beta 1$  subunit in *Sternopygus*.** Expression pattern of the two splice forms in brain (B) electric organ (E), heart (H), and skeletal muscle (M). Top and bottom panel are two independent RT-PCR reactions by different primer pairs, but both covering the third exon.



**Figure 3.5 Gene structure and alternative splicing of sodium channel  $\beta 1$  subunit.** Exons (filled blocks) are labeled in order by the numbers above. The sizes (in bp) of exons and introns (line between boxes) are noted below. Empty arrow marks the location of start codon. Black arrows mark the stop codons in the two splice forms.

rat $\beta$ 1	177	EMVYCYK	KIAAAT	EAAQEN	ASEYLAIT	SESKEN	NCTGVQ	VAE	218
sm $\beta$ 1L	180	EMVYCYR	KIAAAGEE	ALRESAA	EYLAIA	SESKD	NCTGV	VAE	221
sm $\beta$ 1S	180	EMVYCYR	KIAAAGEE	ALRESAA	KTP	LKLHP			209

▼

**Figure 3.6 ClustalW alignment of the intracellular domains of  $\beta$ 1 subunits in rat and *Sternopygus macrurus*.** Alignment shows the difference between the translation products of the two splicing variants, compared with rat  $\beta$ 1 subunit. Identical amino acids are shaded. Filled triangle indicates tyrosine 181 (originally numbered in Isom et al., 1992) is changed to threonine in  $\beta$ 1S.

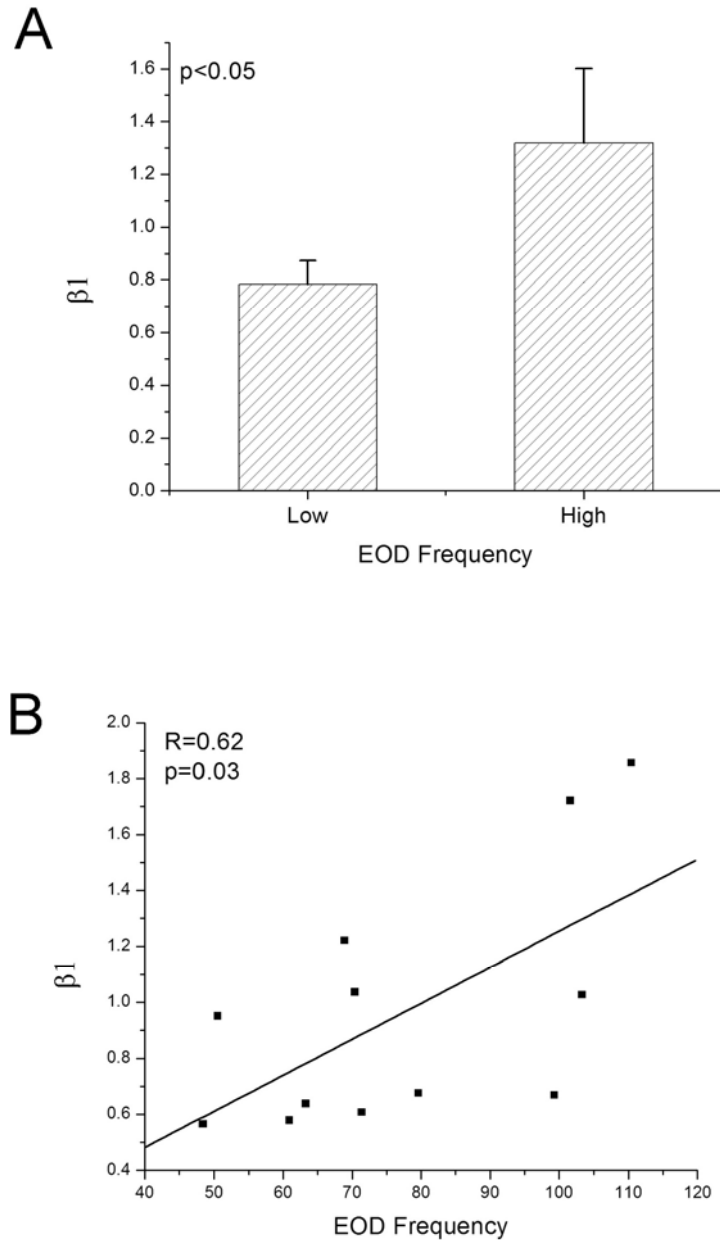


**Figure 3.7 mRNA level of sodium channel  $\beta 1$  subunit correlates with EOD frequency.**

A. High EOD frequency fish ( $n=4$ ) show higher mRNA level of  $\beta 1$  than low EOD frequency fish ( $n=8$ ). t-test  $p<0.05$ . B. mRNA levels of  $\beta 1$  in individual fish correlate with their EOD frequencies.  $R=0.63$ ,  $p=0.03$ .

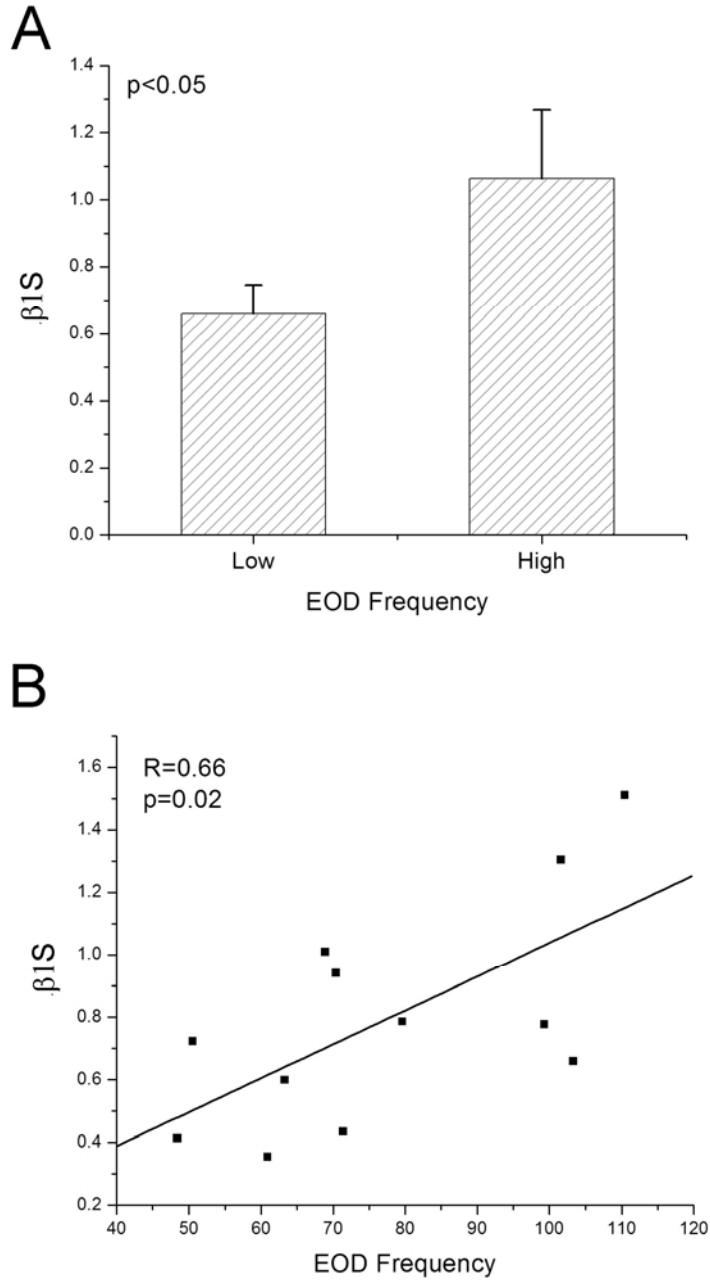


**Figure 3.8 mRNA level of  $\beta 1S$  splice form correlates with EOD frequency.**  
 A. High EOD frequency fish ( $n=4$ ) show higher mRNA level of  $\beta 1S$  than low EOD frequency fish ( $n=8$ ). t-test  $p < 0.05$ . B. mRNA levels of  $\beta 1S$  in individual fish correlate with their EOD frequencies.  $R=0.66$ ,  $p=0.02$ .

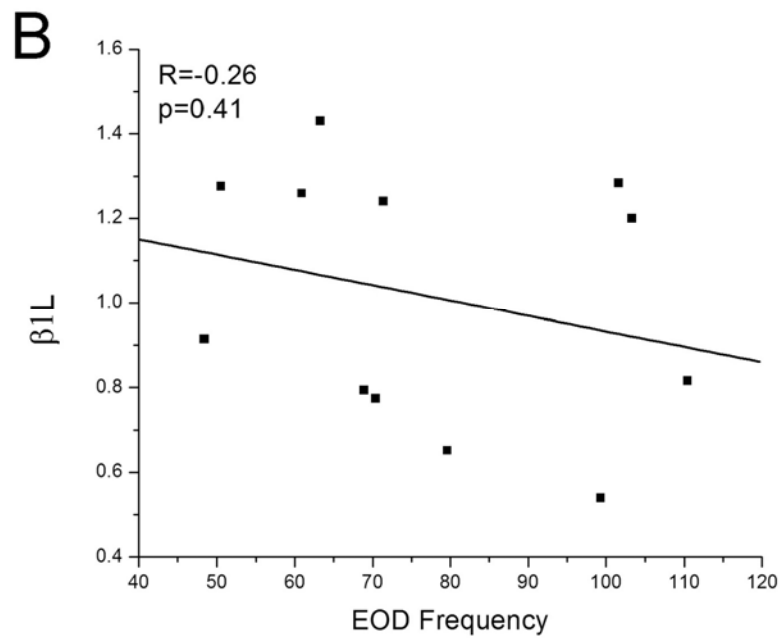
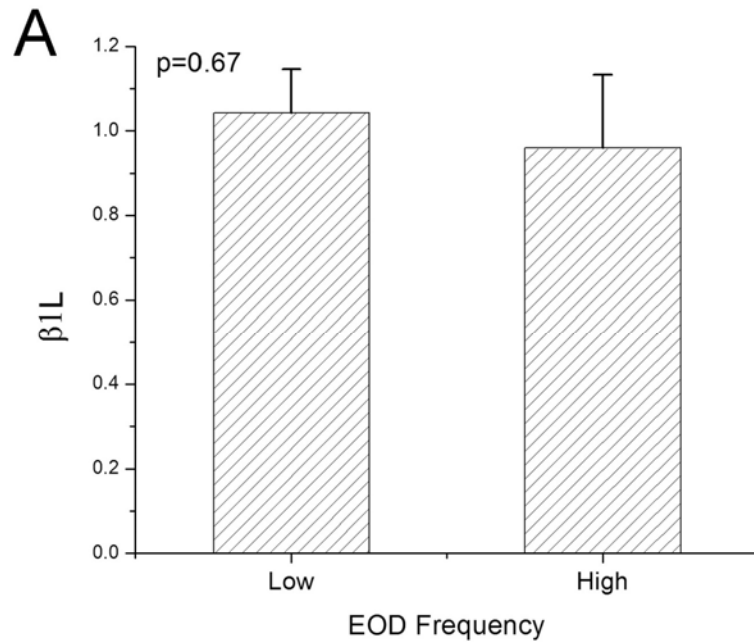


**Figure 3.9 mRNA level of  $\beta 1L$  splice form does not correlate with EOD frequency.**  
 A. No significant difference is seen between high EOD frequency fish ( $n=4$ ) and low EOD frequency fish ( $n=8$ ) in the mRNA level of  $\beta 1L$ . t-test  $p < 0.05$ . B. mRNA levels of  $\beta 1L$  in individual fish do not correlate with their EOD frequencies.  $R = -0.26$ ,  $p = 0.41$ .

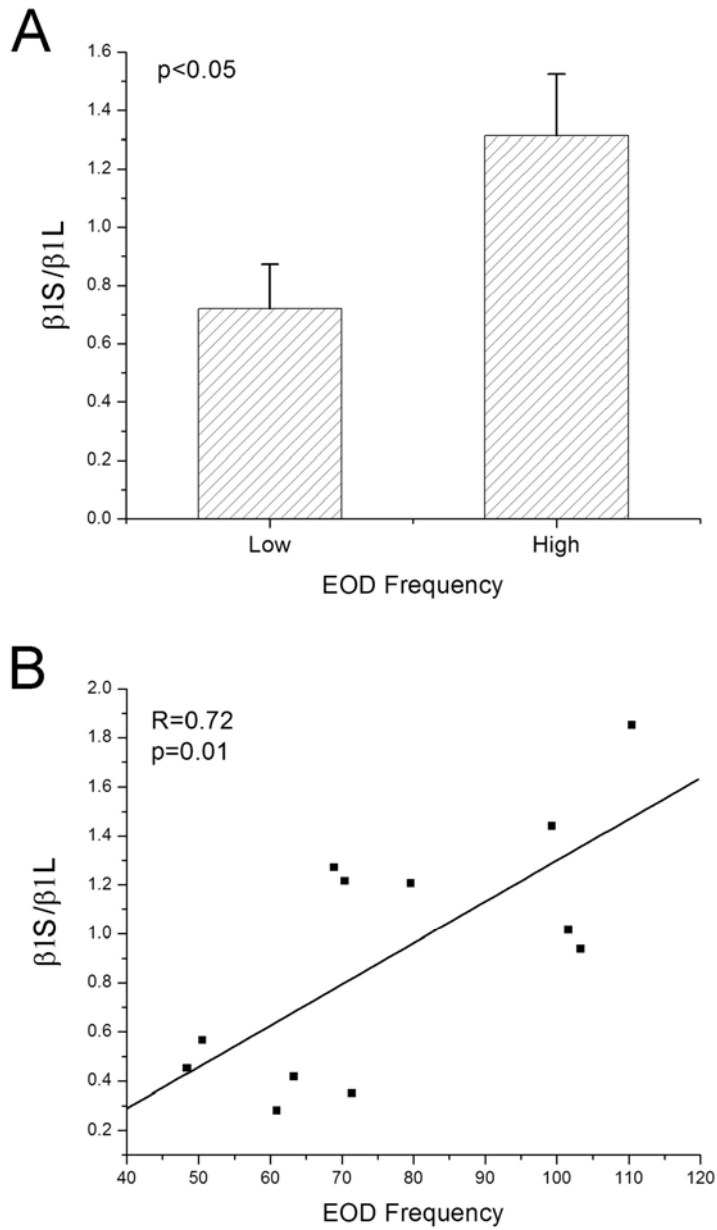


**Figure 3.10 The mRNA splicing preference, represented by  $\beta 1S/\beta 1L$  ratio, correlates with EOD frequency.** A. High EOD frequency fish (n=4) show higher ratio of  $\beta 1S/\beta 1L$  than low EOD frequency fish (n=8). t-test  $p < 0.05$ . B. The ratios of  $\beta 1S/\beta 1L$  in individual fish correlate with their EOD frequencies.  $R = 0.72$ ,  $p = 0.01$ .

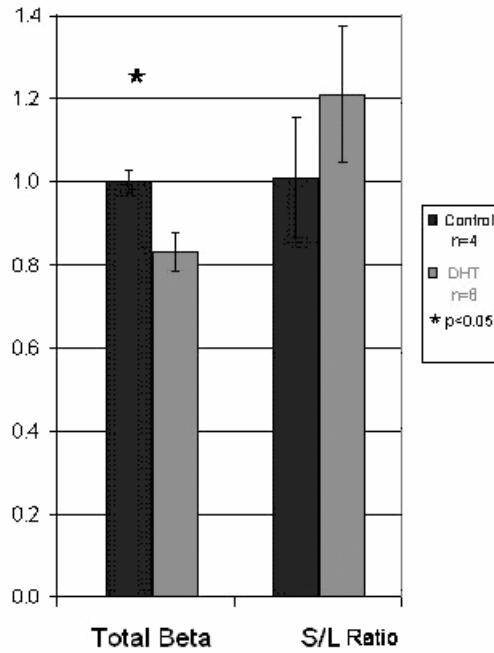


**Figure 3.11 DHT implants (n=8) lowered the mRNA level of  $\beta 1$  but did not change the splicing preference, compared to control group (n=4).**

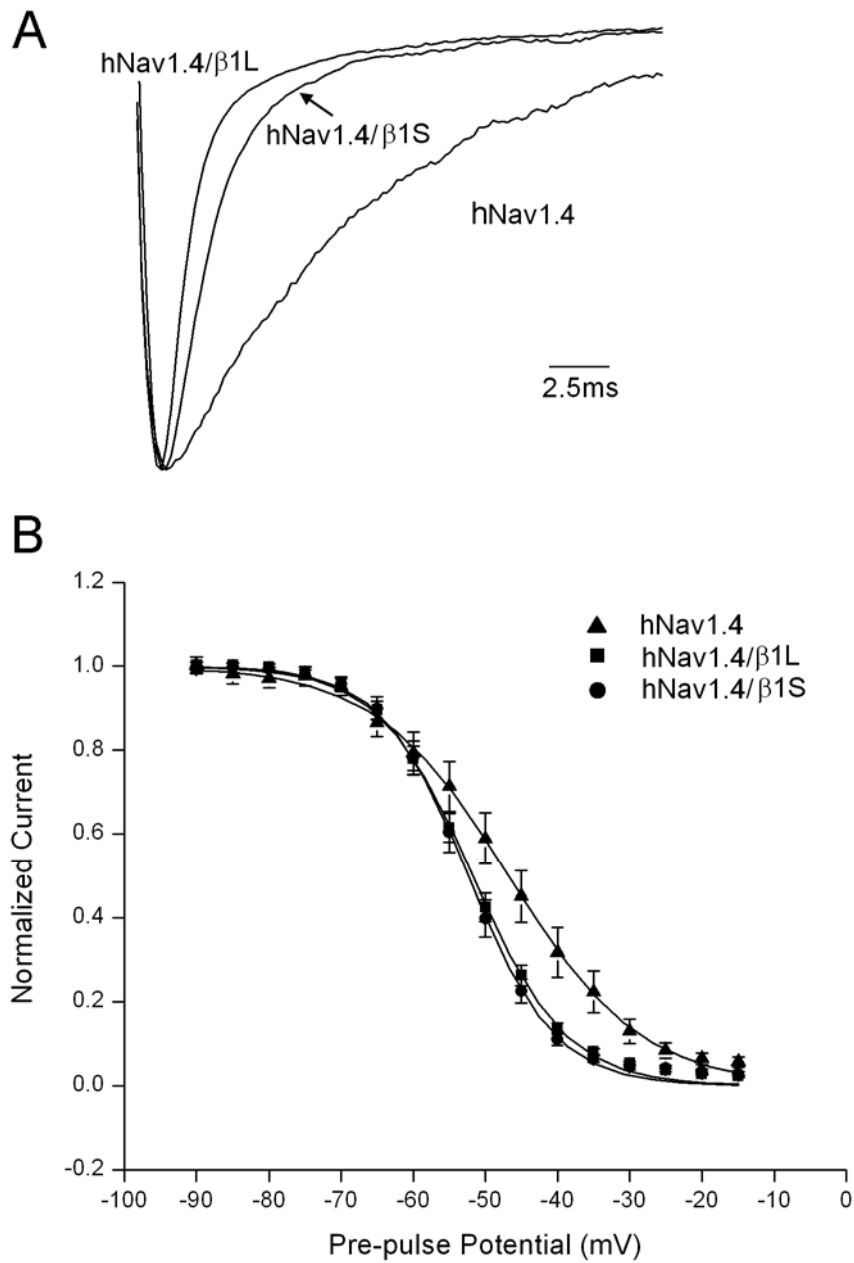


**Figure 3.12 Both  $\beta 1$  subunits of *Sternopygus* dramatically affect the kinetics of hNav1.4.** A. Representative traces show both  $\beta 1$  subunits dramatically increase the speed of inactivation and have no visible effect on activation. B. Steady-state inactivation curves show both  $\beta 1$  subunits negatively shift the voltage dependence of inactivation of hNav1.4.

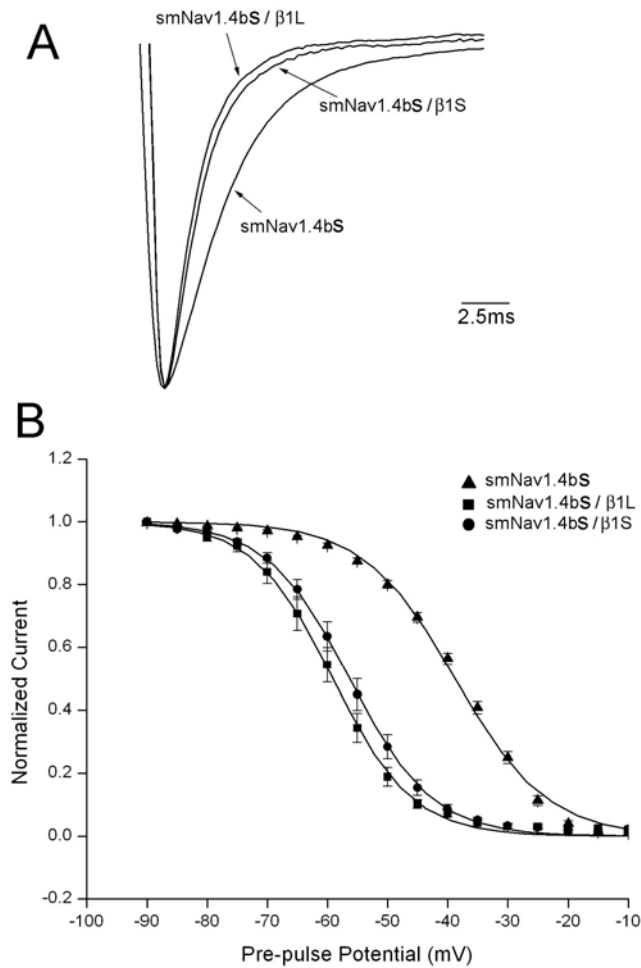


**Figure 3.13 Both  $\beta$ 1 subunits affect the kinetics of smNav1.4bS.** A. Representative traces show both  $\beta$ 1 subunits sped the inactivation and seemingly the activation too. B. Steady-state inactivation curves show both  $\beta$ 1 subunits significantly shifted the voltage dependence of inactivation of smNav1.4bS to a more negative membrane potential.

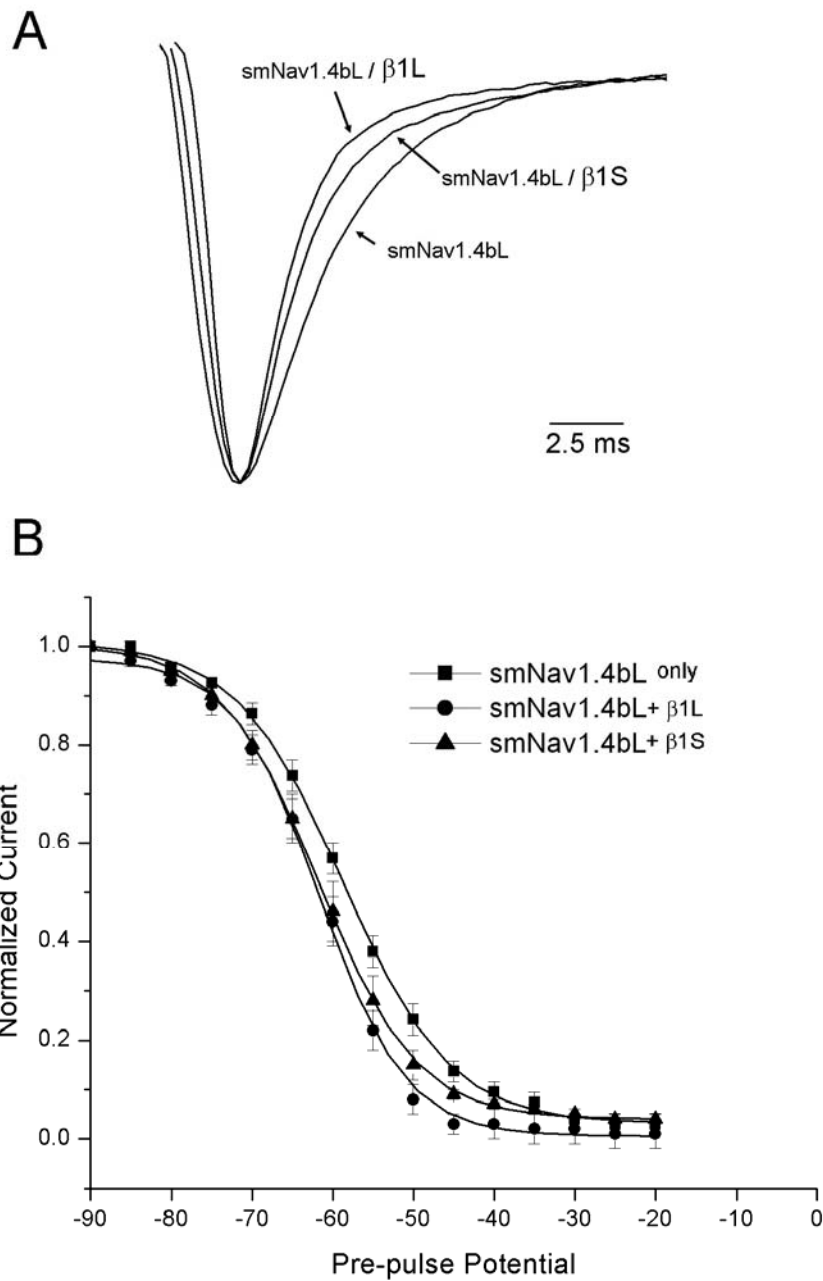


**Figure 3.14 Both  $\beta$ 1 subunits affect the kinetics of smNav1.4bL.** A. Representative traces show both  $\beta$ 1 subunits sped the inactivation. B. Steady-state inactivation curves show both  $\beta$ 1 subunits barely changed the voltage dependence of inactivation of smNav1.4bL.

---

## CHAPTER 4

### General Discussion

---

Variation of membrane excitability is essential for many cellular functions. Controlling membrane excitability needs the expression of appropriate ion channels in appropriate amounts. Previous studies in our lab on *Sternopygus* have provided a model system with solid background for addressing this question with molecular biology approaches. First, electrocytes membrane conducts only sodium, potassium and chloride currents, making this model relatively simple. Secondly, the electric organ contains a large number of cells with similar cellular excitability, allowing me to harvest ample tissue with a uniform cellular phenotype from a single individual (Ferrari and Zakon, 1989; Ferrari et al., 1995), and the strong correlation between the gradual changes of EOD frequency and of sodium current inactivation kinetics simplifies the measurement procedure and maximizes the RNA amount isolatable. Thirdly, the only two sodium channel  $\alpha$  subunits have been identified in the electric organ of *Sternopygus* before this study (Lopreato et al., 2001), which further simplifies the system and allows us to conceive how a cell may regulate its long-term excitability with virtually the least number of sodium channels available. Finally, androgens such as DHT can lower the EOD frequency and alter the sodium current kinetics, thus providing a powerful tool for us to manipulate the system and examine the changes on the molecular level. In addition to the background studies from our lab, recent progress in genome sequencing projects of

the zebrafish (*Danio rerio*) and the fugu (*Takifugu rubripes*) greatly facilitates the molecular biology studies in *Sternopygus*.

Even starting with such a simple model system, however, a quite complex pattern of mRNA control of cellular excitability has been identified in this study (Fig. 4.1 and 4.2). It involves multiple levels of regulations on both sodium channel  $\alpha$  and  $\beta 1$  subunits, including regulations of mRNA abundance, preferential transcription initiation, alternative mRNA splicing, and hormonal repression of gene expression.

In addition, this study identified a novel Nav1.4 ortholog with a uniquely longer N terminus and showed the first evidence that the N terminus of a sodium channel affects its inactivation. This study also identified a novel sodium channel  $\beta 1$  subunit and its function. Both these findings will enrich our understandings in structure, function and evolution of sodium channels.

### **Two sodium channel $\alpha$ subunits in electrocytes of *Sternopygus***

Our lab started the functional study of these channels by cloning the partial cDNAs sequences of the two sodium channel  $\alpha$  subunits, Nav1.4a and Nav1.4b, in electrocytes (Lopreato et al., 2001). In this study, I identified the full-length cDNA sequences of these two genes in *Sternopygus macrurus* and further identified the two mRNA variants of smNav1.4b.

smNav1.4b variants (smNav1.4bL and smNav1.4bS) are the only voltage-gated sodium channels in skeletal muscle, thus we expected they have fast inactivation kinetics, as sodium currents in muscles of other species inactivate quickly (Kirsch and Sykes, 1987; Coutts et al., 2006). Their expression in *Xenopus* oocytes confirmed this.

Furthermore, electrocytes show preferential expression of smNav1.4bL, which has a faster  $\tau_h$  and a more negative voltage dependence of inactivation.

The *Sternopygus* electrocyte also expresses smNav1.4a, which is located only in electrocytes (Lopreato et al., 2001; Zakon et al., 2006). This gene has not yet been exogenously expressed so its biophysical characteristics are not known. Nevertheless, the sodium current in electrocytes inactivates much slower than in muscle. smNav1.4a is specifically expressed in the electric organ. Thus, smNav1.4a, as the only additional sodium channel in electric organ than muscle, is expected to be the channel contributing to the slow inactivation of the sodium current in electrocytes. Further exogenous expression of smNav1.4a is needed to confirm this hypothesis.

### **Regulation of sodium channel mRNA abundance may determine cellular excitability**

Differential regulation on mRNA abundances of multiple ion channels results in the alteration of channel constitution on the membrane, which in turn directly changes the cellular excitability. This has been seen in other systems, such as DRG neurons containing multiple sodium channels (Nav1.1, Nav1.3, Nav1.6, Nav1.7, Nav1.8 and Nav1.9) (Waxman et al., 1994; Dib-Hajj et al., 1996; Dib-Hajj et al., 1998). Changes in the expression of these channels may contribute to the axotomy-induced change in excitability, but proofs for a direct correlation are still incomplete partially due to the complexity of the system (Flake et al., 2004).

In this study, the electric organ of *Sternopygus* expresses only two voltage-gated sodium channels, smNav1.4a and smNav1.4bL (smNav1.4bS is at a very low level thus

negligible), and these channels presumably have different kinetic characteristics. With the minimal number of voltage-gate channels available, the electrocytes in *Sternopygus* show sodium channel inactivation kinetics in a gradient manner. Therefore, it provides a unique and simple model system to study the general mechanism of how the gene expression of ion channels may regulate cellular excitability.

Real-time quantitative RT-PCR experiments showed the expression level of smNav1.4bL, but not smNav1.4a, correlated with the EOD frequency. Therefore, smNav1.4a, abundant in electric organ and presumably a slow sodium channel, may express at a fairly constant level and set the kinetic baseline of the slow sodium current. While on the other hand, smNav1.4bL, a channel with extraordinary inactivation properties, may act as a fast component and provides fine tuning of sodium current inactivation rate by regulation of the expression level. Across the EOD frequency range, smNav1.4bL expression shows a 2~3 fold difference while smNav1.4a expression is relatively stable, and the two genes are expressed at generally equal levels in medium EOD frequency fish, suggesting the differential expression of these two genes may greatly change the composition of sodium channels on membrane and causes different kinetics of sodium currents (Fig. 4.2).

### **$\beta$ 1 subunit expression: an independent regulation mechanism**

Sodium channel  $\beta$ 1 subunit forms a non-covalent bond with  $\alpha$  subunit in 1:1 ratio. A previous study showed when unsaturated,  $\beta$ 1 alters the kinetics of  $\alpha$  subunit in a gradient manner (Meadows et al., 2002). It leads to the hypothesis that gradient expression of  $\beta$ 1 may contribute to the individual variation of cellular excitability in

*Sternopygus macrurus*. Indeed, the mRNA abundance of both  $\beta 1$  subunits together correlates with EOD frequency. Furthermore, the mRNA splicing, and the mRNA abundance of  $\beta 1S$  but not  $\beta 1L$ , both correlate with EOD frequency as well (Fig. 4.2). The cause and the functional advantage of this selective regulation on  $\beta 1S$  are not clear yet. The two  $\beta 1$  subunits do not show statistically different effects in the modulation on the kinetics of  $\alpha$  subunit, while on the other hand, their difference is located in the intracellular domain, which is involved in the interaction with  $\alpha$  subunits and cytoskeleton proteins. Therefore, one possibility is that  $\beta 1S$ , as a novel  $\beta 1$  subunit, may have a higher affinity to the  $\alpha$  subunits, especially smNav1.4a. Since adding  $\beta 1$  subunits to smNav1.4bL does not change the kinetic much in *Xenopus* oocytes, and the extended N terminal segment of smNav1.4bL functions like an internal  $\beta 1$  subunit,  $\beta 1$  subunit appears unnecessary for smNav1.4bL to change the sodium current kinetics. Therefore, a higher affinity between  $\beta 1S$  and smNav1.4a would allow  $\beta 1S$  to participate in the regulation of membrane excitability more effectively.  $\beta 1S$  and smNav1.4a, both evolutionally novel, may both undergo positive selections in the cytoplasmic domains for the higher affinity. Whether or not this explanation is true, the upregulation of  $\beta 1$  expression, independent to the regulation of  $\alpha$  subunit expression, shifts the sodium channels to faster inactivation and voltage dependence to a more negative membrane potential.

In real-time quantitative RT-PCR experiments, I observed statistically significant correlations of smNav1.4b and  $\beta 1$  with EOD frequency. However, several outliers, especially in high frequency EOD fish, were still of concern. Interestingly, these outliers deviate in opposite directions from the regression lines of smNav1.4b and  $\beta 1S$  (Fig. 4.3 A

& B). Virtual addition of the expression levels of these two genes results in a much stronger correlation (Fig. 4.3C) and the deviations from the regression lines of smNav1.4b and  $\beta 1S$  of all the 12 individuals negatively correlate (Fig. 4.3D), implying the regulations of smNav1.4b and  $\beta 1$  subunit may be independent, but compensate each other. Quantitative modeling and more data are still needed to further investigate this phenomenon.

### **Multiple levels of controls on multiple genes**

Cellular excitability is determined by all ion channels on the membrane. Thus, the regulation of cellular excitability may involve controls on multiple ion channels. Moreover, the expression of ion channel protein on the membrane is determined by multiple steps, including transcriptional events, mRNA splicing, mRNA degradation, translation, post-translation modification and protein trafficking. Due to the technical difficulty of isolation and quantitative measurement of individual sodium channel protein, my dissertation focuses only on the regulations of mRNA, but still reveals a complex pattern.

First, of the genes I studied, smNav1.4bL shows a preferential expression over smNav1.4bS in electrocytes. Since the two variants differ in the first exon, thus this is likely to be caused by differential initiation of transcription. In fact, 5'RACE revealed multiple initiation sites in both transcripts, suggesting multiple promoters may participate in this process and may be under tissue-specific regulations.

Secondly, the mRNA levels of smNav1.4bL and  $\beta 1$ , but not smNav1.4a, correlate with the EOD frequency. mRNA abundance can be affected by many procedures, such as

transcription initiation, transcription elongation, mRNA stability, pre-mRNA splicing, mRNA transport and polyadenylation. Among these, transcriptional control is believed to be the most common way of regulation. In this study, DHT, whose receptor acts as a transcriptional factor, affects the mRNA abundances of these genes, further supporting the hypothesis that the regulations I observed are mainly transcriptional.

Thirdly, alternative mRNA splicing probably also contributes to the cellular excitability of electrocytes. In high EOD frequency fish, although the total level of  $\beta 1$  is higher, only  $\beta 1S$  mRNA level is elevated. One possibility is that the degradation of  $\beta 1L$  increases with the increased transcription. However, this is not likely because most mRNA degradations in eukaryotes studied so far go through either deadenylation or decapping (Caponigro and Parker, 1996; Jacobson and Peltz, 1996), but the 5' and 3' ends of  $\beta 1L$  and  $\beta 1S$  are the same thus presumably indistinguishable for these pathways. A more plausible cause may be that certain mechanism exists to keep the  $\beta 1L$  mRNA level constant, thus the increased input of mRNA precursor leads to increase the level of  $\beta 1S$  only. This mechanism may involve exon boundary recognition to differentiate  $\beta 1S$  from  $\beta 1L$ . In addition, the two variants of smNav1.4b may also undergo differential mRNA splicing. Their first introns share the same 3' end, but the 5' end of the first intron of smNav1.4bL is included in the first intron of smNav1.4bS. The recognition mechanism to discriminate these splicing sites is not clear but remains an interesting question.

In summary, these results suggest that transcription initiation, transcriptional regulation abundance regulation and mRNA splicing of sodium channel  $\alpha$  and  $\beta 1$  subunits all contribute to the control of cellular excitability of electrocytes. Moreover,

another study (Few, 2003) showed the mRNA levels of multiple potassium channels also correlate with EOD frequency, suggesting the presence of a homeostatic control of multiple genes to precisely regulate cellular excitability. A pattern of co-variations of sodium current inactivation and potassium current activation has been seen in electrophysiological recordings in the electrocytes (Mcanelly and Zakon, 2000).

DHT implants lowered the mRNA abundances of both  $\alpha$  and  $\beta 1$  subunits of sodium channel in electric organ, and DHT level is naturally higher in male than in female fish. The expression levels of multiple potassium channel  $\alpha$  subunits are also repressed by DHT (Few, 2003). Thus, androgen may play a pivotal role to control the sexually dimorphic cellular excitability of electrocytes by gene repression. The mechanism of gene repression by steroid hormones is largely not clear. One possibility is DHT and androgen receptor may bind to the DNA sequence in the vicinity of these genes and affect the chromatin structure. Another possibility is that DHT may enhance the expression of other transcriptional factors, which repress the expressions of these genes. Identification of common binding sites of either androgen receptor or other transcriptional factors in the genomic DNA sequences around these genes may elucidate the mechanism.

### **Does expression of sodium channel subunits explain individual variation in sodium current?**

Since I undertook this study to test if sodium channel  $\alpha$  and  $\beta 1$  subunits were involved in the regulation of sodium currents in *Sternopygus* electrocytes, a comparison between sodium currents in the native environment (Ferrari et al., 1995) and in oocytes

with and without  $\beta 1$  co-expression is instructive. The voltage dependence of activation of the native sodium current does not vary with EOD frequency and has a  $V_{1/2}$  of  $\sim -25$  mV, which agrees with values reported here for  $\alpha$  subunits alone or with  $\beta 1$  subunits (Table 3.2). Importantly, in the native currents in the electrocytes of low EOD frequency fish to high EOD frequency fish, the  $V_{1/2}$  of inactivation ranges from  $\sim -40$  to  $\sim -60$  mV, and the  $\tau_h$  varies from  $\sim 0.5$  to  $4.0$  msec. The values at the end of high EOD frequency fish agree well with the values of smNav1.4bL without or with  $\beta 1$ , in both the  $V_{1/2}$  of inactivation (mean value  $-59 \sim -62$  mV) and the  $\tau_h$  (mean value  $1.31 \sim 0.78$  msec). Although smNav1.4bS is expressed at a very low level in electric organ, its kinetic parameters are also contained in the range of natural variation ( $V_{1/2}$ :  $-43$  mV without  $\beta 1$  and  $-59$  mV with  $\beta 1$ ,  $\tau_h$ :  $2.63$  msec without  $\beta 1$  and  $1.81$  msec with  $\beta 1$ ), more toward the values at the end of low frequency fish, providing the hint that the parameters of smNav1.4a, though not successfully expressed but presumably slower than smNav1.4b, might cover the end of low EOD frequency fish.

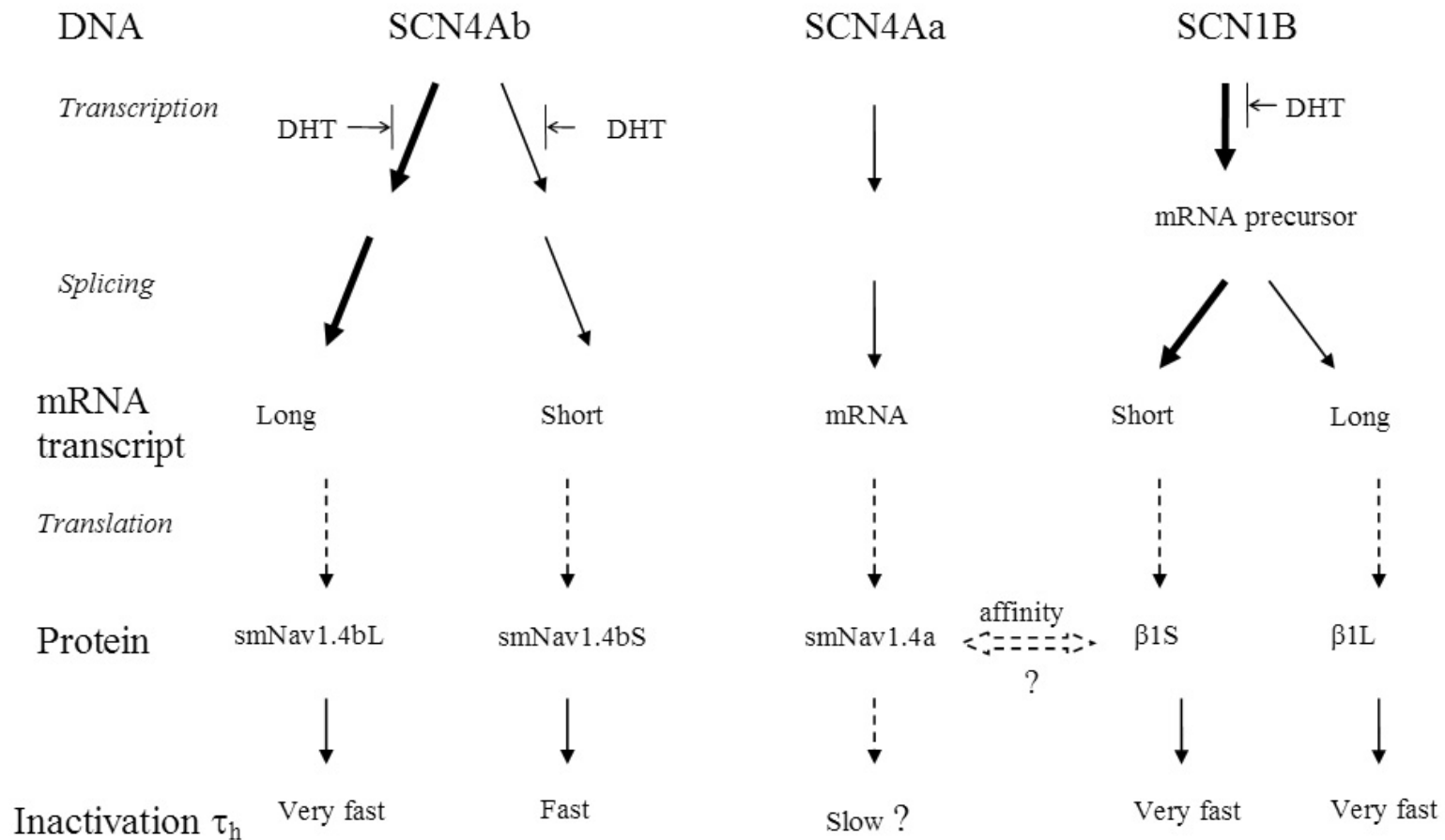


**Figure 4.1 Working model for the regulation of sodium channel subunits in the electric organ of *Sternopygus macrurus*.** Flow charts show the cellular processes (in italic fonts) from genomic DNA to mRNA, then to protein and finally the inactivation kinetics of sodium current. Bold arrows indicate upregulations in high EOD frequency fish; dashed arrows label the processes not proved or not included in this study; two question marks indicates two immediate goals needed to be studied. Figure also shows the gene repression by DHT.

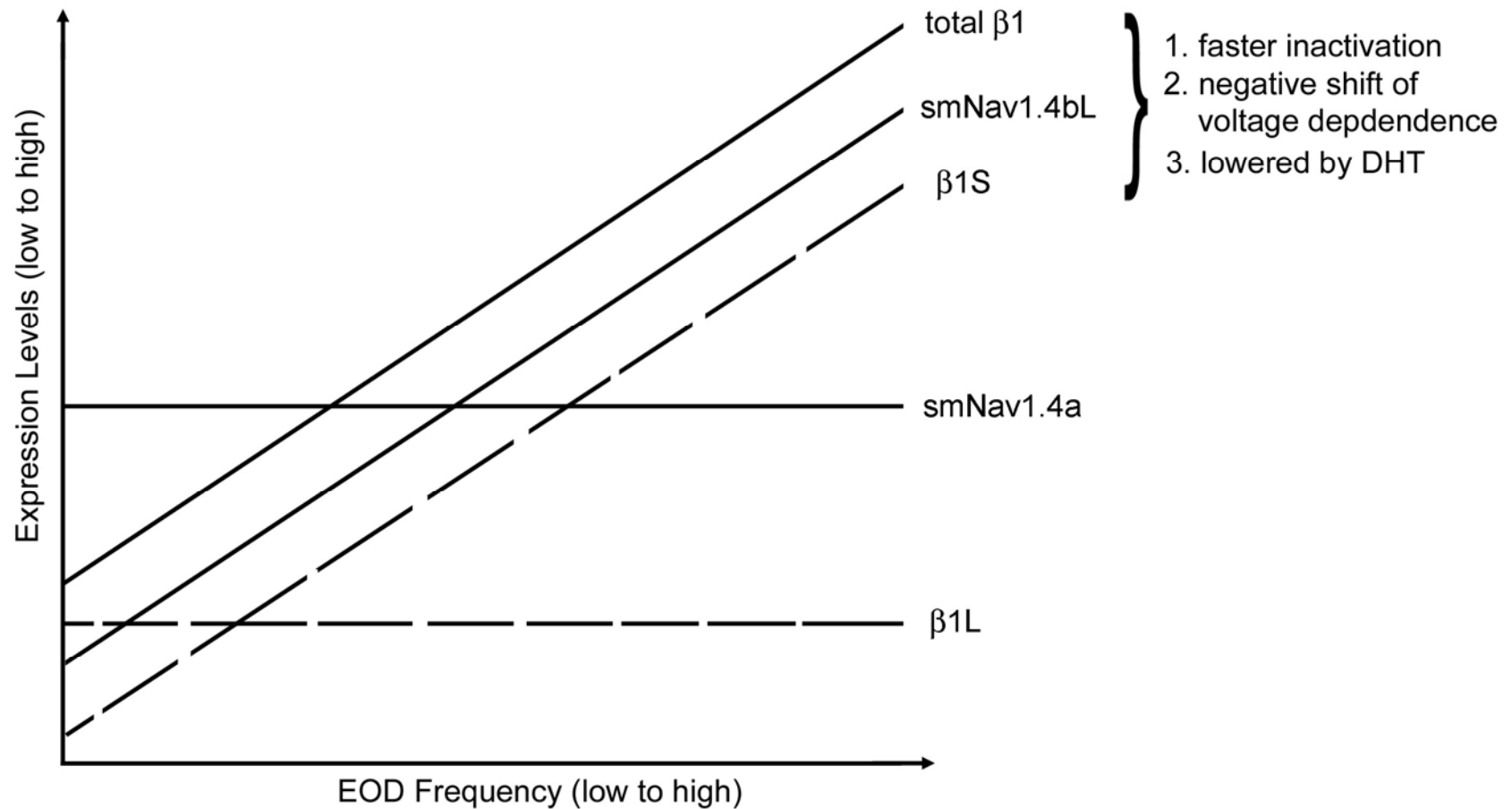


**Figure 4.2** Schematic illustration of the relations of expression levels of multiple sodium channel subunits with EOD frequency. Three genes, smNav1.4bL, smNav1.4a and  $\beta 1$  are shown in solid lines (smNav1.4bS expression is low in electrocytes thus not shown). Broken lines show the expression levels of each splice form of  $\beta 1$ . The mRNA levels of smNav1.4bL,  $\beta 1S$  and total  $\beta 1$  correlate with EOD frequency, while smNav1.4a and  $\beta 1L$  not. Right corner shows the common characteristics of  $\beta 1$ ,  $\beta 1S$  and smNav1.4bL.

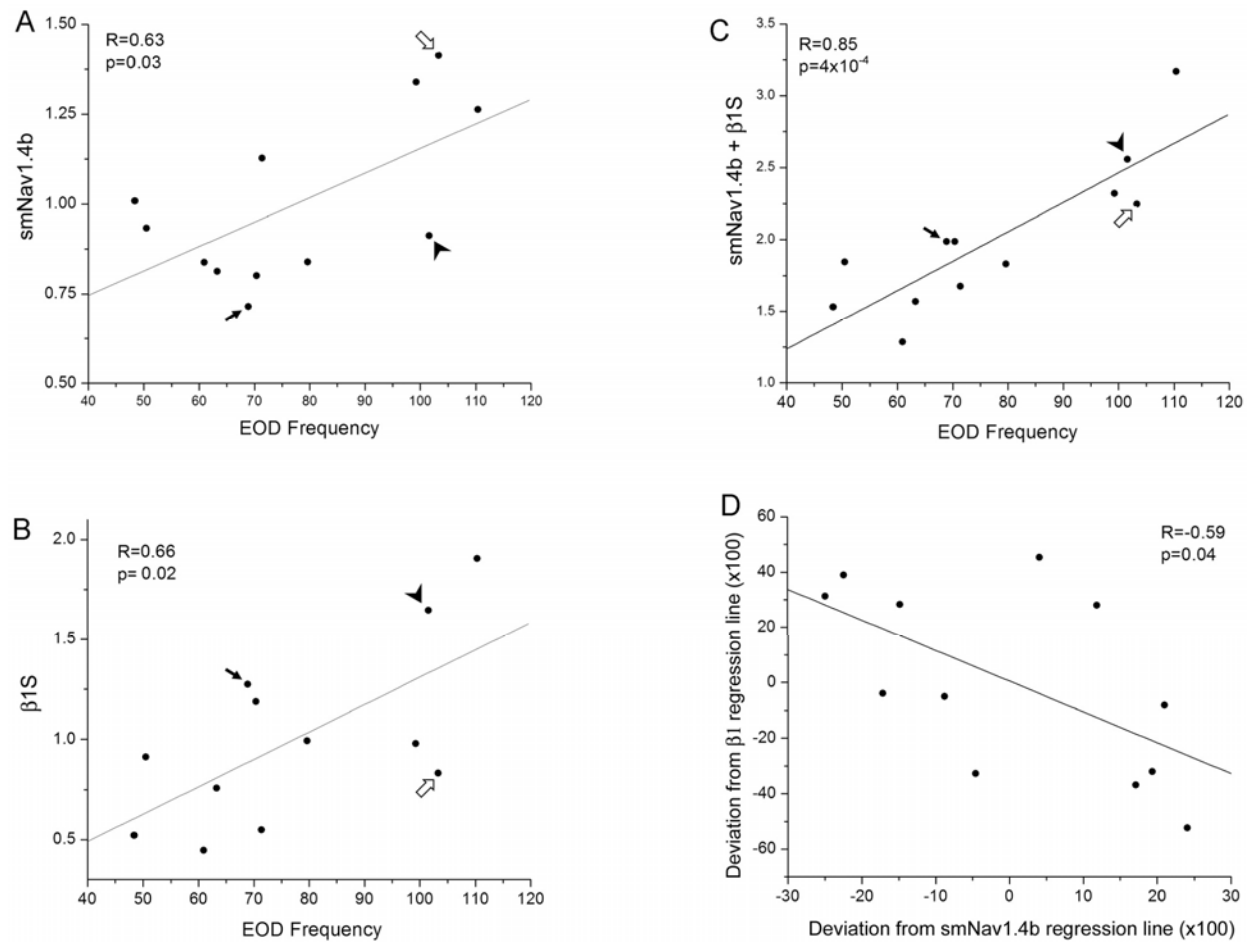


**Figure 4.3 The expressions of smNav1.4b and  $\beta 1S$  show compensation to each other.** (A) and (B) Real-time quantitative RT-PCR results with Taqman method. Data points were normalized by group average. (C) Virtual sum of the mRNA levels of smNav1.4b and  $\beta 1S$  correlate with the EOD frequency, suggesting possible compensation of the two regulation mechanisms. (D) Negative correlation between the deviations from the regression lines of smNav1.4b and  $\beta 1S$  of each individual fish. Three individuals with deviations in opposite directions are labeled in A, B and C.

## Appendices

### Appendix 1. cDNA sequence of smSCN4Aa(smNav1.4a)

GATGCTGTTCTTAGTTTATAATGACTACAAGTAATCATTTGAGCTTGAATACCAGTACTTTTCCTCATT  
AAAGTGTTACTACAAACCTTTTCACTTTTCATTAGAGCAAGCAAAAAAATTATTTTAGCATTGTTTGC  
ATACTAACGTTTCGCCATTGGTTGTGGAATACTGCGGTTCTACCTCTGGGATATTGCTATTCTGAA  
ACATCTCTGTGTCTTGAGCTCAGGATAGAGATTCCACTCTGAGGTGGTATCTTTTCGCAATGCAA  
ACATGGCACACCTGGTCTCTCCGCCAGGCCCGAAGTGTTCGCCCGTTTACCCCGGAGTCACTGGC  
GGAGATCGAGAGGCTTACCGAGCTGCGGAACAGGGGAGAAGGAAGTAGAGGGGACGGAGCTGG  
AGGCGGGCGCCCAAGGCACCCAGCCGTGACCTGGAAGCGGGGAAACCCCTGCCCATAATCTAC  
GGAGACCCACAAAGGACCTGCTCAACACACCCCTGGAGGATCTGGACCCCTACTTCAAACA  
AAAGAGAACATTTATTGCGATTAGCAAGGGAAACACTATCAACAGATTCAATGCCGAAGCAG  
CTTTCAACACTTTTCAAGCCATTTAACTCCATGAGAAGAGCAGCCATTAAGTTCTTGTGCAT  
TCGTTATTTAGTTTCGATTATCATGGTTCATCCTCGCCAACTGCATACTCATGACTATT  
TTTGAACCTTCCCTGGTGTAAAATTGTGGAATATGTTCTTACCGGTATATATACCTTTGAA  
AACTATAATCAAAGTGTGTCCAGAGGGTTCTGTTTTGGACCGTTTACATTCTTTCGCGATCC  
GTGGAAGTGTCTGGATTTCATGGTGATCAGTATGGCGTACATCACAGAGTTTCGTTGATCTT  
GGCAACATGTTCGGCGCTTAGGACGTTCCGTGTGCTCCGAGCTCTCAGGACAATCACCGTTA  
GTCCAGGATTGAGAACGATCGTCGCAGCTCTGATCCAGTCCGGTGAAGAAGATGGGTGACG  
TAATCATCCTGACCCCTCTTTGCCCTGTCCGTGTTTACCCTGGTCGGTCTGTCAGCTCTT  
CATGGGGAACCTCCGTCACAAATGCATACGCTGGCCCTCCCAACACCACCCTCGACTAC  
AACACCACCTTGGACAACAGCGCTTTCAACTTACGGCCTACGTCGAAAACAAAGAAAATC  
AGTACTTTCTCGATGGTGCTTTGGATCCCTTACTATGTGGTAACAATTCTGATGCTGGGA  
AGTGCCCTGAAGGCTACACGTATGAAGGTTGAGAGGAACCCGAACACTACGGCTACACG  
AACTACGACAGCTTTCAGCTGGGCTTTTCTGTCTCTGTTTCAAGTCTATGGTGCAGGACT  
ACTGAGGACTACTGGGAGAACCTGTATCAGCAGACTCTCCGTGCTGCAGGGGAAGAC  
CTACATGCTCTTCTTCGTCAATTGTCAATTCCTGGGCTCCTTCTACCTCGTCAACCTC  
ATCCTGGCTGTGGTCGCCATGGCGTATGATGAGCTGAACGTGGCCCTGCAGGCCGAGGCT  
CAAGAGAAAAGAGGCCGAGTTCCAGAGAATGCTGGAGCAGCTCAGGAACCAAGAGCAAC  
AGCTGCAGGCTGGCAGTAGGGAGTCTTTGGCCAGTCAAGTCACTCAGAGCATCTCATCGG  
GATGACGGACGATGAGGATGATGTCACGAAGGGCTGTAACGGCAAGGTCACCCCCCATCT  
GGTCATTAACAGAGTGCCATCTAAGGTGAAGTCATCAATAGAGGAGCGGAACCTTGGAC  
ACTAAGTCCATAGACTCCAGGCGACACAGCGTGATGTTCTTGGATGAACCGGGCCTGCG  
CCAGAGGACTGCAGATATCGCCAGTGTGCTCACAGCTGAAGAGGTGGAATTGGCCAAG  
AGGGCATGTCTCCAATCTGGTATAAAATCACTGGCTTCTTCTCAAGTGAACCTGTGT  
GCCCTGGAGGATGTTGAAGAAATTTGGCCATTTATAGTATGATCCTTTTCAATGACCT  
TGGGATCCTTATGAGACTATGGAGCACTACTTGCATAATACTGAATACACTGTTTCA  
TATGGAGCACTACCCCATGAGCGAAACCTTTCAACACACTGCTCACCATAGGGAACCT  
GGTGTTTACTACCATCTTTACCGCTGAAATGGTGTGAAGATCATCGCCCTGGACCTT  
ACTACTACTTCCAGGTGGGCTGGAACATCTTCGACTGCATCATCGTCACTCTCAGTCT  
GGTGGAGCTAAGCCTATCCAACATGCCGGGCCTGTCTGTGCTCAGATCCTTTTCTG  
TTGATGCGTATTTTTCAAGCTGGCCAAGTCTGGCCACGCTCAACATGCTGATCAAGA  
TCATCGGCAACTCAATGGGCGCCCTGGGGAACCTGACCTTCGTGTTGGCCATCGTCA  
TCTTTCATCTTCGCCGTGGTGGGCTTCCAGCTGTTTCGGGAAGAGCTACAAGGACA  
ACGTTGTGCAAGGTGAGCGCGGACTGCACGCTGCCTCGCTGGCACATGAACGACTT  
CTTCCACTCCTTCTGATCGTGTTCGTCATCCTGTGCGGCGAGTGGA  
TCGAGACCATGTGGGACTGCATGGAGGTGGACGGAGTGCCCATGTGCCTCACCGTCT  
TCATGATGGTTCATGTCATCGGAAACCTGGTGTGCTGAACCTGTTCTTGCCTTGCTT  
CTCAGCTCATTTCAGCTGCGACAATCTTGCCGCGCCAGACGATGACAGTGAAGTT  
ACCAACATCCAGATCTCCATTGTGCGCATCAGCAGAGGGATAAGCTGGGTGAAGAA  
ATTCAATTGTAGGCACAGCCTGGTGGATCATGGGCAGGAAGCCCCACGGTGATGAT  
GGGGAGGAGAGAAGGAGACAACGAGGACAGAAAGGACACTTTGCCCTTAAACTAC  
CTTGTATGGTGGGAAGATGTAGATGGGATTACCAACTATGTTGTAGAGTCTACGGT  
TCTGAATGTGCCTATTGCCAAGGGGGAGTCTGAGGTTGAGGATGATGAATCAGTGG  
ATTTGTCAACTGAAGAGAACATGATAAACTGAAGGGTGTCTCTCGATGATGACTCT  
TCGATTTGCAGTTTCAGTGGACTACGAGCTTCTACAACCCCTCTGTGAGGAAGAG  
GAGGAAAAAAGGAGCCTGTTGATCCAGAAGCCTGTTTTACAGAAAACCTGTGTG  
AGGTACTTTCCATGTCTGGATGTGACATCACACAGGGGAAAGGGAAGATCTGGT  
GGAACCTCCGCTGCACCTGCTACAACATCGTGAACATCGTGAACATCAC  
TATTTTGAACACTTTCTCATCTTTCATGATTTCTCCTCAGTGTGGAGCACTGGC  
ATTTCGAGGATTTAATCGAACCGCGCAGGGTCAATTAAGACCATGTTGGAGTAT  
GCAGACATAGTCTTTCACATATATTTTCTGTTGGTGGAGATGTTTTCTGAAGT  
GGACTGCATATGGGTTTTAAAGCGTACTTACCAGTGCCTGGTGTGGCTGGAT  
TTTTATTGTTGATGTGTGCTCAGTTATTAGCTTAGTAGCCAATGTGTTGGGCT  
ATGCAGAGCTGGGACCAGTCAATCGCTCAGAACTTTTCCAGGCTTTCAGGCTT  
TTCGACCTTTACGTGCCCTTTCCAGATTTGAAGGAATGAGGGTGGTAG

TGAATGCATTGCTCGGTGCCATCCCCTCCATCATGAACGTTCTATTGGTGTGTCTGATCTTCTGGCTGATC  
TTCAGCATCATGGGGTCAACTTGTGGCGGAAAGTTCTACCGCTGCATTAACACCACCACAGATGAGGT  
TCTGTCCACAGAGCAAGTGAACAACAGGAGTGAATGCATGGCACTAATGCACACTAATGAGGTGCGTTGGG  
TCAACCTTAAGGTCAACTACGACAATGTGGGCCAGGGATATCTCTCCTTGCTTCAAGTGGCCACATTTAAA  
GGGTGGATGGACATCATGTATGGTGCAGTGGACTCTAGAGAGGTAGAGGATCAGCCATCATATGAGATTAA  
CCTCTACATGTACCTGTACTTTGTTCATCTTCATCACATTTGGATCCTTTTTTATCCTCAACCTTTTCATTG  
GTGTTCATCATTGACAATTTAACC GGCAAAAACAAAAGTTAGGAGGAGATGACCTCTTTATGACAGATGAA  
CAAAAAAGTATTATGCTGCCATGAAGAAGCTGGGTCCCAAGAAACCACTCAAACCTATAACCCCGTCTTC  
GAATATGGTTCAAGGGGTGGTGTTCGACTTCATCTCCCAAAAGTTCTTTGACATTTCCATCATGGTTCTCA  
TCTGCCTCAACATGGTGCATCATGTATGGTGGAGGCGGACAGACAGAGTGAAGAGAAAGAGAATGTCTCTAT  
CAGATCAATATCATATTTTATTGTTCATCTTCACCGGAGAGAGTTTACTCAAGTTGTTGGACTTAGACATTA  
CTTCTTCACTATCGGATGGAATATTTTTGATCTCATCGTTCTCATCCTTTCTATAATTTGGTATTTTGTCTGA  
TGGACATAATTGAGAAGTACTTTGTGTCCCCTACTCTGTTCCGTGTTCATCCGCTTGGCTAAGATTGGTCTG  
GTGTTGCGTCTCATCAGAGGGGCGAGGGGCATAAGGACGCTGTTATTTGCCCTTATGATGTCACCTCCCTGC  
ACTTTTCAACATTGGCCTTCTTCTTTTTCTTATTATGTTTCATGTTTTCCATCTGTGGAATGTCTAACTTTG  
CCTATGTGAAAAGCAAGCCGGCGTTCGATGAAATCTTCAGCTTCGAGACTTTTGGGAGTGGCATCGTCTGC  
CTGTTTCGAAATCACACCTCCGCCGGCTGGGATGGGCTTCTCCTCCCAATGCTAAACAGTGGTCTCTCTGA  
CTGTGACCCTGATGCGGAACACCCTGGATCAGATATGAGGGGCAACTGTGGGAGTCCAACCATTGGCATCG  
TGTTCTTCTGCAGCTACATCATCTTGTGCTTCTTAGTGGTAGTGAACATGTACATCGCCGTCTCTGGAG  
AACTTCAATGTGGCACAAGAGGAGAGCAGTGACCCACTCTGTGAGGATGACTTTCAAATGTTTGTATGAGAC  
CTGGGAAAAGTTTCGATGTCCACGGTACACAATATTTGGACTACAATCGTGTGTTTACTTTGTTGATGCAC  
TGCATGAACCCATGCGTATTTCCCAAGCCCAATAGACTCAAGCTGGTTAAAATGGACCTGCCTGTTTTCAGAG  
GGAGACAAAATCCACTTTGTGGACATTCTGCTGGCTGTCACCTCAGGAGGTCTTGGGGGACACCATTGAGAT  
GGCGGCCATGAGGCTAAGCATCGAGACTAAGGTCAAGATGAGCTCCCCAGCCTCGCCTCATTTCGAGCCCA  
TTATCACCCTCTGAGAAGGAAGGAGGAGGAGCAGGCGGCCAAGGTGATCCAGAGGGCGTACCGCCAACAC  
CTCCTCAGACGTGCCTTTCGCTATGCCTCCTTTCTGCACTGCACCAGGCAGAAGAAGGTGAGCAAGCACAA  
TGGCGTGGCGCCAGACAAGGAGGGTCTGATTGCACAGAAGATGAATACCCTGTACGGCGGAGGCCAGAGC  
TTGCCATGGCCCTGGAGCTTCAGCCAAGGTCCATGGTAGCCAATCCAGAATGCCTGATTTCCGAATACCA  
TTCTCCTACTCCCGGACACCAGCTCAGCCAATCTGATCCCAATAGAAGTCACAAATGAGGCGTCTCCA  
CTCTGCACCCATGGTTCAGGCATAACCGATCACAGTCAAGGGCCACGGTCAAGGAATCAACAATATAATGGA  
CACACAGTGTAGCGTGGCACCAGACTCTTCCATGTGGAGAGTGAAGTGTAAAAATGGAACATCATG  
CACAAAGCTGGTAATCCGCAGTGCCTTTTGTCTGAAAGGATTGCGCATCACTGTTAAGAAATTGCTGAGCT  
CTAGAAAGCAATGAAATTATGTTTGGTGTCTGATAACGATGTTTTAATCACTACATAAACTTTTTAAA  
CATCTCATTGGAAGTATTTGTCTGAGGGCAGTGGTGGCTAAGTGGTTAAGACGACTAATAACCTGGAGG  
TTGCCATTCAAGCCCCCTCTGCCACTGTTGGGCCCTGAGCAAGGCCCTTAACCCTTGATTGCTCAAG  
ATGTATTAGTGGTAATTGTAAGTCGCTTTGGATAAAAGCGTCAGCTAAATGCCATAAATGTAAATGTCTT  
GTTGCGTGGTCCCTACTCAGAATTACAATGGTAGTCTCTGACAGACTTCAGAATTACAATGGTAATGCTT  
TGACAGACTTCAGAATTACAGTGGTAATGCTTTGACAACTTCAGAATTACAGTGGTAATGCTTTGACAA  
ACTTCAGAATTACAATGGTAATCCTTTAACAGACTTCAGAATTACAATGGTAATCCTCTAATAGACTTCAG  
AATTACAATGGTAATCCTTTAATAGACTTCAGAATTACAATGGTAATCCTTTGACAGGCTTCAGATTTGCC  
AGACTACTGCTTTCTTCTCCCTCTCCTACGATTTTCAACATTTTTTCTACATTCATATCACCTTTTGTAGT  
GTTCCCTTTTTAAAAGAAAAATTGTCAGGAATTTCTTCTTTTTTTCTTATTTTTTTTTAACTAATTAC  
CCACTAAAATATAATTTACTTCTTCATCCGAGAGTTGCATTTACTTGTATCTGTAATTTGTGTTGATGTCT  
CACTTCCCTTGCACTGTTTATAAACCTACAGGTGCATGGGCTGCCACTTTACTGCAGGGAAATGGAATGAGT  
AAGGCAGATGCCATTCACCTACATGGAAGGCACTCAGTCACTGGGGAGTATGTGCAGCTATATAATGCA  
TACATAAACTGTGCGGTACACTTACCTGTAGCATTTAATACCAGATCTTTTCTTAGTACTGTTCCAGGCT  
TTCTCAGGTTTCGAAAACACTCGCCAATGTCTTTGTTGCATCTAACCACACTTTTTATGTATGCTTCATTA  
AGTTGCGCTCCATCCGCACTGTGACCAAATTTTGAATGTGTGATGTTATTTATATCCCATATTTCAGG  
TGGCAAGTGTGTTGAGCAGCGCAAATTCATGTAAGTTTTCTGTAAGTGTGTTTGTGTTGTTGTTGTTGTT  
AAATCCTTTTGCCTAAAACTTAAATTGACTGATAATAAGAACAAAAATTGAAGGAGGCATTAATATGAAG  
TTTTATTGGATAACTTTTATTAGGCTTAATGTCATCACCCGATTCCATTAATCAATCAATAACAGTGCTAA  
AGGAATTTGGGTAAATGTTATATTTATAATTTTGAACATCCCAAAGTAAACCCCTCAAATTTATGCCCTA  
AGTGA AAAACAGTATTTAATGGTTAATAATTGCAGTCTGTGCATTTTTGATTAAAAATATCTTTGCTCCAA  
ACTTAATTAAGTGTCCACATGTTATGAGCCATAAAGAAATATGGCAAGAGAAATGGCAGAAAACATTTA  
ATTYATTGATGGTATTTAAAATTTATTTTCAAATAGCATGTTCTTTTGTAAATGCGTGGCTTGGAGAGGTT  
CTGTGGAGGCCAGACCTTAAGTTTTAATACAATGACAAATGCCTTACTCCTGAAAGTGTGTGAATGAATAA  
AAAACACTTTTTGAGTTTTCTTYAAAAAAAAAAAAAA

## Appendix 2. cDNA sequence of smSCN4Ab (smNav1.4b)

### Exon1S

TAAGACCCCAATGCATAAGCAACAGCTGCCACGCAGCGCGCACTCTGAGATTGGGGGGAAAAGTTCTCGCC  
CAGGACTTAGACGAAAAGTAACCTTCGGTGTAAACTACAGCTAAAAGGAAATTTCTGTTTTACTGGATAA  
GG

### Exon1L

GTAGAACTGGCTGAGGCTGACTTGAACGTGCGCAAACCACGTCAAGCAGACGCATGCGGAGACTTACTGG  
TTAGCTCCAAGTTCTCGGTTGTAAGCAGGTTTGCAGGCAGAC**ATG**CCCAAGCAAAGATCACGCTGCTGGA  
GGTATGGCAGAGGAATCGTACAGCACATGTGAAGAAGTCAGAAAACTCAAACATATGGCCGCATCAGGTG

### Exon2 and following sequence

GAGCGGCTGAGAGACCCCGAGGTGGTGACATCCCTCGTCAAGCAGAATGCGAAGATGGTGCGCCTGCTCCC  
CACCGCAGGCCCTGATGTTTTCCGCCGCTTACGCCGGATACGCTGGTGGAGATCGAGCGGCGCATGGCAG  
AGGAGGCTGCAGAGCTGCAGCACCGGAAGTCCCTGAACATCGAGATTCCCGAGGATGAACTGCCCAAACCC  
TCTAAAGATCTGGAAGCCGGCAAGCCCCTGCCCTTTCATCTATGGAGACCCACCACCTGAGTTCCTCAACAT  
ACCTCTGGAAGAGTTGGATCCCTACTACAAAGCCAAGAAAACCTTTCATCGTAATCAGCAAAGGGAAAACGA  
TCAACAGATTCAACGCTGAGCCTGCCTGTTACATTATAAGTCCATTTAACCCAATTCGCAGAGCAGCCATC  
AGAACACTCATAACATTGTTTTCAGTATGTTTATCATGGTAACAATCCTGTCAAACCTGTGTGTTTCATGAC  
TATGAGCAACCCCCACAATGGAGCAAAACTGCAGAGTACGTTTTTCACAGGTATCTATACTTCGAAGCAC  
TGGTAAAATCTTCTCCAGAGGTTTCTGTGTTGGAGACTTACATTTCCTTAGAGATCCATGGAACCTGGCTG  
GATTTTCATGGTATCAGCATGGCGTACACTACGGAGTTTGTGGACCTGGGAAACGTGTGGCTCTGAGGAC  
CTTCCGTGTTCTCCGAGCACTGAAAACAATTACTGTAATTCCTGGTCTGAAAACCAATTGTTGGCGCACTCA  
TCCAGTCTGTGAAGAAGCTGGGAGACGTGATGATCCTGACCGTCTTCTGTCTCAGTGTCTTTGCCCTCATT  
GGCCTGCAGTGTTTCATGGGGATCCTGCGCCACAAGTGTGTCTTGTGGCCTAGTTTGTCCAAAACAACAC  
AAACACCACCTTTGACTGGGAGGAGTACGTGTCAAATGAAGAAAACCTACTACTTTTCTCCAGGTAATAAGG  
ACGCACCTTCTGTGGAAACAGTTCTGATTCTGGGCGGTGTCCAGAAGGATACGTATGTTTTGAAGGCAGGC  
AAGAACCCAAATTACGGCTACACCAGTTACGACAATTTTGGGTGGGCCTTTCTGGCCCTGTTCCGTCTTAT  
GACGCAGGACTTCTGGGAAAACCTGTTCCAATTGACTCTACGGGCAGCGGGGAAGACCTACATGATCTTCT  
TCGTAGTTATCATCTTCTGGGCTCCTTCTACCTGATCAACCTCATTCTGGCCGTGGTTGCTATGGCATA  
GCTGAACAGAACGAGGCCACTATAGCCGAGGCAAAGGAGAAGGAGGAAGAGTACGCGCGAATCATGGAGCA  
GCTCAAACAGAAGCATGCCAAGGTGAGTACGACGTTGCGGATGACAATCAAAGCCTTGACAGGACGGCA  
AACAGAGAACAGACCATGACTGCATTGCACTGAAATCCCTTTTCAGAGGGAAAGATATCAAAGTCAATGGG  
TGCAAGGGAAGCATGGACCAGCTTGAAGAGCCCCACCCACACAACAGGAAAGCCAGTGTGTGAGCGCTAC  
CAGCAATGCCTTAGATGAATTAGAGGAGTTAGAAAGGCCATGCCCTCCTTGCTGGTACAAGTTTGAGACA  
TTTTCTGAAGTGGGACTGCTGTGCACCATGGATCAAATTCAGAAGTGGGTGCACCTTCATTGTGATGGAC  
CCTTTTGTGGACCTAGGCATCACTATCTGCATCGTCTGAACTGTGTTTCATGGCCATGGAACACTATCC  
CATGACTCAAGATTTGAAAACGGTCTTGATCACTGGCAACTTGGTCTTTACAGGCATCTTACGGCCGAGA  
TGGTGTCAAGATCATTGCGATGGACCCGTAATACTACTTTTCAGGTTGGCTGGAACATTTTTGACAGCATC  
ATTGTGACAATGAGTCTCGTGGAGCTGGGCTTGGCCAACGTGGAGGGACTCTCAGTGTCTCAGGTCCTTCCG  
TCTCATGCGTGTCTTCAAGTTGGCCAAGTCAATGGCCACTCTCAACATGCTGATTAAGATCATCGGCAACT  
CGGTGGGCGCGTTGGGCAACCTGACCCCTCGTGTGGCCATCATCGTCTTTCATCTTTGCCGTGGTGGGCATG  
CAGCTGTTCCGGGAAGAGCTACAAGGACTGTGTGTGCAAGATTTCAGAAGACTGCGAGCTGCCTCGCTGGCA  
CATGAGTGACTTCTTCACTCCTTCTGATCGTGTTCGCGTGCTGTGTGGCGAGTGGATCGAGACGATGT  
GGGACTGCATGGAGGTAGCCGGTCAAAGCATGTGCCTCATCGTCTTTCATGATGGTCATGGTGATTGGCAAC  
TTGGTGGTCTTGAATCTTTTCTCGCCTTGCTTCTTAGCTCTTTTAGTGGAGATAATCTGTATCATCAGAG  
TGATGATGGTGAATGAACAACCTGCAGATCGCCATTGCAAGAATCACCACAGCTATTGATTGGGTCAAGG  
CCTTTTTTATTGGACATATAAGTAGTTTGTAGGCTTAAAACCTAAGGATGAGGAGAAGAAAGAGAACGAC  
CATGGAGACTTCAAAGGCAGCAATGATCTTGTGATGAACCACATGGACTCAGGGGAAGAGCCTGAACCTGA  
GGTGATAAAGCTGGTACCTTCTCAAATTGCCATTGAGGCTCCAATTGCAAAAAGTTGAGTGTGCTTACAAA  
GAATTAACGATGATGACGGCGCTCCTACAGATGAAGACAAGAATCTGAAAGACATAGATGCAGATGGCTCA  
TCCATCTGCAGTACGGTGGACATAACAACCTGAGGTGGTGGAGACAGAATATGTTGAAGAAGAAGACTCCAA  
CACCCAGAGGACTGTTACACAGAGAAATGCATCACGCGCTGTCCATGCCTGGATGTGGACATCACCCAGG  
GCAGAGGAAAGTTATGGTGGAACTTCCGCAAGACCTGTTTCATCATTGTGGAACACAACCTATTTTTGAACT

TTTATCATCTTCATGATTCTCCTCAGCAGTGGTGCCTTTGGCTTTTTGAGGATGTTTACATTGAGCAACGAAG  
AGTGATTAATAATCATCCTTGAGTATGCAGATCAGATCTTCACCTACATCTTTGTTGTTGAGATGCTCTTAA  
AATGGGTTGCCATATGGTTTTCAAGACATACTTCACAAATGCATGGTGCCTGGCTGGACTTCCTGATTGTTGAT  
GTCTCTCTGATCAGCTTGACAGCTAACATTCTAGGTTACTCTGAACTTGGTCCCATCAAATCCCTGCGGAC  
ACTGAGGGCTCTGAGACCCTTCGTGCCTTATCCAGATTTGAAGGAATGAGGGTGGTGGTCAATGCCCTGG  
TTGGAGCCATCCCCTCAATATTCAACGTCATGCTCGTGTGCCTGATTTTTCTGGTTGATCTTTAGTATAATG  
GGAGTAAACCTGTTTGTGCGAAAGTTCTACTATTGCTTTAATACCACCTTAGAGGTTACATACCTGATAGA  
TGAGGTAAACAACAAGAGTGAAGTGCATCGCACTCATCGATGCTGGTTTAGACGCACGATGGATGAACGCGA  
AGGTCAACTTTGATAATGTGGGCATGGGCTACCTCTCCTTACTACAAGTGGCAACATTTAAAGGATGGATG  
GAAATCATGTATGCTGTGTTGATTCTCGTGAAGTGGAGAGCCAACCATCATATGAGATAAACATCTACAT  
GTACCTCTACTTTGTTATTTTTCATCATCTTTGGATCCTTCTTCACTCTCAATTTATTGTTGTTTATCA  
TTGATAATTTCAACCAACAAAAATCCAAGTTAGGTGGACAGGACTTATTATGACAGAGGAACAGAAAGAAA  
TACTACAATGCCATGAAGAAACTAGGTTCTAAGAAACCACAGAAACCTATCCCACGCCCCCAGAAGTGCCTT  
TCAGGGCCTCATCTTCGACTTTGTACGAAGCAGTTCTTTGACTTCACAATAATGGGACTAATCTGCCTGA  
ACATGATCACCATGATGGTGGAGACTGATGACCAGAGCATCGAAGCCGAAAAACATCCTATACATGATTAAT  
TTAGTCTTCATTGTGATCTTCAGTGGAGAGTGTGTTGCTGAAGCTCATTGCCCTTAGACAATACTTCTTCTC  
CATTGGATGGAATGTTTTGATTTTTATTGTGGTGAATCTTTCAATTGCAGGCTTACTGCTGGCAGACATCA  
TTGAGAAGTATTTTCGTGTCACCCACCCTTTTCCGTGTCATCCGACTTGCCAGAATAGGTGCTGCTCCTGCGT  
CTGATCCGAGGGGCCAAGGGCATCCGGACACTGCTGTTTGCCTGATGATGTCCCTCCCTGCCCTCTTCAA  
CATTGGCCTCCTCCTCTTTTTGATCATGTTTCATTTTTTCAATATTTGGCATGTCCAACCTTCGTTATGTTA  
AAAAAGAGGCAGGCATTGATGACATGTTCAATTTTTGAGACCTTTGGAAACAGCATCATATGTCTGTTTCATG  
ATCACAACCTTCTGCAGGTTGGGATGACTTCTAGGTCTATGCTAAACAGTGCCCCCTCCAGACTGTGACCC  
GAAGATGGAACATCCCGAACATATGTGAGGGGTGATTGTGGGAACCCTGCAGTGGGAATAGCATTTTTCT  
GCACCTACATTGTGATGTCCTTCTTGTGGTGGTCAACATGTACATTGCCATCATTCTGGAGAACTTCAAT  
GTGGCAACAGAGGAGAGCAGTGAAGCCATTAAGTGAAGGATGACTTTGAGATGTTCTACAGCACCTGGGAAAA  
GTTTGTATCCAGATGCTTCACAGTTCATCAGTTACAACCTACTGTCCGATTTCTGTGACACACTAAAAGAGC  
CACTGAGGATCCCAAAGCCAAACACAATCAAGCTGATTACCATGAACCTCCCAATGGTCGCAGGAGAGAAG  
ATCCACTGTGTTGACATCCTGCTAGCTCTCACTATTGATGTACTGGGTGAGTCAGGGGGAACAGACATGCT  
CAAATTTGACCATAGAGGAAAAAATTCATGGCGAATAACCCACAAAGGTGTCTTACGTGCCAATCACCACCA  
CCCTGCGACGCAAGCAAGAGGACGTGGCTGCAAGAGTTATCCAAAGAGCCTACCGCAAACATATGCTTAAA  
TGTCAACTCAAGCAACTGAAGAAAAGGCATAATGAAACATCTGGGACAGTTGAGATGTTGACAGATGAGTT  
AAACCAGCTCTACAGAGATCGAGTGACAGAGGAGAGGCCTTCTGTGTCTTTTTGGTCTCCCGAAAAACAAGG  
CCAAAACAGAAATGGGCAAGTACAAGAAAAGCCTTTCTTTCAGTTAAGTTGCAGAATGAAAGGTCTTTGCAT  
TCTGTCCCTTTCTCCATCCCTGCAACTTCTGCTTATGTGGACAGTTTGAAGAGAGTCTGTTGTGTAGAAAGA  
GCTGAGCGCATGAAAGTGTTTTTAGTTACATAATGCACCAAGATGACGCCTTTTTATTAAAGGGTTTTGTTGG  
CATTTTTGAGGTATATAAAAAGTAAATAGAATCTCAGACATTCATCAAGAAGTGTAACTGCTAACAGACTG  
TAAGCTTTTTACTCTCCTGGTCCCCTGCAGGAATGGGGTGCAGTGGCGTGGGACCTTGCTTTTTAGATCAGTG  
GTGCTCAGATCTGAACTTCAAACGGAAGCTGAATTTTTGTGGTGGTTAAATGAACTGGCTGGACACTGTCA  
CCACATCTTCAAGTTAAAGGGGGGGGGGGGGGGTTCATCCGTGAACAGTCTGATGCAGCAGCCCAATACA  
TTAAGACATTTTTTACATTACAAGATGCAGCATGACATGTTTTCTGTATGCRAAAAAAAAAAAAAAAAAA

### Appendix 3. Exon and intron sequences of SCN1B

#### Exon1

GAGTGTGCTTGTGTGCTTGAGACGCGAAGGGACGCTGCTCCTCAGTGAAGATGTCTGCAGTGCAGCTGCTG  
TGGATGCCGTTGGTGTGTGTGTGGTGCACGGTGGGCTCAGCAATGGGGCATGTGTGGAGGTGGACTCGGA  
CACAGAGGCGGTTCGTGGGCCAAGGCTTCAAACCTGGGTTGCATCTCCTGTAAGATGAGGGGGGAGGTAGAGG  
CCTCCGCCACTGTGGACTGGTGGTTTCATGGCCAAAGGGGAGAGCGAGTTTAGCCACATCTACAGTTATGCT  
GATATGGTGGGCATGGTTAATGACGAACGCTTCTGGACCGCTGGACTGGATGGGCAGCAAGAACACATT  
CGACCTGCAAGACGGCTCCATCTACATCGTCAACGTTACCTTAAATGACACGGGCACCTACCGCTGTTACT  
TTGACCGAACGCTCACCTTCAGCTACTACGAGTACCGCACCAACACCACCAAGTACATCACCATTAATGTG  
GCACCTAAG

#### Intron1

GGTGTGAGGGTGGATGAGGTTAAAGCATGCCAACACTACCAAACACAAAACAAGCTGGGTTAAAAGAAA  
GARCGGGCTTGTATACAGAGCCTGATTCGGGACTGTATTGAACACAGCATCCTAACCGGATGTCAAAGCA  
ATAACACAGGAAGCAAGGACGAATCTTTGTGTTCATGAAAGTAAAGAGTGTTCCAAGGCAACGGCCCCCTGG  
GCTTTTCATCTCTCTGAGTGGCTTTGACTAGCGAACACCTGCTTATAAATCAACAGGTAATCGATGTATG  
AAACAGCCACCATTCTAATAAAACAATCCTGGTGTAGCATTACCACTTACCCGCTTATGCGGGTAAGTTTAT  
TTTCTTTTGTTCATCAAAAAGCAGCTTGTGTTGAAAGTAAATGCATCTTTGATATACCCTCAAATATCA  
CATTACTGAATACATTTATTTAACATTTCTTTAGGTGTATCATAACAATTTGTGTAAGTCAGTTTCTGA  
CCACAGGACCTTTCTTTGTATGTGTCTAGATGACACACCAGTCTCTACTCAGCAGTGACCTGTGTCTTAGT  
CCAGCTGTGGACATGTGGGCAGAACTGACCAGTGATAAAAACAGTGGAGGGCTGTAGATAAACTAGCAAA  
AGATGTCTACAATCTGTAATGTATAGCTACAAATTGCACCTATAATAGGTTTGTCCAATATAGAGTGTGC  
TGAGTAAAGGTTAAACTGTGTGGTCCCAAGATCATCTTGACTTTCCCATGCTCTTGCCCTAAAGAGAAGC  
CAGACCAGATGATGATGATGATGATCATCACAACACCAGCTCAAAAGAAAGGCATTGGCTCACACTCAAG  
TGTTGCATAGGTTGAGCTGGAGCTGGGTAATAAAGGGCGCGTGCAAGAGCCCATGATGGGGTGGGAGACC  
GAGGGGGACTCTGGGAGAAGAGCAGCCCATATGAGCCTTCTGCTGCCCAAGGCAGGCTGAGTCACTATGAC  
TGCTGCAGTACGCTAGTGGAACACTGCCAGTATCTATCTCCTCTTAGAAAAAATGGTAATACATTACAC  
TTTTAGGGGGATTGAGTGTGCCTGATTGTAGGTAAATAGAGACCCTTTGGTTGAGAGATGATATTACGCT  
ACACCAGCTAAACCATTATGTAGTGCACGGCAGTATATGTCAACAGCTTTCTGAATGAGGCTCACCCATAG  
TACTAACTCAAGTAGTTTACAACACAGCATGACTCAAAAATGTCAATACATTCTGAAACATCAACATGTTG  
ATATACTCAATATTCCAGGAGCCTAAGATTTAACTAAGATTTATTCTGTGTGYA

#### Exon2

GCATCGCGTGGCATGGCGTCGATCCTGTGAGAGGTGATGATGTATGTGTCAATCATTGGGCTGCAGCTATG  
GCTGCTGGTGGAGATGGTCTACTGCTACAGGAAGATAGCCGCCGAGGAGAGGAGGCACTGAGAGAGAGCG  
C

#### Intron2

GTGAGTAACACTTCAAACCTACTAATAGTGTCTGTGAGGTTAACTCCCTCCCTTTCTCTCTCTCTCTCTCC  
CACTCAGACACGCTAAAAATCCAATCTTCTTTCCATTCCATATTTATGTCCATTACTCCAGCGGATTCCTC  
TACTTAACTAAAGTGTATTTTACGATTTTACACTTACATGTTTACCTTTTGTGGTGGCATGCCAAGTGT  
CGGTCTGCTACTCTCCTGATTTTCTTTTCTTTCTTTGTTCTTCTGTCTGGTCTTACTCTCTCAG

#### Exon3

GGCTGAGTATTTAGCTATAGCCTCCGAGAGCAAAGATAACTGCACAGGTGTGGCAGTAGCAGAATAACGCA

#### Intron3

GGTGGGTTTATGAACGCCCCAGCCCCCAGGCCTCTTTTTCCGAAAGCCTTGATCAGGAATTGCCAAAACA  
GCACCACACCTGGTTAGAGCTGCGCTTCCAAAAAGCCAATAAAGGCTCATAATGTGCAATTTACTGTCTGC  
AGTCTTTGTAAAGTTTCAAATGTTAACAGCACCAACACTAGCCTGTGAGCTGACAGCAGTTCTGACTAGG  
CTTTTGAAGTCTTTATCTTTTTCCCCCTCTTCTTGGGTGTGCTCAGTAAATGNAAGGGCTTTAACTA  
ACAGACTTTGGTTTCAATTTTCA



**Appendix 4. Intron 1L (between exon 1L and exon2) of smNav1.4b, 808bp**

GTAAGTGTATGATGCTGGAATACTTTTTGTTTGTCTTTGTTTTGGGATTTTTTTTTGCT  
TTGGTTTGTTTAGTTTTGGAAGAGCAGGTAGCAAAGTGTAGACAGCTTATCATATAAAG  
GCTTATAAATGCTTATCATATAAATGCTTATAAATGCTTATCATATAAACACATCATAT  
ACACGCTTATTTTATGCACAAGGACCTGCAGTAATATGTTCTGGTCAATGTATCATTGC  
AATACAAGCTAAGTAATAGCACTATTTACTTTTTTTGTAAGAAATCAAAACATCTGTGA  
ACAATATATTAATATCTGCTGGAGTATTGAATCATAATAAATAATAAGTATCTTAAAA  
TCTTGACACATCTGTTCTAAGCATTAAAGCGTTAAGATTTTAGTTTATATTAATATACT  
AATGTGATCTATATTTTTCATACCCATTATTTGTTTCAATTTGGCTATAAAATAAATTTGA  
TTTGATTAATTAGATTAATAATTAGATATAAAAAGTGTGGCGGTGTTGTAAAATGGAGCAC  
TCTGCATCTTGAATATAACCTTTTTGAAGCGTCTTTTAATTGTTACAGTCAGGAGCACAA  
CATGGATGAGATAGAGGATAATGTGTCATTCTCCAAGTGAAAGCTGTTGAGTGTCTCA  
GCTCATTATAATGAGCACTGACCTGTCAAATCTAATGCGCAGTGTCCATAACAAGGTC  
ACTGTCTTCTCCTCTTCTCCTCTTCTCCTCTTCTCTTTTCTCCTCTCTGCTCACCTCAC  
ATCTCTGTTTTCTTTTCTTCTCTTCTCTCGTCTTCCCCTAG

**Appendix 5. Genomic DNA sequence immediately upstream of exon1L of smNav1.4b (1202bp known, obtained by 5' RAGE)**

GGAGACTGACATGGACTGAAGGAGTAAAGGGGGGGGGGCATGTTCCACTCAGAGTCTG  
TTGCTGGCAGTTTCTGTGCGCAAGGGTGGACTTCCTGGAAGCCCCGGCCCCCTCCGGTTT  
CTGGATTAGCCGCTCTTCTCACAAGCATTCCTACTGGATAAGAGAAAGTTTTCAGAACATC  
AAGTCTACCCAAGAGTTTCCAGAAATTCCTACTCAAGCAGCACAAAAGAAGAAAGGGCC  
TCCTGTTGATGCAGTCTCGTTCATCTTTGAGAAACAAAAAAGGAAGAAAAAGAAAA  
TGAAGAAAAGACTCAAGACAAAAGAGGGGACAGAAAACAGACCTCTCACAGAAGAGC  
TGAAGGAGCAGAAGACTGGGCGAAAACTGTTGAAATCCTGTAATAATTTACATAAAAT  
ATCTGATGCTATTTGCAAAGAACAACCTGGATAAGAATAACAGTGGGCCCTGTAGTAG  
CATTGCTTTCATGTTAACATTCTGAAATCTACAACCCCATCCAATTACCTTCCATGTCA  
CTGTTAAGTACATGAATGAAATTTGGTGCATGATCAGATTTAAATTAATAATTTGCAATT  
TTAAATATTTCCATATATGCTAACTTCTAAAGATTACACCCTTTAGGTGCTTGATCTTC  
AATTAACTACTCAACCCCACTGTGAGGGTATAATCATTGTGAGGGTATAATCATTGTTGGG  
CTCCATTGTTTACAAAGGCAAATAAAAGAAGAATGCTATTATGTCTGTCACTGGCTGTC  
AGTTACTGGCTATCAGTTCCTTGTGTTTACAACCTCTAGGACTTAGAGATGAACAGTATGA  
CAGAAACAGCTCCCTCTGCCCTTCAACACATTCAGTAGTACACCTTGGGACCACTTTGT  
TGTCCTGAAATCTTACATCTTTCAGCCACCACCCATAGTTTTATGGAATCAAACTTTT  
AATTGTAAGATTTTAGGAATTTCCATATGTTTTATAAGTGACATTGCATAAAACAATAA  
AATGATCATTAAATCATGGAATGAAAGAATCATTGAGACATCTAGTTCCTACTGTCCCT  
GAAGCTCCCCAGGCTCTCCAGAGGATGAATAGAGTCTTTGTTTCTGGACTGTTTTGAG  
ATTTGTGAGGGGCGGTATCTGATCCAAGCCAGTAGAACTGGCTGAGGCTGACTTGAA  
CTGTGCGCAAACCACGTCAAGC

Appendix 6. pNHE vector.

TGTAA TACGA CTCAC TATAG GGCGA ATTAA TTCGA GCTCG  
 T7 promotor SacI

GTACC CAGCT TGCTT GTTCT TTTTG CAGAA GCTCA GAATA  
*KpnI*

AACGC TCAAC TTTGG CAGAT CAATT CCCCG GGGAT CC  
*XmaI* *BamHI*

GAATTC Insert GAATTC  
*EcoRI* *EcoRI*

TTTAG AGCAA GCTTG ATCTG GTTAC CACTA AACCA GCCCA  
*HindIII*

AGAAC ACCCG AATGG AGTTT TTAAG CTACA TAATA CCAAC  
 TTACA CTTTA CAAAA TGTTG TCCCC CAAAA TGTAG CCATT  
 CGTAT CTCCT CCTAA TAAAA AGAAA GTTTT TTCAC AAGCA  
AAAAA AAAAA AAAAA AAAAA AAAAA AAAAA AACCC CCCCC  
*Poly-(A)*

CCCCC CCCCC TGCAG GCATG CAAGC TAGCA GCACA CTGGC  
*PstI* *SphI* *NheI*

GGCCG TTACT AGTGG ATCCG AGCTC GGTAT ACGAC ATGTT  
*SpeI*

TCCTG CGATA GCTTG AGTAT CAATA GCTCA CCTAA ATAGC

TTGGC GTAAT CATGG TCATA GCTGT TTCCT GATGC TAGCT  
M13 Reverse *NheI*

TGAGT ATTCT ATAGT GTCAC C  
 Sp6 promotor

\* Region shown contains promotor sites and cloning region sequence (510bp). All the rest sequence outside this T7-Sp6 region (2674bp) is the same as pGEM3Z

## References

- Agnew, W. S., Moore, A. C., Levinson, S. R. and Raftery, M. A. (1980). Identification of a large molecular weight peptide associated with a tetrodotoxin binding protein from the electroplax of *Electrophorus electricus*. Biochem Biophys Res Commun **92**(3): 860-6.
- Becker, M. N., Brenner, R. and Atkinson, N. S. (1995). Tissue-specific expression of a *Drosophila* calcium-activated potassium channel. J Neurosci **15**(9): 6250-9.
- Behrens, R., Nolting, A., Reimann, F., Schwarz, M., Waldschutz, R. and Pongs, O. (2000). hKCNMB3 and hKCNMB4, cloning and characterization of two members of the large-conductance calcium-activated potassium channel beta subunit family. FEBS Lett **474**(1): 99-106.
- Beneski, D. A. and Catterall, W. A. (1980). Covalent labeling of protein components of the sodium channel with a photoactivable derivative of scorpion toxin. Proc Natl Acad Sci U S A **77**(1): 639-43.
- Bennett, P. B., Jr., Makita, N. and George, A. L., Jr. (1993). A molecular basis for gating mode transitions in human skeletal muscle Na<sup>+</sup> channels. FEBS Lett **326**(1-3): 21-4.
- Black, D. L. (2003). Mechanisms of alternative pre-messenger RNA splicing. Annu Rev Biochem **72**: 291-336.
- Black, J. A., Langworthy, K., Hinson, A. W., Dib-Hajj, S. D. and Waxman, S. G. (1997). NGF has opposing effects on Na<sup>+</sup> channel III and SNS gene expression in spinal sensory neurons. Neuroreport **8**(9-10): 2331-5.
- Bohm, R. A., Wang, B., Brenner, R. and Atkinson, N. S. (2000). Transcriptional control of Ca(2+)-activated K(+) channel expression: identification of a second, evolutionarily conserved, neuronal promoter. J Exp Biol **203**(Pt 4): 693-704.
- Brenner, R., Thomas, T. O., Becker, M. N. and Atkinson, N. S. (1996). Tissue-specific expression of a Ca(2+)-activated K<sup>+</sup> channel is controlled by multiple upstream regulatory elements. J Neurosci **16**(5): 1827-35.
- Cantrell, A. R., Smith, R. D., Goldin, A. L., Scheuer, T. and Catterall, W. A. (1997). Dopaminergic modulation of sodium current in hippocampal neurons via cAMP-dependent phosphorylation of specific sites in the sodium channel alpha subunit. J Neurosci **17**(19): 7330-8.
- Caponigro, G. and Parker, R. (1996). Mechanisms and control of mRNA turnover in *Saccharomyces cerevisiae*. Microbiol Rev **60**(1): 233-49.
- Catterall, W. A. (2000). From ionic currents to molecular mechanisms: the structure and function of voltage-gated sodium channels. Neuron **26**(1): 13-25.
- Chen, C., Westenbroek, R. E., Xu, X., Edwards, C. A., Sorenson, D. R., Chen, Y., Mcewen, D. P., O'malley, H. A., Bharucha, V., Meadows, L. S., Knudsen, G. A., Vilaythong, A., Noebels, J. L., Saunders, T. L., Scheuer, T., Shrager, P., Catterall, W. A. and Isom, L. L. (2004). Mice lacking sodium channel beta1 subunits display defects in neuronal excitability, sodium channel expression, and nodal architecture. J Neurosci **24**(16): 4030-42.

- Chen, L. Q., Santarelli, V., Horn, R. and Kallen, R. G. (1996). A unique role for the S4 segment of domain 4 in the inactivation of sodium channels. J Gen Physiol **108**(6): 549-56.
- Chen, T. C., Law, B., Kondratyuk, T. and Rossie, S. (1995). Identification of soluble protein phosphatases that dephosphorylate voltage-sensitive sodium channels in rat brain. J Biol Chem **270**(13): 7750-6.
- Chew, L. J. and Gallo, V. (1998). Regulation of ion channel expression in neural cells by hormones and growth factors. Mol Neurobiol **18**(3): 175-225.
- Chou, P. Y. and Fasman, G. D. (1974). Prediction of protein conformation. Biochemistry **13**(2): 222-45.
- Cormier, J. W., Rivolta, I., Tateyama, M., Yang, A. S. and Kass, R. S. (2002). Secondary structure of the human cardiac Na<sup>+</sup> channel C terminus: evidence for a role of helical structures in modulation of channel inactivation. J Biol Chem **277**(11): 9233-41.
- Coutts, C. A., Patten, S. A., Balt, L. N. and Ali, D. W. (2006). Development of ionic currents of zebrafish slow and fast skeletal muscle fibers. J Neurobiol **66**(3): 220-35.
- Dib-Hajj, S., Black, J. A., Felts, P. and Waxman, S. G. (1996). Down-regulation of transcripts for Na channel alpha-SNS in spinal sensory neurons following axotomy. Proc Natl Acad Sci U S A **93**(25): 14950-4.
- Dib-Hajj, S. D., Black, J. A., Cummins, T. R., Kenney, A. M., Kocsis, J. D. and Waxman, S. G. (1998). Rescue of alpha-SNS sodium channel expression in small dorsal root ganglion neurons after axotomy by nerve growth factor in vivo. J Neurophysiol **79**(5): 2668-76.
- Dib-Hajj, S. D., Tyrrell, L., Black, J. A. and Waxman, S. G. (1998). Na<sub>v</sub>N, a novel voltage-gated Na channel, is expressed preferentially in peripheral sensory neurons and down-regulated after axotomy. Proc Natl Acad Sci U S A **95**(15): 8963-8.
- Dick, G. M., Hunter, A. C. and Sanders, K. M. (2002). Ethylbromide tamoxifen, a membrane-impermeant antiestrogen, activates smooth muscle calcium-activated large-conductance potassium channels from the extracellular side. Mol Pharmacol **61**(5): 1105-13.
- Dick, G. M., Rossow, C. F., Smirnov, S., Horowitz, B. and Sanders, K. M. (2001). Tamoxifen activates smooth muscle BK channels through the regulatory beta 1 subunit. J Biol Chem **276**(37): 34594-9.
- Dick, G. M. and Sanders, K. M. (2001). (Xeno)estrogen sensitivity of smooth muscle BK channels conferred by the regulatory beta1 subunit: a study of beta1 knockout mice. J Biol Chem **276**(48): 44835-40.
- Dobrzycka, K. M., Townson, S. M., Jiang, S. and Oesterreich, S. (2003). Estrogen receptor corepressors -- a role in human breast cancer? Endocr Relat Cancer **10**(4): 517-36.
- Drews, V. L., Lieberman, A. P. and Meisler, M. H. (2005). Multiple transcripts of sodium channel SCN8A (Na(V)1.6) with alternative 5'- and 3'-untranslated regions and initial characterization of the SCN8A promoter. Genomics **85**(2): 245-57.

- Dunlap, K. D., Mcanelly, M. L. and Zakon, H. H. (1997). Estrogen modifies an electrocommunication signal by altering the electrocyte sodium current in an electric fish, *Sternopygus*. J Neurosci **17**(8): 2869-75.
- Fahmi, A. I., Forhead, A. J., Fowden, A. L. and Vandenberg, J. I. (2004). Cortisol influences the ontogeny of both alpha- and beta-subunits of the cardiac sodium channel in fetal sheep. J Endocrinol **180**(3): 449-55.
- Ferrari, M. B., Mcanelly, M. L. and Zakon, H. H. (1995). Individual variation in and androgen-modulation of the sodium current in electric organ. J Neurosci **15**(5 Pt 2): 4023-32.
- Ferrari, M. B. and Zakon, H. H. (1989). The medullary pacemaker nucleus is unnecessary for electroreceptor tuning plasticity in *Sternopygus*. J Neurosci **9**(4): 1354-61.
- Ferrari, M. B. and Zakon, H. H. (1993). Conductances contributing to the action potential of *Sternopygus* electrocytes. J Comp Physiol [A] **173**(3): 281-92.
- Fettiplace, R. and Fuchs, P. A. (1999). Mechanisms of hair cell tuning. Annu Rev Physiol **61**: 809-34.
- Few, W. (2003). Regulation of Electrical Excitability: Individual, Gender and Hormonally-Induced Variation in Potassium Channel Expression in the Electric Organ. Doctoral Dissertation, The University of Texas at Austin.
- Few, W. P. and Zakon, H. H. (2001). Androgens alter electric organ discharge pulse duration despite stability in electric organ discharge frequency. Horm Behav **40**(3): 434-42.
- Fjell, J., Cummins, T. R., Dib-Hajj, S. D., Fried, K., Black, J. A. and Waxman, S. G. (1999). Differential role of GDNF and NGF in the maintenance of two TTX-resistant sodium channels in adult DRG neurons. Brain Res Mol Brain Res **67**(2): 267-82.
- Fjell, J., Cummins, T. R., Fried, K., Black, J. A. and Waxman, S. G. (1999). In vivo NGF deprivation reduces SNS expression and TTX-R sodium currents in IB4-negative DRG neurons. J Neurophysiol **81**(2): 803-10.
- Flake, N. M., Lancaster, E., Weinreich, D. and Gold, M. S. (2004). Absence of an association between axotomy-induced changes in sodium currents and excitability in DRG neurons from the adult rat. Pain **109**(3): 471-80.
- Garnier, J., Osguthorpe, D. J. and Robson, B. (1978). Analysis of the accuracy and implications of simple methods for predicting the secondary structure of globular proteins. J Mol Biol **120**(1): 97-120.
- Gold, M. S., Weinreich, D., Kim, C. S., Wang, R., Treanor, J., Porreca, F. and Lai, J. (2003). Redistribution of Na(V)1.8 in uninjured axons enables neuropathic pain. J Neurosci **23**(1): 158-66.
- Grabowski, P. J. and Black, D. L. (2001). Alternative RNA splicing in the nervous system. Prog Neurobiol **65**(3): 289-308.
- Grieco, T. M., Malhotra, J. D., Chen, C., Isom, L. L. and Raman, I. M. (2005). Open-channel block by the cytoplasmic tail of sodium channel beta4 as a mechanism for resurgent sodium current. Neuron **45**(2): 233-44.
- Guiramand, J., Montmayeur, J. P., Ceraline, J., Bhatia, M. and Borrelli, E. (1995). Alternative splicing of the dopamine D2 receptor directs specificity of coupling to G-proteins. J Biol Chem **270**(13): 7354-8.

- Hilborn, M. D., Vaillancourt, R. R. and Rane, S. G. (1998). Growth factor receptor tyrosine kinases acutely regulate neuronal sodium channels through the src signaling pathway. *J Neurosci* **18**(2): 590-600.
- Hobson, A. J. and Isom, L. L. (2003). Cloning and expression of novel voltage gated Na<sup>+</sup> channel subunits in the genome of *Danio rerio*. **Program No. 8.3. 2003 Abstract Viewer/Itinerary Planner. Washington, DC: Society for Neuroscience 2003: Online.**
- Hobson, A. J., Meadows, L. S. and Chen, C. L. (2004). Identification and expression of multiple beta1 orthologs from zebrafish. No. 262.8. 2004 Abstract Viewer/Itinerary Planner. Washington, DC: Society for Neuroscience 2004: online.
- Hong, K., Guerchicoff, A., Pollevick, G. D., Oliva, A., Dumaine, R., De Zutter, M., Burashnikov, E., Wu, Y. S., Brugada, J., Brugada, P. and Brugada, R. (2005). Cryptic 5' splice site activation in SCN5A associated with Brugada syndrome. *J Mol Cell Cardiol* **38**(4): 555-60.
- Hopkins, C. D. (1974). Electric communication in the reproductive behavior of *Sternopygus macrurus* (Gymnotoidei). *Z Tierpsychol* **35**(5): 518-35.
- Hopkins, C. D. (1999). Design features for electric communication. *J Exp Biol* **202**(Pt 10): 1217-28.
- Isom, L. L. (2001). Sodium channel beta subunits: anything but auxiliary. *Neuroscientist* **7**(1): 42-54.
- Isom, L. L. (2002). Beta subunits: players in neuronal hyperexcitability? *Novartis Found Symp* **241**: 124-38; discussion 138-43, 226-32.
- Isom, L. L. and Catterall, W. A. (1996). Na<sup>+</sup> channel subunits and Ig domains. *Nature* **383**(6598): 307-8.
- Isom, L. L., De Jongh, K. S., Patton, D. E., Reber, B. F., Offord, J., Charbonneau, H., Walsh, K., Goldin, A. L. and Catterall, W. A. (1992). Primary structure and functional expression of the beta 1 subunit of the rat brain sodium channel. *Science* **256**(5058): 839-42.
- Isom, L. L., Ragsdale, D. S., De Jongh, K. S., Westenbroek, R. E., Reber, B. F., Scheuer, T. and Catterall, W. A. (1995). Structure and function of the beta 2 subunit of brain sodium channels, a transmembrane glycoprotein with a CAM motif. *Cell* **83**(3): 433-42.
- Isom, L. L., Scheuer, T., Brownstein, A. B., Ragsdale, D. S., Murphy, B. J. and Catterall, W. A. (1995). Functional co-expression of the beta 1 and type IIA alpha subunits of sodium channels in a mammalian cell line. *J Biol Chem* **270**(7): 3306-12.
- Jacobson, A. and Peltz, S. W. (1996). Interrelationships of the pathways of mRNA decay and translation in eukaryotic cells. *Annu Rev Biochem* **65**: 693-739.
- Jaillon, O., Aury, J. M., Brunet, F., Petit, J. L., Stange-Thomann, N., Mauceli, E., Bouneau, L., Fischer, C., Ozouf-Costaz, C., Bernot, A., Nicaud, S., Jaffe, D., Fisher, S., Lutfalla, G., Dossat, C., Segurens, B., Dasilva, C., Salanoubat, M., Levy, M., Boudet, N., Castellano, S., Anthonard, V., Jubin, C., Castelli, V., Katinka, M., Vacherie, B., Biemont, C., Skalli, Z., Cattolico, L., Poulain, J., De Berardinis, V., Cruaud, C., Duprat, S., Brottier, P., Coutanceau, J. P., Gouzy, J., Parra, G., Lardier, G., Chapple, C., Mckernan, K. J., Mcewan, P., Bosak, S., Kellis, M., Volff, J. N., Guigo, R., Zody, M. C., Mesirov, J., Lindblad-Toh, K.,

- Birren, B., Nusbaum, C., Kahn, D., Robinson-Rechavi, M., Laudet, V., Schachter, V., Quetier, F., Saurin, W., Scarpelli, C., Wincker, P., Lander, E. S., Weissenbach, J. and Roest Crolius, H. (2004). Genome duplication in the teleost fish *Tetraodon nigroviridis* reveals the early vertebrate proto-karyotype. Nature **431**(7011): 946-57.
- Ji, S., Sun, W., George, A. L., Jr., Horn, R. and Barchi, R. L. (1994). Voltage-dependent regulation of modal gating in the rat SkM1 sodium channel expressed in *Xenopus* oocytes. J Gen Physiol **104**(4): 625-43.
- Kazarinova-Noyes, K., Malhotra, J. D., Mcewen, D. P., Mattei, L. N., Berglund, E. O., Ranscht, B., Levinson, S. R., Schachner, M., Shrager, P., Isom, L. L. and Xiao, Z. C. (2001). Contactin associates with Na<sup>+</sup> channels and increases their functional expression. J Neurosci **21**(19): 7517-25.
- Kazen-Gillespie, K. A., Ragsdale, D. S., D'andrea, M. R., Mattei, L. N., Rogers, K. E. and Isom, L. L. (2000). Cloning, localization, and functional expression of sodium channel beta1A subunits. J Biol Chem **275**(2): 1079-88.
- Kirsch, G. E. and Sykes, J. S. (1987). Temperature dependence of Na currents in rabbit and frog muscle membranes. J Gen Physiol **89**(2): 239-51.
- Krishek, B. J., Xie, X., Blackstone, C., Haganir, R. L., Moss, S. J. and Smart, T. G. (1994). Regulation of GABAA receptor function by protein kinase C phosphorylation. Neuron **12**(5): 1081-95.
- Lemaillet, G., Walker, B. and Lambert, S. (2003). Identification of a conserved ankyrin-binding motif in the family of sodium channel alpha subunits. J Biol Chem **278**(30): 27333-9.
- Li, M., West, J. W., Lai, Y., Scheuer, T. and Catterall, W. A. (1992). Functional modulation of brain sodium channels by cAMP-dependent phosphorylation. Neuron **8**(6): 1151-9.
- Liman, E. R., Tytgat, J. and Hess, P. (1992). Subunit stoichiometry of a mammalian K<sup>+</sup> channel determined by construction of multimeric cDNAs. Neuron **9**(5): 861-71.
- Lin, Z., Haus, S., Edgerton, J. and Lipscombe, D. (1997). Identification of functionally distinct isoforms of the N-type Ca<sup>2+</sup> channel in rat sympathetic ganglia and brain. Neuron **18**(1): 153-66.
- Lin, Z., Lin, Y., Schorge, S., Pan, J. Q., Beierlein, M. and Lipscombe, D. (1999). Alternative splicing of a short cassette exon in alpha1B generates functionally distinct N-type calcium channels in central and peripheral neurons. J Neurosci **19**(13): 5322-31.
- Liu, X. and Baird, W. (2001). Rapid amplification of genomic DNA ends by Nla III partial digestion and polynucleotide tailing. Plant Molecular Biology Reporter **19**: 261.
- Lopreato, G. F., Lu, Y., Southwell, A., Atkinson, N. S., Hillis, D. M., Wilcox, T. P. and Zakon, H. H. (2001). Evolution and divergence of sodium channel genes in vertebrates. Proc Natl Acad Sci U S A **98**(13): 7588-92.
- Makita, N., Bennett, P. B., Jr. and George, A. L., Jr. (1994). Voltage-gated Na<sup>+</sup> channel beta 1 subunit mRNA expressed in adult human skeletal muscle, heart, and brain is encoded by a single gene. J Biol Chem **269**(10): 7571-8.
- Makita, N., Sloan-Brown, K., Weghuis, D. O., Ropers, H. H. and George, A. L., Jr. (1994). Genomic organization and chromosomal assignment of the human

- voltage-gated Na<sup>+</sup> channel beta 1 subunit gene (SCN1B). Genomics **23**(3): 628-34.
- Malhotra, J. D., Kazen-Gillespie, K., Hortsch, M. and Isom, L. L. (2000). Sodium channel beta subunits mediate homophilic cell adhesion and recruit ankyrin to points of cell-cell contact. J Biol Chem **275**(15): 11383-8.
- Malhotra, J. D., Koopmann, M. C., Kazen-Gillespie, K. A., Fettman, N., Hortsch, M. and Isom, L. L. (2002). Structural requirements for interaction of sodium channel beta 1 subunits with ankyrin. J Biol Chem **277**(29): 26681-8.
- Mantegazza, M., Yu, F. H., Catterall, W. A. and Scheuer, T. (2001). Role of the C-terminal domain in inactivation of brain and cardiac sodium channels. Proc Natl Acad Sci U S A **98**(26): 15348-53.
- Mattick, J. S. and Gagen, M. J. (2001). The evolution of controlled multitasked gene networks: the role of introns and other noncoding RNAs in the development of complex organisms. Mol Biol Evol **18**(9): 1611-30.
- Mcanelly, L., Silva, A. and Zakon, H. H. (2003). Cyclic AMP modulates electrical signaling in a weakly electric fish. J Comp Physiol A Neuroethol Sens Neural Behav Physiol **189**(4): 273-82.
- Mcanelly, L. and Zakon, H. H. (1996). Protein kinase A activation increases sodium current magnitude in the electric organ of *Sternopygus*. J Neurosci **16**(14): 4383-8.
- Mcanelly, M. L. and Zakon, H. H. (2000). Coregulation of voltage-dependent kinetics of Na<sup>(+)</sup> and K<sup>(+)</sup> currents in electric organ. J Neurosci **20**(9): 3408-14.
- Mccormick, K. A., Isom, L. L., Ragsdale, D., Smith, D., Scheuer, T. and Catterall, W. A. (1998). Molecular determinants of Na<sup>+</sup> channel function in the extracellular domain of the beta1 subunit. J Biol Chem **273**(7): 3954-62.
- Mccormick, K. A., Srinivasan, J., White, K., Scheuer, T. and Catterall, W. A. (1999). The extracellular domain of the beta1 subunit is both necessary and sufficient for beta1-like modulation of sodium channel gating. J Biol Chem **274**(46): 32638-46.
- Mcewen, D. P., Meadows, L. S., Chen, C., Thyagarajan, V. and Isom, L. L. (2004). Sodium channel beta1 subunit-mediated modulation of Nav1.2 currents and cell surface density is dependent on interactions with contactin and ankyrin. J Biol Chem **279**(16): 16044-9.
- Mcphee, J. C., Ragsdale, D. S., Scheuer, T. and Catterall, W. A. (1995). A critical role for transmembrane segment IVS6 of the sodium channel alpha subunit in fast inactivation. J Biol Chem **270**(20): 12025-34.
- Mcphee, J. C., Ragsdale, D. S., Scheuer, T. and Catterall, W. A. (1998). A critical role for the S4-S5 intracellular loop in domain IV of the sodium channel alpha-subunit in fast inactivation. J Biol Chem **273**(2): 1121-9.
- Meadows, L., Malhotra, J. D., Stetzer, A., Isom, L. L. and Ragsdale, D. S. (2001). The intracellular segment of the sodium channel beta 1 subunit is required for its efficient association with the channel alpha subunit. J Neurochem **76**(6): 1871-8.
- Meadows, L. S., Malhotra, J., Loukas, A., Thyagarajan, V., Kazen-Gillespie, K. A., Koopman, M. C., Krieglner, S., Isom, L. L. and Ragsdale, D. S. (2002). Functional and biochemical analysis of a sodium channel beta1 subunit mutation responsible for generalized epilepsy with febrile seizures plus type 1. J Neurosci **22**(24): 10699-709.

- Mills, A. and Zakon, H. H. (1991). Chronic androgen treatment increases action potential duration in the electric organ of *Sternopygus*. *J Neurosci* **11**(8): 2349-61.
- Mohler, P. J., Rivolta, I., Napolitano, C., Lemaillet, G., Lambert, S., Priori, S. G. and Bennett, V. (2004). Nav1.5 E1053K mutation causing Brugada syndrome blocks binding to ankyrin-G and expression of Nav1.5 on the surface of cardiomyocytes. *Proc Natl Acad Sci U S A* **101**(50): 17533-8.
- Morgan, K., Stevens, E. B., Shah, B., Cox, P. J., Dixon, A. K., Lee, K., Pinnock, R. D., Hughes, J., Richardson, P. J., Mizuguchi, K. and Jackson, A. P. (2000). beta 3: an additional auxiliary subunit of the voltage-sensitive sodium channel that modulates channel gating with distinct kinetics. *Proc Natl Acad Sci U S A* **97**(5): 2308-13.
- Murphy, B. J., Rossie, S., De Jongh, K. S. and Catterall, W. A. (1993). Identification of the sites of selective phosphorylation and dephosphorylation of the rat brain Na<sup>+</sup> channel alpha subunit by cAMP-dependent protein kinase and phosphoprotein phosphatases. *J Biol Chem* **268**(36): 27355-62.
- Navaratnam, D. S., Bell, T. J., Tu, T. D., Cohen, E. L. and Oberholtzer, J. C. (1997). Differential distribution of Ca<sup>2+</sup>-activated K<sup>+</sup> channel splice variants among hair cells along the tonotopic axis of the chick cochlea. *Neuron* **19**(5): 1077-85.
- Novakovic, S. D., Eglen, R. M. and Hunter, J. C. (2001). Regulation of Na<sup>+</sup> channel distribution in the nervous system. *Trends Neurosci* **24**(8): 473-8.
- Numann, R., Catterall, W. A. and Scheuer, T. (1991). Functional modulation of brain sodium channels by protein kinase C phosphorylation. *Science* **254**(5028): 115-8.
- Offord, J. and Catterall, W. A. (1989). Electrical activity, cAMP, and cytosolic calcium regulate mRNA encoding sodium channel alpha subunits in rat muscle cells. *Neuron* **2**(5): 1447-52.
- Patterson, J. M. and Zakon, H. H. (1996). Differential expression of proteins in muscle and electric organ, a muscle derivative. *J Comp Neurol* **370**(3): 367-76.
- Patton, D. E., Isom, L. L., Catterall, W. A. and Goldin, A. L. (1994). The adult rat brain beta 1 subunit modifies activation and inactivation gating of multiple sodium channel alpha subunits. *J Biol Chem* **269**(26): 17649-55.
- Qin, N., D'andrea, M. R., Lubin, M. L., Shafae, N., Codd, E. E. and Correa, A. M. (2003). Molecular cloning and functional expression of the human sodium channel beta1B subunit, a novel splicing variant of the beta1 subunit. *Eur J Biochem* **270**(23): 4762-70.
- Qu, Y., Curtis, R., Lawson, D., Gilbride, K., Ge, P., Distefano, P. S., Silos-Santiago, I., Catterall, W. A. and Scheuer, T. (2001). Differential modulation of sodium channel gating and persistent sodium currents by the beta1, beta2, and beta3 subunits. *Mol Cell Neurosci* **18**(5): 570-80.
- Qu, Y., Isom, L. L., Westenbroek, R. E., Rogers, J. C., Tanada, T. N., McCormick, K. A., Scheuer, T. and Catterall, W. A. (1995). Modulation of cardiac Na<sup>+</sup> channel expression in *Xenopus* oocytes by beta 1 subunits. *J Biol Chem* **270**(43): 25696-701.
- Ramanathan, K., Michael, T. H., Jiang, G. J., Hiel, H. and Fuchs, P. A. (1999). A molecular mechanism for electrical tuning of cochlear hair cells. *Science* **283**(5399): 215-7.

- Ratcliffe, C. F., Qu, Y., McCormick, K. A., Tibbs, V. C., Dixon, J. E., Scheuer, T. and Catterall, W. A. (2000). A sodium channel signaling complex: modulation by associated receptor protein tyrosine phosphatase beta. Nat Neurosci **3**(5): 437-44.
- Rosenblatt, K. P., Sun, Z. P., Heller, S. and Hudspeth, A. J. (1997). Distribution of Ca<sup>2+</sup>-activated K<sup>+</sup> channel isoforms along the tonotopic gradient of the chicken's cochlea. Neuron **19**(5): 1061-75.
- Rossie, S. and Catterall, W. A. (1987). Cyclic-AMP-dependent phosphorylation of voltage-sensitive sodium channels in primary cultures of rat brain neurons. J Biol Chem **262**(26): 12735-44.
- Sashihara, S., Oh, Y., Black, J. A. and Waxman, S. G. (1995). Na<sup>+</sup> channel beta 1 subunit mRNA expression in developing rat central nervous system. Brain Res Mol Brain Res **34**(2): 239-50.
- Sashihara, S., Waxman, S. G. and Greer, C. A. (1997). Downregulation of Na<sup>+</sup> channel mRNA in olfactory bulb tufted cells following deafferentation. Neuroreport **8**(5): 1289-93.
- Shang, L. L. and Dudley, S. C., Jr. (2005). Tandem promoters and developmentally regulated 5'- and 3'-mRNA untranslated regions of the mouse Scn5a cardiac sodium channel. J Biol Chem **280**(2): 933-40.
- Smith, M. R. and Goldin, A. L. (1997). Interaction between the sodium channel inactivation linker and domain III S4-S5. Biophys J **73**(4): 1885-95.
- Smith, R. D. and Goldin, A. L. (1996). Phosphorylation of brain sodium channels in the I-II linker modulates channel function in *Xenopus* oocytes. J Neurosci **16**(6): 1965-74.
- Spampanato, J., Escayg, A., Meisler, M. H. and Goldin, A. L. (2001). Functional effects of two voltage-gated sodium channel mutations that cause generalized epilepsy with febrile seizures plus type 2. J Neurosci **21**(19): 7481-90.
- Spampanato, J., Kearney, J. A., De Haan, G., McEwen, D. P., Escayg, A., Aradi, I., Macdonald, B. T., Levin, S. I., Soltesz, I., Benna, P., Montalenti, E., Isom, L. L., Goldin, A. L. and Meisler, M. H. (2004). A novel epilepsy mutation in the sodium channel SCN1A identifies a cytoplasmic domain for beta subunit interaction. J Neurosci **24**(44): 10022-34.
- Srinivasan, J., Schachner, M. and Catterall, W. A. (1998). Interaction of voltage-gated sodium channels with the extracellular matrix molecules tenascin-C and tenascin-R. Proc Natl Acad Sci U S A **95**(26): 15753-7.
- Sun, W., Cohen, S. A. and Barchi, R. L. (1995). Localization of epitopes for monoclonal antibodies directed against the adult rat skeletal muscle sodium channel (rSkM1) using polymerase chain reaction, fusion proteins, and western blotting. Anal Biochem **226**(1): 188-91.
- Sutkowski, E. M. and Catterall, W. A. (1990). Beta 1 subunits of sodium channels. Studies with subunit-specific antibodies. J Biol Chem **265**(21): 12393-9.
- Unguez, G. A. and Zakon, H. H. (1998). Phenotypic conversion of distinct muscle fiber populations to electrocytes in a weakly electric fish. J Comp Neurol **399**(1): 20-34.
- Unguez, G. A. and Zakon, H. H. (1998). Reexpression of myogenic proteins in mature electric organ after removal of neural input. J Neurosci **18**(23): 9924-35.

- Valverde, M. A., Rojas, P., Amigo, J., Cosmelli, D., Orio, P., Bahamonde, M. I., Mann, G. E., Vergara, C. and Latorre, R. (1999). Acute activation of Maxi-K channels (hSlo) by estradiol binding to the beta subunit. Science **285**(5435): 1929-31.
- Vassilev, P. M., Scheuer, T. and Catterall, W. A. (1988). Identification of an intracellular peptide segment involved in sodium channel inactivation. Science **241**(4873): 1658-61.
- Vinogradov, A. E. (1999). Intron-genome size relationship on a large evolutionary scale. J Mol Evol **49**(3): 376-84.
- Wagner, E. J. and Garcia-Blanco, M. A. (2001). Polypyrimidine tract binding protein antagonizes exon definition. Mol Cell Biol **21**(10): 3281-8.
- Wallace, R. H., Wang, D. W., Singh, R., Scheffer, I. E., George, A. L., Jr., Phillips, H. A., Saar, K., Reis, A., Johnson, E. W., Sutherland, G. R., Berkovic, S. F. and Mulley, J. C. (1998). Febrile seizures and generalized epilepsy associated with a mutation in the Na<sup>+</sup>-channel beta1 subunit gene SCN1B. Nat Genet **19**(4): 366-70.
- Walters, M. R. and Nemere, I. (2004). Receptors for steroid hormones: membrane-associated and nuclear forms. Cell Mol Life Sci **61**(18): 2309-21.
- Waxman, S. G., Kocsis, J. D. and Black, J. A. (1994). Type III sodium channel mRNA is expressed in embryonic but not adult spinal sensory neurons, and is reexpressed following axotomy. J Neurophysiol **72**(1): 466-70.
- Whiting, P., Mckernan, R. M. and Iversen, L. L. (1990). Another mechanism for creating diversity in gamma-aminobutyrate type A receptors: RNA splicing directs expression of two forms of gamma 2 phosphorylation site. Proc Natl Acad Sci U S A **87**(24): 9966-70.
- Wu, F. F., Gordon, E., Hoffman, E. P. and Cannon, S. C. (2005). A C-terminal skeletal muscle sodium channel mutation associated with myotonia disrupts fast inactivation. J Physiol **565**(Pt 2): 371-80.
- Xiao, Z. C., Ragsdale, D. S., Malhotra, J. D., Mattei, L. N., Braun, P. E., Schachner, M. and Isom, L. L. (1999). Tenascin-R is a functional modulator of sodium channel beta subunits. J Biol Chem **274**(37): 26511-7.
- Xie, J. and Black, D. L. (2001). A CaMK IV responsive RNA element mediates depolarization-induced alternative splicing of ion channels. Nature **410**(6831): 936-9.
- Xie, J. and Mccobb, D. P. (1998). Control of alternative splicing of potassium channels by stress hormones. Science **280**(5362): 443-6.
- Yang, P., Kupersmidt, S. and Roden, D. M. (2004). Cloning and initial characterization of the human cardiac sodium channel (SCN5A) promoter. Cardiovasc Res **61**(1): 56-65.
- Yu, F. H., Westenbroek, R. E., Silos-Santiago, I., McCormick, K. A., Lawson, D., Ge, P., Ferriera, H., Lilly, J., Distefano, P. S., Catterall, W. A., Scheuer, T. and Curtis, R. (2003). Sodium channel beta4, a new disulfide-linked auxiliary subunit with similarity to beta2. J Neurosci **23**(20): 7577-85.
- Zakon, H. H., Lu, Y., Zwickl, D. J. and Hillis, D. M. (2006). Sodium channel genes and the evolution of diversity in communication signals of electric fishes: Convergent molecular evolution. Proc Natl Acad Sci U S A.

- Zakon, H. H. and Unguez, G. A. (1999). Development and regeneration of the electric organ. J Exp Biol **202**(Pt 10): 1427-34.
- Zakon, H. H., Yan, H. Y. and Thomas, P. (1990). Human chorionic gonadotropin-induced shifts in the electrosensory system of the weakly electric fish, *Sternopygus*. J Neurobiol **21**(5): 826-33.
- Zhang, H., Kolibal, S., Vanderkooi, J. M., Cohen, S. A. and Kallen, R. G. (2000). A carboxy-terminal alpha-helical segment in the rat skeletal muscle voltage-dependent Na<sup>+</sup> channel is responsible for its interaction with the amino-terminus. Biochim Biophys Acta **1467**(2): 406-18.
- Zwerling, S. J., Cohen, S. A. and Barchi, R. L. (1991). Analysis of protease-sensitive regions in the skeletal muscle sodium channel in vitro and implications for channel tertiary structure. J Biol Chem **266**(7): 4574-80.

## VITA

He Liu was born in Yi'an, Heilongjiang Province, P.R. China on September 17, 1976, the son of Wen-Sheng Liu and Yu-Wen Wang. After completing his work in Harbin No.3 High School, Harbin, Heilongjiang, in 1994, he entered University of Science and Technology of China in Hefei, Anhui, P.R. China. He received the degree of Bachelor of Molecular and Cell Biology in July 1999. In September 1999 he entered the Graduate School of The University of Texas.

Permanent Address: 3-603, #100 Herun St., Harbin, Heilongjiang, 150076  
P.R.China.

This dissertation was typed by the author.